

1990 ANNUAL REPORT

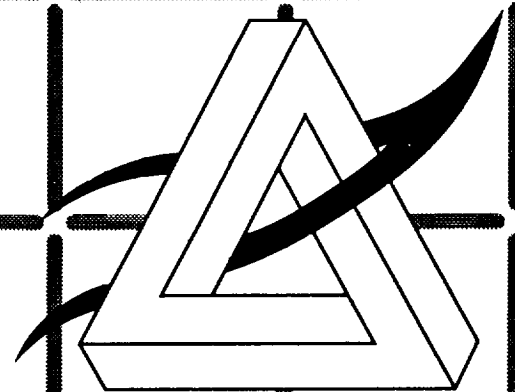
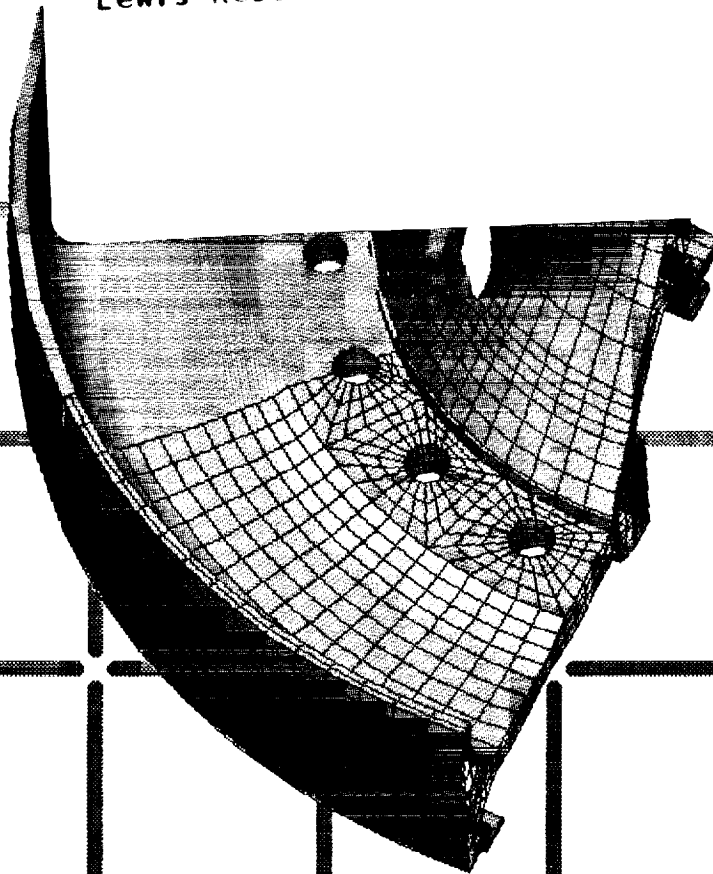
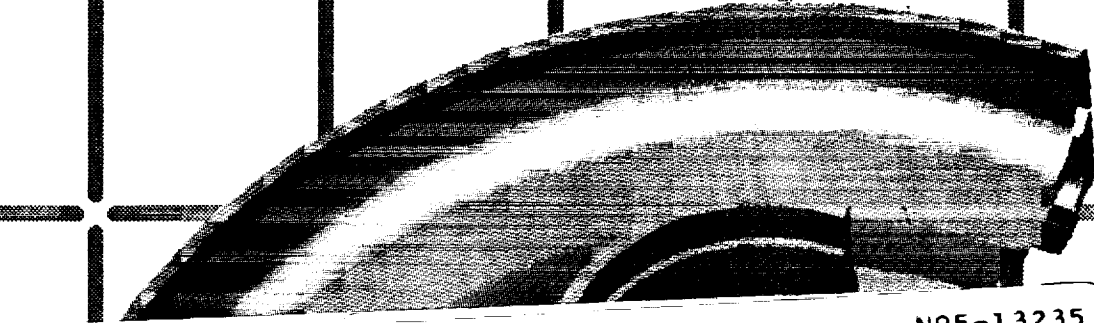
Structures Division

(NASA-TM-108081) ACTIVITIES OF THE
STRUCTURES DIVISION, LEWIS RESEARCH
CENTER Annual Report, 1990 (NASA.
Lewis Research Center) 71 p

N95-13235

Unclas

G3/39 0028248



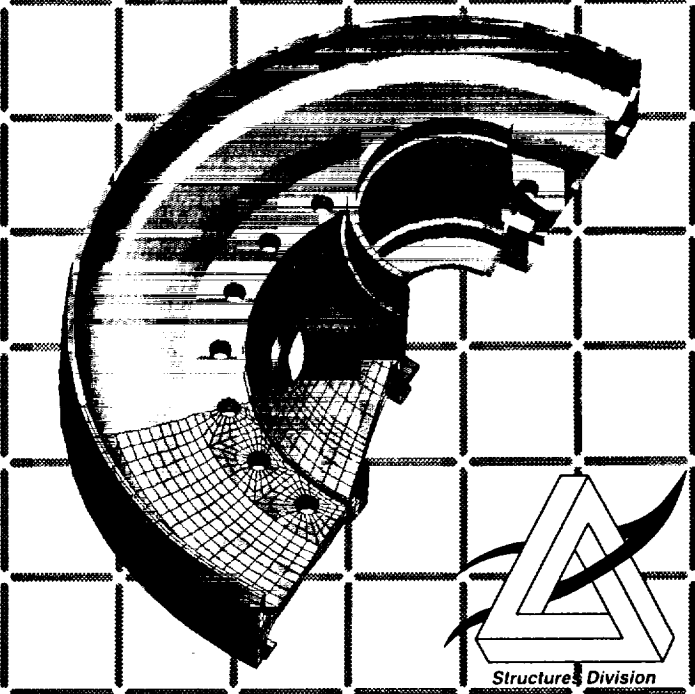
Structures Division

1990 ANNUAL REPORT

Structures Division

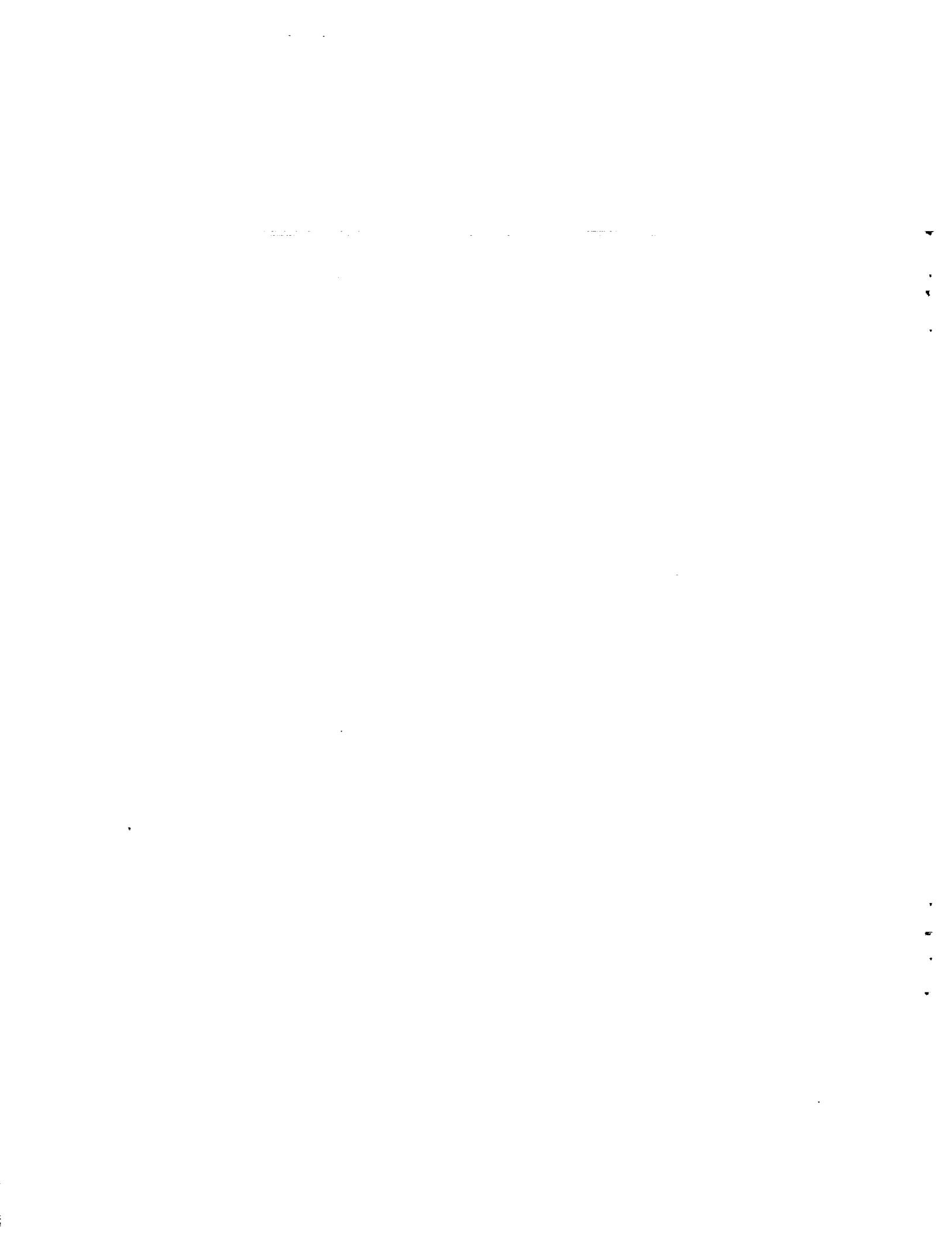


1990 ANNUAL REPORT
Structures Division



1990 ANNUAL REPORT
Structures Division

NASA
National Aeronautics and
Space Administration
Lewis Research Center
Cleveland, Ohio 44135



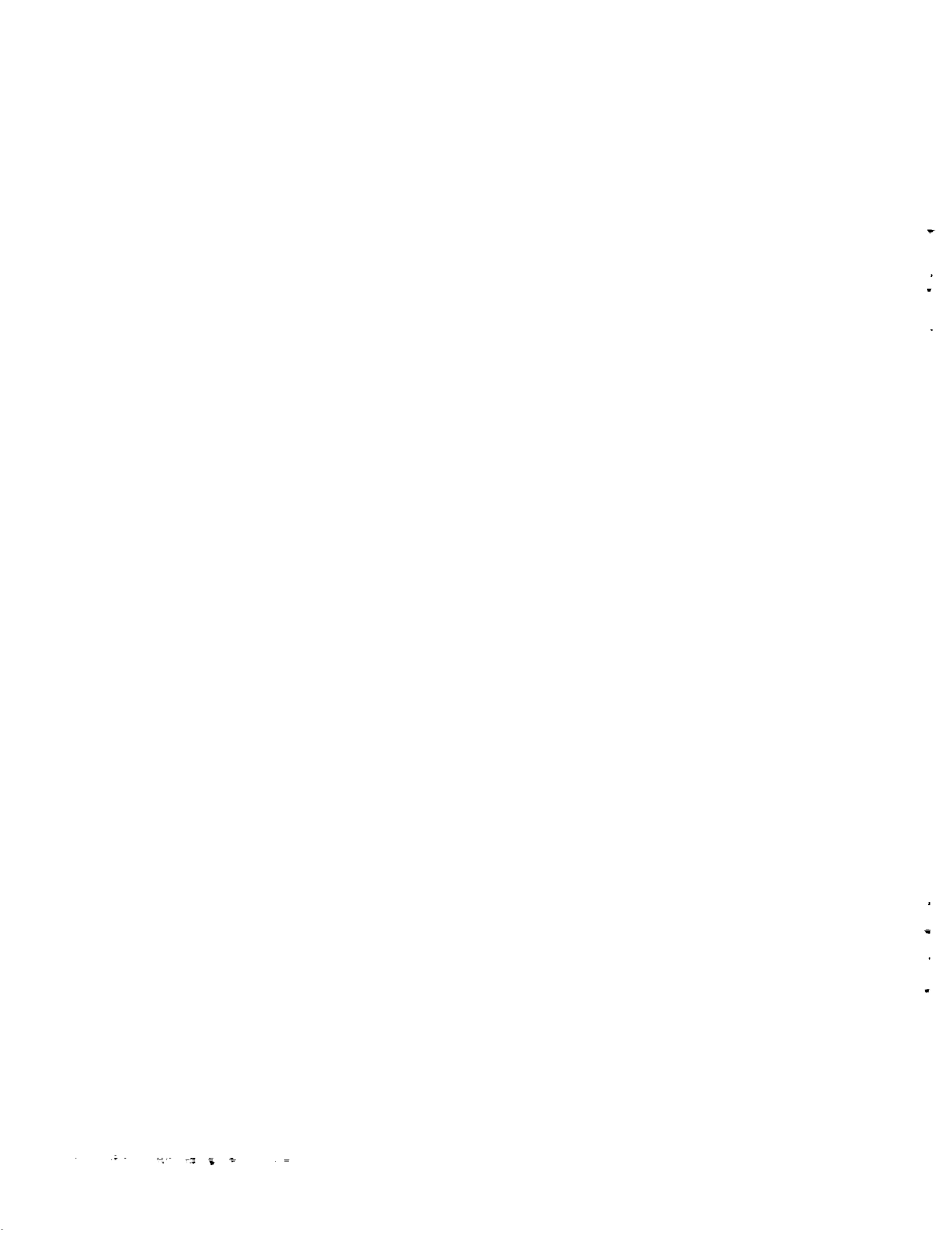
INTRODUCTION

The purpose of the NASA Lewis Research Center, Structures Division's 1990 Annual Report is to give a brief, but comprehensive, review of the technical accomplishments of the Division during the past calendar year. The report is organized topically to match the Center's Strategic Plan.

Over the years, the Structures Division has developed the technology base necessary for improving the future of aeronautical and space propulsion systems. In the future, propulsion systems will need to be lighter, to operate at higher temperatures and to be more reliable in order to achieve higher performance. Achieving these goals is complex and challenging. Our approach has been to work cooperatively with both industry and universities to develop the technology necessary for state-of-the-art advancement in aeronautical and space propulsion systems.

The Structures Division consists of four branches: Structural Mechanics, Fatigue and Fracture, Structural Dynamics, and Structural Integrity. This publication describes the work of the four branches by three topic areas of Research: Basic Discipline; Aeropropulsion; and Space Propulsion. Each topic area is further divided into Materials; Structural Mechanics; Life Prediction; Instruments, Controls, and Testing Techniques; and Mechanisms. The publication covers 78 separate topics with a bibliography containing 159 citations. We hope you will find the publication interesting as well as useful.

Larry Pinson
Chief, Structures Division



Contents

Basic Disciplines

Materials

High-Temperature Fatigue Behavior of an SiC/Ti-24Al-11Nb Composite	1
Thermomechanical Fatigue Behavior of SCS-6/Ti-15-3	1
Interfacial Failure Mechanisms in a Metal Matrix Composite	2
Effect of Fiber Layup on Fatigue of Metal Matrix Composite	3
Ultrasonic Measurement of Material Pore Fraction Modeled and Analyzed	4
Optimal Fabrication Process for Unidirectional Metal Matrix Composites: A Computational Simulation	5
Evaluation of Thermomechanical Damage in SiC/Titanium Composites	6
Computational Simulation of Damping in Composite Structures	6
Micromechanical Tailoring and Fabrication Optimized Concurrently for Metal Matrix Composites	7
Finite Element Computational Simulation of a Three-Dimensional Fiber Push-Out Test	8
Metal Matrix Composites Microfracture: Computational Simulation	9
Compliant Layer Effects on Metal Matrix Composite Behavior	10
Probabilistic Micro- and Macromechanics of Polymer Matrix Composites	10

Structural Mechanics

Developments Made in the Physics of Viscoplasticity	11
Multi-Objective Shape and Material Optimization of Composite Structures Including Damping	12
Computational Simulation of Metal Matrix Composites	13
NASTRAN Improved for Low-Velocity Impact Analysis	13
Neural Nets Capture Design Expertise	14
Transverse Crack Detection in Composites Improved	15
Computational Simulation of Structural Fracture in Composites	16
Probabilistic Composite Analysis	17
Application of Artificial Neural-Network Concepts to Structural Mechanics Problems	18
Simplified Design Procedures for Fiber-Composites Structural Components/Joints	18
Fiber Substructuring Captures Greater Local Detail of Composite Response	19
The Computational Simulation of the Global Fracture Toughness of Composite Structures	20
Reduction of Thermal-Residual Stress in Advanced Metallic Composites Via a Compensating/Compliant Layer Concept	20
Metal-Matrix Composite Analyzer Verification Status	21
Probabilistic Simulation of Uncertainties in Composite Uniaxial Strengths	22
Probabilistic Laminate Tailoring With Probabilistic Constraints and Loads	22
Fundamental Aspects of and Failure Modes in High-Temperature Composites	23
Progressive Damage and Fracture in Composites Under Dynamic Loading	24
Flutter Analysis of a Supersonic Cascade in Time Domain Using a Euler Solver	25
Multi-Input, Multi-Data (MIMD) Parallel Fortran Configuration File Generator	26
Dynamic Substructuring by the Boundary-Flexibility Vector Method of Component-Mode Synthesis	26
Active Vibration Control Test Results	27
Global Approach Identifies Structural Joint Properties	28
Structural Shape Optimization	28
Space Station Structures Analyzed by Probabilistic Structural Methods	29

Life Prediction

Multiaxial Fatigue-Life Modeling at High Temperatures	30
Nonlinear Cumulative Fatigue-Damage Model Validation	30
Crack Bridging in Metal Matrix Composites Modeled Analytically	31

High-Temperature Fatigue Modeled for a Tungsten/Copper Composite	32
Characterization of Failure Mechanisms of Fiber-Reinforced Ceramic Composites Using In-Situ Nondestructive Evaluation Monitoring (NDE) Techniques	33
New Method for Determining Probability of Failure Initiation in Rotating Structures	33
<i>Instruments, Controls and Testing Techniques</i>	
Inductively Heated Susceptors for Thermomechanical Testing of Ceramic Matrix Composites	34
Flat Tensile Specimen Design for Advanced Composites	35
Stable Poisson Loaded Specimen for Mode I Fracture Testing of Ceramic Materials	35
In-Situ X-Ray Monitoring of Damage Accumulation in SiC/RBSN Tensile Specimens	36
Ultrasonic Theory and Experimental Technique Developed to Nondestructively Evaluate Ceramic Composites	37
Improved Transverse Crack Detection in Composites	38
<i>Mechanisms</i>	
Contact Area Temperature Profile of an Engaging Sprag Clutch	39
Active Vibration Control (AVC) Test Results	40
Hybrid Magnetic Bearing Developed for Cryogenic Applications	40
Bearing Elastohydrodynamic Lubrication Formula Made Simple	41
Closed-Form Solution for Hoop Stress in a Ball-Race Contact	42
Space Mechanisms Technology Needs	43

Aeropropulsion

<i>Materials</i>	
Computed Tomography Guides Machining and Structural Modeling	44
<i>Structural Mechanics</i>	
Probabilistic Analysis of Blade Disks and the Effect of Mistuning	44
Structural Tailoring of Select Composite Structures	45
Demonstration of Capabilities of the High-Temperature Composites Analyzer Code	46
Three-Dimensional Full Potential Method for the Aeroelastic Modeling of Propfans	47
Application of an Efficient Hybrid Scheme for Aeroelastic Analysis of Advanced Propellers	47
Full Potential Solver Used for Time-Domain Flutter Analysis of Cascades	48
Reduced Order Models for Nonlinear Aerodynamics	49
Updated Flutter Analysis of Supersonic Fan Stator	49
Aeroelastic Analysis of Propfans Adapted for Concurrent Processing	50
Linearized Unsteady Aerodynamic Analysis for Application to Turbomachinery Flutter and Forced Response	50
Blade Aeroelastic Stability Analysis for Cruise Missile Counter Rotation Propfan Models	51
Counter Rotation Propfan Unstalled Flutter Experimentally Investigated	52
<i>Life Prediction</i>	
Fatigue-Life Prediction of Intermetallic Matrix Composites	53
Ultrasonic and Radiographic Evaluation of Advanced Aerospace Materials: Ceramic Composites	53
<i>Mechanisms</i>	
Actively Controlled Hydraulic Force Actuator	54

Space Propulsion

Materials

Fatigue Mean Stress Equations for Space Shuttle Main Engine Turbopump Blade Alloys56

Mechanisms

Cryogenic Dampers Verification56

Structural Mechanics

Viscoplastic Analysis Performed for Rocket-Thrust Chamber57

Aeroelastic Stability Characteristics of the Space Shuttle Main Engine High-Pressure

Oxidizer Turbopump Turbine Rotor58

Life Prediction

A Method for Predicting Cumulative Creep-Fatigue Damage Interaction59

Nondestructive Evaluation/Health Monitoring Opportunities for Space Propulsion Systems59

1990 Bibliography62

Section 1: Introduction to the Project

The purpose of this project is to analyze the impact of climate change on the global economy.

This report will discuss the various factors contributing to climate change and the resulting economic consequences.

The findings of this study will provide valuable insights into the long-term effects of climate change on the world's financial systems.

The data presented in this report is based on a comprehensive review of current research and economic models.

Basic Disciplines

Materials

High Temperature Fatigue Behavior of an SiC/Ti-24Al-11Nb Composite

The intermetallic composite SiC/Ti-24Al-11Nb has generated considerable interest for aerospace applications due to its high strength-to-density ratio. Recent investigations have examined various aspects of this composite such as fiber-matrix chemical interactions, fiber-matrix bond strength, tensile properties, and thermal cycling. For this composite system to be a viable option for aerospace applications, an understanding of its fatigue behavior and damage mechanisms is necessary. The current study, part of an ongoing NASA Lewis program, examined the fatigue response of unidirectional SiC/Ti-24Al-11Nb isothermally fatigued at 425 and 815 °C. The influence of testing method control on failure mechanisms and fatigue behavior was of major concern to this investigation. Tension-tension fatigue tests were conducted in both strain-control and load-control tests at 425 and 815 °C.

Fatigue life results for the SiC/Ti-24Al-11Nb composite at 425 and 815 °C were presented on a maximum strain basis. Fatigue lives of the strain- and load-controlled tests were compared on a maximum strain basis since, in the absence of cracking or debonding, the axial strain is identical for both fiber and matrix. Stresses in the two constituents, however, differ considerably. Fatigue behavior is characterized by distinctive regions (I, II, and III) as shown in Figure 1. Regions

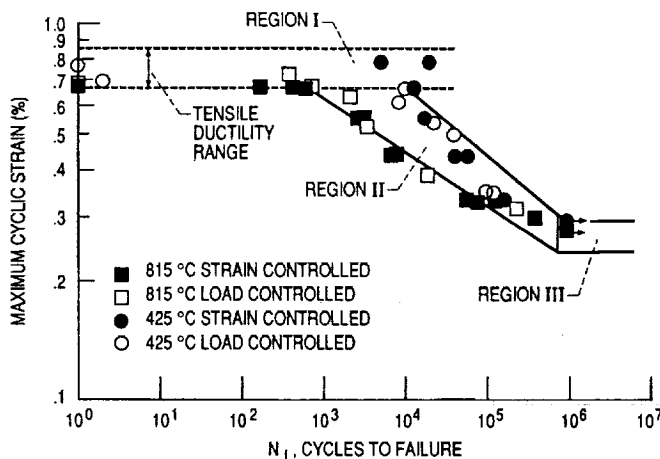


FIGURE 1. - FATIGUE BEHAVIOR BY REGION.

I and III did not vary with test temperature, while Region II was clearly temperature dependent. These three regions were similar in shape to those of the "fatigue life diagram," which was first introduced by Talreja for polymer-matrix composites. SiC/Ti-24Al-11Nb fatigue failure within Region I was catastrophic and appeared to be fiber dominated although other mechanisms may be operative. Fatigue behavior in Region II was progressive since the strain-controlled tests first exhibited gradual decreases in stress and then abrupt, simultaneous decreases in strength and modulus during the life of the composite. It was estimated that this abrupt drop in stress was associated with approximately eight fibers (9 percent) fracturing at one time. Since this region was temperature dependent and the fiber stresses were just below the lower portion of the fiber's ultimate tensile-strength scatterband, the dominating failure mechanism appeared to be a combination of initial matrix cracking followed by fiber fractures. In the high-cycle fatigue regime of Region III, an apparent endurance limit at 0.29 percent strain was observed. Since the applied strains in this region were low, and there was no apparent decrease in modulus, it is believed that the majority of damage resulted from matrix cracking.

The concept of the fatigue life diagram for PMC materials at room temperature has been extended to SiC/Ti-24Al-11Nb at elevated temperatures. The fatigue life diagram delineates three distinct regions of composite fatigue behavior. From the fatigue life diagram, it was observed that in Regions I and III Low Cycle Fatigue (LCF) lives did not vary with test temperature, while in Region II lives were temperature and maximum strain dependent. Distinctly different damage mechanisms operate in each region.

Lewis contacts: Paul A. Bartolotta,
(216) 433-3338; and Pamela K. Brindley,
(216) 433-5529

Thermomechanical Fatigue Behavior of SCS-6/Ti-15-3

Metal Matrix and Intermetallic Matrix Composites (MMC and IMC) are being developed for a number of high-temperature aerospace applications. The advantage of these composite materials is that they offer superior strength/density ratios compared to monolithic materials, particularly at elevated temperatures. This level of performance typically is achieved by using high-strength ceramic fibers and low-density matrix materials. One obvious problem with this approach is that it combines materials with widely differing physical properties. This mismatch raises questions regarding the performance of MMC and IMC materials under the complex thermomechanical

cal loading conditions typical of aerospace service. Investigating the thermomechanical behavior of this class of materials was viewed as being a logical first step in addressing this concern.

In general, cyclic lives of SCS-6/Ti-15-3 determined under thermomechanical fatigue (TMF) conditions were greatly reduced from those obtained under comparable isothermal conditions. Also, for the case of high-stress, in-phase loadings, lives were reduced by several orders of magnitude from those obtained under comparable isothermal and bithermal (nonisothermal) conditions. For example, the isothermal specimen experienced a fatigue life of approximately 4000 cycles at 538 °C. Specimens subjected to true in-phase loading conditions from 93 to 538 °C consistently failed upon the second loadup.

Fractography and metallography reveal crack initiation and propagation mechanisms different from those found under isothermal conditions. Oxidation patterns and scanning electron microscope imagery from out-of-phase specimens clearly suggest that crack initiation sites occurred almost exclusively at surface and near-surface, fiber-matrix interface locations. Metallographic sections reveal that the primary cyclic fatigue damage consists of transverse matrix cracking. Fractographs taken from in-phase specimens reveal extensive fiber pull-out and ductile matrix failure across the entire fracture surface. In fact, the in-phase fracture surfaces closely resemble those displayed by specimens subjected to tensile tests. In contrast to the out-of-phase tests, longitudinal and transverse sections clearly reveal extensive fiber damage in the absence of matrix cracking. Fiber cracking was found in both the transverse (more predominant) and longitudinal directions.

The results indicate the importance of understanding the temperature-time-stress history on the behavior of these materials and the limitations of using isothermal test results to model the fatigue behavior of these materials.

Lewis contact: Michael Castelli,
(216) 433-8464
Headquarters program office: OAST

Interfacial Failure Mechanisms in a Metal Matrix Composite

Metal matrix composites (MMC) are candidate materials for use in the next generation of both NASA and commercial aerospace vehicles. These materials typically consist of stiff, strong ceramic fibers embedded in a metal matrix. When these two composite constituents are combined during the processing, a chemical bond, better known as the interface, is created with properties different than those of its constituents. In the case of silicon-carbide, fiber-reinforced titanium metal matrix composites, the interface not only consists of the chemical bond but also of vapor-deposited carbon layers surrounding the silicon-carbide fibers.

It has been shown that the interface is the weakest link in these composites. However, details of the mechanisms by which the interface fails are unknown. Mechanical properties of these interfaces, required for proper analytical modeling of the composite, are very sketchy. This is due to the inability to isolate and test the interface.

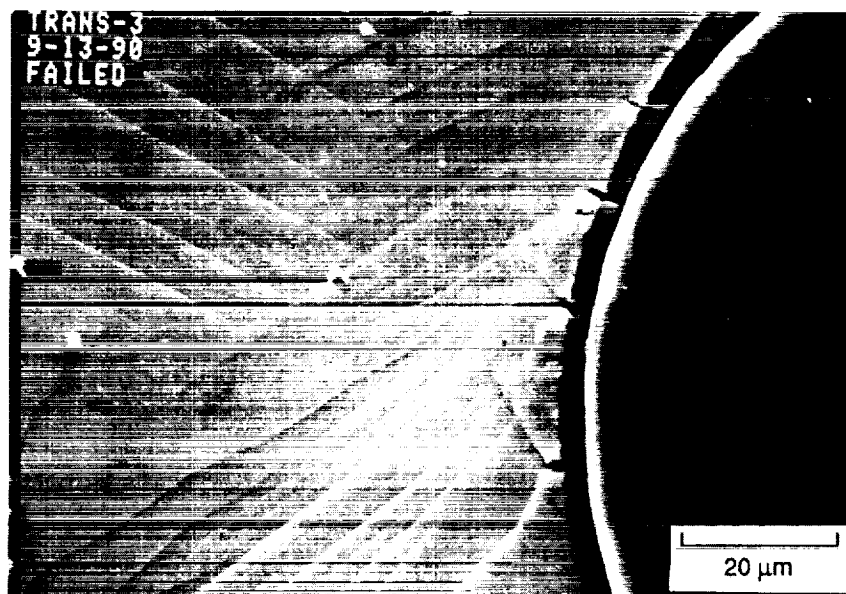


FIGURE 2. - TYPICAL MICROGRAPH OBTAINED DURING MMC TESTING INSIDE THE SCANNING ELECTRON MICROSCOPE.

A testing program was conducted to determine reasons for the composite interface failure. The study also determined failure strength of the interface and residual stresses present at the interface due to the mismatched coefficients of thermal expansion (CTE) of fiber and the matrix.

Testing, as shown in Figure 2, was performed using a fatigue loading stage-mounted inside a scanning electron microscope. This unique facility, designed at NASA Lewis, allows high magnification viewing of the specimens during a loading cycle.

Results show that there are a number of different active failure mechanisms of the interface which are a function of the fiber location and spacing. The most generally observed mechanism, shown in the figure, consisted of the failure of one or more of the interface layers, followed by debonding of the interface from the fiber, and plastic deforming which spread into the matrix from the crack tip. Observations of a large number of interface failures resulted in obtaining a statistical distribution of the failure strength of the interface. Also, a statistical distribution of the residual stresses created by CTE mismatch was obtained by repeated loading of the specimen and determining the stresses under which debonding of the fiber took place.

The results of this study will facilitate a better durability assessment of MMC components as well as an improved design of the next generation of composite materials.

Lewis contact: Jack Telesman,
(216) 433-3310,
Headquarters program office: OAST

Effect of Fiber Layup on Fatigue of a Metal Matrix Composite

Metal matrix composites (MMC) are currently being developed for high temperature, structural applications in engines and hypersonic flight vehicles. Both applications require stiff, light-weight materials capable of carrying significant thermal and mechanical loads. Because of the severe environment, these materials will be subjected to significant cyclic straining. Accurate fatigue life prediction schemes need to be developed for these materials. Before this can be accomplished, a better understanding of the fatigue response is required. This study describes the fatigue behavior of various SiC/Ti-15V-3Cr-3Sn-3Al laminates and presents preliminary information on the damage mechanisms which occur during the fatigue process.

Composite specimens were tested in tension-tension, load-controlled fatigue. The ply layups examined were $[0]_8$, $[90]_8$, $[0/90]_{2s}$, $[90/0]_{2s}$, and $[\pm 45]_{2s}$. As shown in Figure 3, for a given stress range, the $[0]_8$ specimens have the longest life, followed by the $[0/90]_{2s}$, the $[90/0]_{2s}$, the $[\pm 45]_{2s}$, and the $[90]_8$ orientations, respectively. Environmental effect was shown to be significant by demonstrating that the vacuum-tested specimens exhibited lives by at least a factor of four longer than their air counterparts. This indicates the embrittling effect that the environment has on this material, even at low temperatures where a thick, surface-oxide scale does not form.

Metallographic observations showed that multiple fatigue cracks initiated at the surfaces of the specimens as well as at fiber/matrix interfaces. In general, damage involved cracking of both matrix and fibers in addition to interfacial debonding. High temperature testing in air resulted in a thick oxide layer

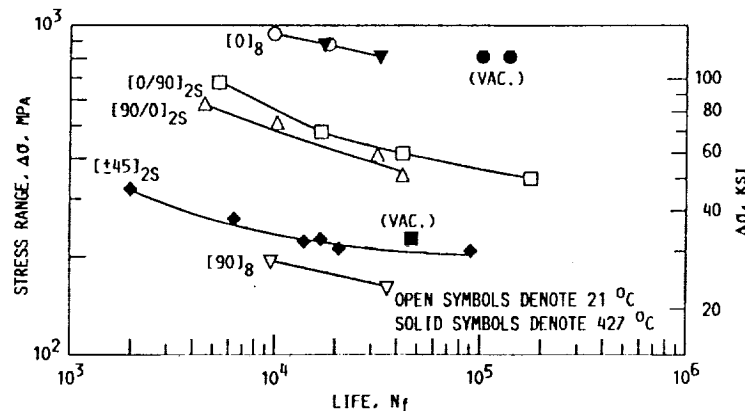


FIGURE 3. - FATIGUE LIFE CURVES FOR VARIOUS SiC/Ti-15-3 LAMINATES.

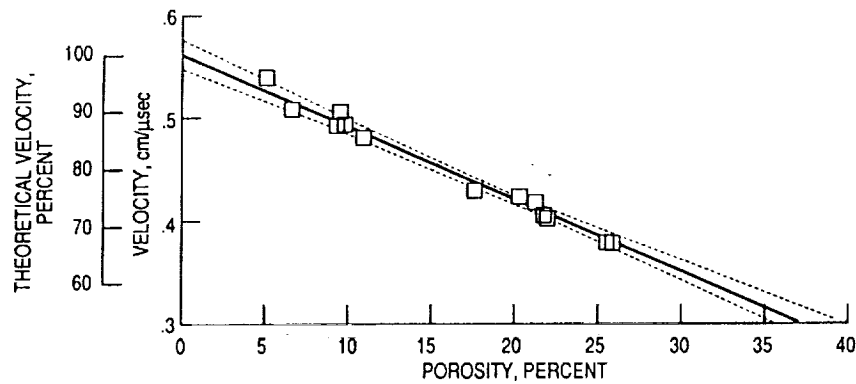


FIGURE 4. -LONGITUDINAL VELOCITY VERSUS PERCENT POROSITY FOR $YBa_2Cu_3O_{7-x}$.

at the fiber/matrix interfaces which was absent when the specimens were tested in vacuum.

These preliminary fatigue tests indicate that fiber layup is important in defining the fatigue behavior. Alignment of the laminate with the applied loads is critical. For example, a $[0]_8$ layup will provide good fatigue resistance only if the applied load is uniaxial and parallel to the fibers. Any off-axis loading will reduce the fatigue life until, in the limit, the life is reduced to the $[90]_8$ fatigue life. Additionally, the fatigue life will be dependent upon damage mechanisms, which could involve constituent cracking, interface debonding, and oxidation. Accurate life predictions can be made only with a thorough understanding of these mechanisms.

Lewis contact: Dr. Bradley A. Lerch,
(216) 433-5522
Headquarters program office:: OAST

Ultrasonic Measurement of Material Pore Fraction Modeled and Analyzed

The physical behavior of many technologically important polycrystalline materials can be affected by the volume fraction of "holes," or pores, present. For example, pore fraction has been shown to affect (1) the strength, toughness, and modulus of structural and refractory materials, such as steel, tungsten, SiC, Si_3N_4 , and Al_2O_3 ; (2) the strength of nuclear fuel materials such as UO_2 ; (3) the thermal shock behavior and strength of porcelain-based ceramics; (4) the dielectric and elastic properties of piezoelectric materials, such as PZT; and (5) the critical current density, diamagnetic response, and modulus of superconducting ceramics such as $YBa_2Cu_3O_{7-x}$.

Pore fraction variations on the order of 1 percent in $YBa_2Cu_3O_{7-x}$ samples can result in an order-of-magnitude variation in critical current density. Where physical properties are directly dependent on the pore fraction, the measurement of pore fraction becomes important in the quality assurance process for the material. Although various methods are available for measuring the pore fraction of polycrystalline materials, some are limited to certain geometries and others are destructive. The ultrasonic velocity method of measuring pore fraction in polycrystalline materials may be useful and convenient in certain laboratory and industrial situations. NASA Lewis has modeled and analyzed the use of ultrasonic velocity as a measure of pore fraction in polycrystalline materials.

Ultrasonic velocity is a relatively simple measurement that requires the material specimen to have one pair of flat and parallel sides. The advantages of this method are that it is nondestructive and that measurements can be made on different regions of a component to map porosity variation.

The semi-empirical model developed, as shown in Figure 4, showed a linear relationship between ultrasonic velocity and pore fraction in polycrystalline materials. Linear regression correlation coefficients with magnitudes greater than 0.95 (indicating a good correlation) were obtained in 31 out of 42 scatter plots of velocity versus pore fraction. Predicted intercepts (theoretical velocities) and slopes (ratio of change in velocity to change in pore fraction) differed from material to material as expected, since each material has different elastic constants and theoretical densities. The value of theoretical velocity predicted from regression and those calculated from elastic properties agreed within approximately 17 percent in 16 out of 16 cases and within approximately 6 percent in 11 out of 16 cases. Batch-to-batch, sample-to-sample, and within-sample pore-fraction variations for a material can be estimated if the velocity-pore fraction relation is known with reasonable confidence for that material.

Bibliography

Roth, D.J., et al.: Review and Statistical Analysis of the Ultrasonic Velocity Method for Estimating the Porosity Fraction in Polycrystalline Materials. NASA TM-102501, 1990.

Lewis contact: Don J. Roth,
(216) 433-6017
Headquarters program office: OAET

Optimal Fabrication Process for Unidirectional Metal Matrix Composites: A Computational Simulation

A problem with most metal matrix composites (MMC) is the high residual thermal microstresses developed during their fabrication. These high residual stresses are attributed to the high-temperature differentials involved in the cooling phase of the fabrication process and the mismatch of thermal expansion coefficients between fibers and matrix. The objective of the in-house research effort as shown in Figure 5 was development of methodology to tailor the temperature and consolidation pressure histories during fabrication for minimal residual stresses, keeping the integrity of the composite ensured.

The thermomechanical response of MMC during the fabrication process is simulated with nonlinear micromechanics including, among other factors, the effects of temperature, the

nonlinearity of the constituent materials, and the gradual buildup of residual microstresses. For the optimal processing, a nonlinear programming problem was formulated and solved with the modified feasible-directions, mathematical-programming method.

The method was evaluated on an ultra-high modulus graphite (P100)/copper composite. Results indicate that for this composite significantly higher consolidation pressures are required than in the current process. The gradual pressure increase was combined with simultaneous reductions in consolidation temperature, indicating that the matrix becomes highly nonlinear and undergoes "plastic" deformation resulting in reduced residual matrix microstress. The predicted optimal process for graphite/copper resulted in an estimated reduction of the maximum residual microstress by 21 percent. Both methodology and obtained results are expected to have an impact on programs related to high-temperature structural applications.

Bibliography

Saravanos, D.A.; Morel, M.R.; and Murthy, P.L.N.: Optimal Fabrication Processes for Advanced Metal-Matrix Composites: A Computational Simulation, Proceedings, 35th International SAMPE Symposium and Exposition. Anaheim, CA, Apr. 2-5, 1990; NASA TM-102559, 1990.

Lewis contact: Dimitris A. Saravanos,
(216) 433-8466,
Headquarters program office: OAET

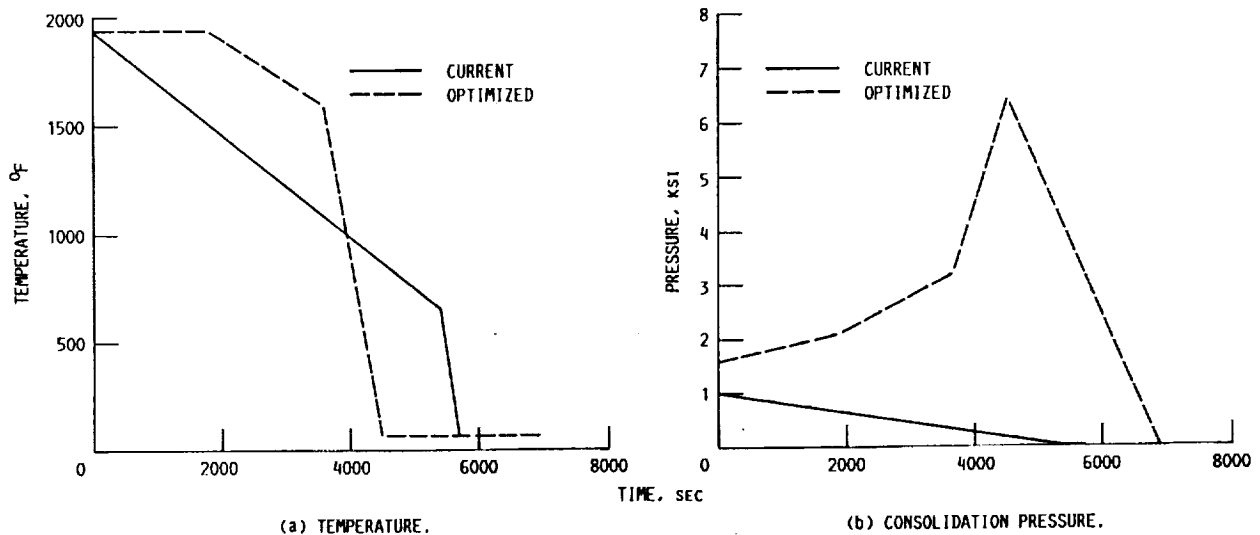


FIGURE 5. - CURRENT AND OPTIMUM CONSOLIDATION TEMPERATURE AND PRESSURE HISTORIES. P100/COPPER.

Evaluation of Thermomechanical Damage in SiC/Titanium Composites

The mechanical behavior of a composite material depends on the properties of the fiber and matrix constituents. Inhomogeneities, which occur during the fabrication process as a result of the addition of fibers and thermal loadings, in-situ matrix properties of SiC/Ti-15-3 composites can vary significantly, as shown in Figure 6, from those of the monolithic matrix. Matrix stiffness, as well as the integrity of the fiber/matrix bond, will also change as the composite material deforms under applied mechanical and thermal loads.

In this study, an indirect measurement of the effective in-situ matrix modulus is obtained using a combined experimental/analytical approach. Resonant frequencies of individual composite test specimens are obtained from vibration testing. Finite element modal analysis is then used to extract the matrix properties from the modal test data. This technique is applied to each test specimen in its original, as-fabricated condition. It is also applied after a heat treatment, and thermal or mechanical loading. The results show how the matrix modulus changes with the different applied loads.

This is an ongoing, in-house research effort, initiated under NASA's High Temperature Engine Materials Technology (HITEMP) program. The experimental/analytical approach described above is currently used by HITEMP researchers as a nondestructive technique for tracking damage initiation and development in metal matrix composites.

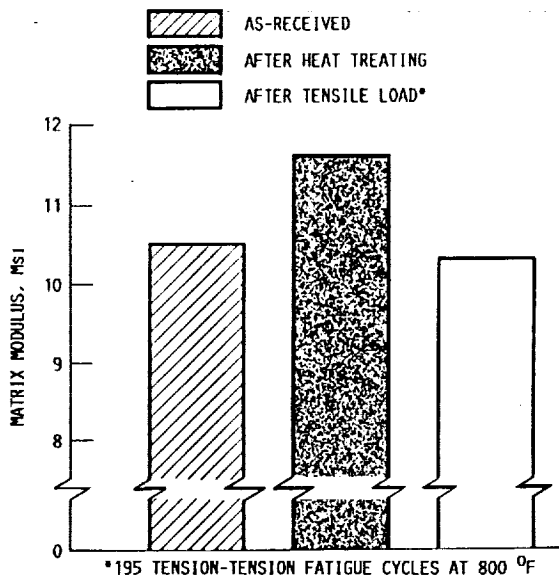


FIGURE 6. - CHANGE IN CALCULATED MATRIX MODULUS FOR (± 45) SPECIMEN DUE TO HEAT TREATMENT AND FATIGUE LOAD.

Bibliography

Grady, J.E.; and Lerch, B.A.: Evaluation of Thermal and Mechanical Loading Effects on the Structural Behavior of a SiC/Titanium Composite. NASA TM-102536, 1990.

Grady, J.E.; and Lerch, B.A.: Evaluation of Thermomechanical Damage in SiC/Titanium Composites, AIAA Journal, May 1991.

Lewis contacts: Dr. Joseph E. Grady,
(216)433-6728
Headquarters program office: OAET

Computational Simulation of Damping in Composite Structures

The significance of passive damping to vibration control, sound control, dynamic stability, fatigue endurance, and overall dynamic performance of structures is broadly recognized. Present light-weight, high-performance requirements imposed on many structural applications restrict the use of nonstructural damping sources. As a result, the use of structural materials, such as polymer-matrix composites, which combine significant damping with other favorable mechanical properties, appears very attractive.

In order to realize significant structural benefits from the damping of composite materials, in-house research was conducted at NASA Lewis. It involved the development of integrated computational mechanics which enable the prediction of damping in plate/shell type thin composite structures. The modal damping of each vibration mode is calculated using a finite element discretization scheme. See Figure 7. A specialty plate finite element was developed for this purpose. All damping contributions due to extensional, flexural and coupling deformations are included. In this manner, the modal damping of thin composite structures, with arbitrary geometry and lamination—including composite structures with geometric or material coupling—is simulated. In addition, the method incorporates micromechanics and laminate theories for composite damping, and can model the effects of constituent material parameters, temperature, moisture, general laminate configurations, and structural geometry. The method was encoded into Structural Tailoring of Engine Blades, STAEBL an in-house structural-analysis research computer code called.

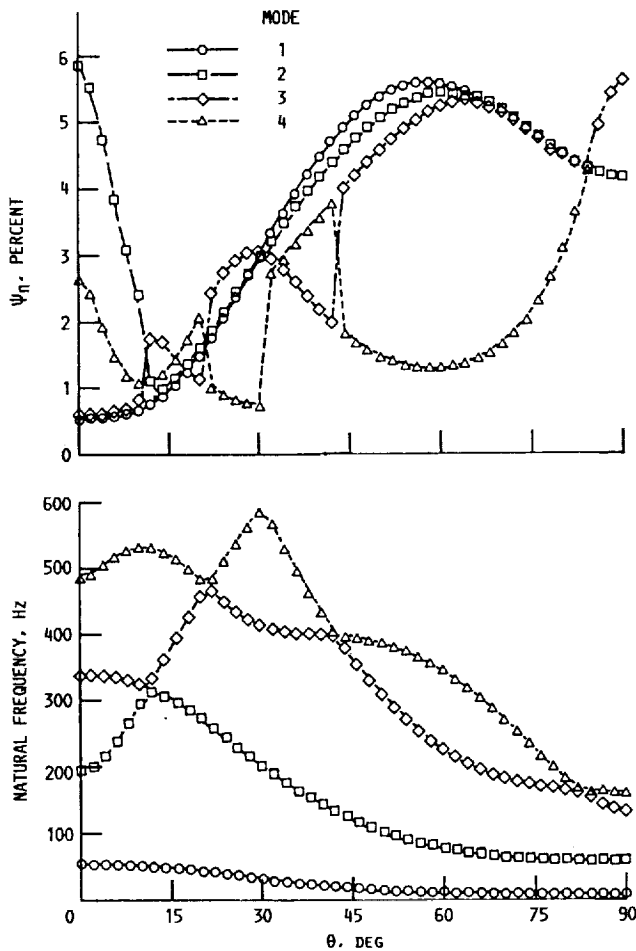


FIGURE 7. - PREDICTED MODAL DAMPING AND NATURAL FREQUENCIES OF (+ θ /- θ) 5S CANTILEVER GRAPHITE/EPOXY BEAM.

Correlations with limited available experimental data on composite beams, illustrate the accuracy of the method. The modal specific damping capacity (SDC) of Gr/Epoxy composite beams, composite plates, and composite shell panels were simulated. Fiber orientation angles and mode order were found to have a strong effect on modal damping. Additional results illustrated that structural modal damping significantly depends on structural geometry and temperature. The effect of fiber-volume ratio on modal SDC was less important. It was further concluded that the aspect ratio and curvature of specimens may have a detrimental effect on damping measurement.

Overall, application examples demonstrated the effectiveness and versatility of the current method. The developed methodology will have a definite effect on ongoing and future programs involving dynamic analysis and design of propulsion components and space structures.

Bibliography

Saravanos, D.A.; and Chamis, C.C.: Computational Simulation of Damping in Composite Structures. *J. of Reinf. Plastics and Composites*, to appear. (Also, NASA TM-102567).

Lewis contacts: Dimitris A. Saravanos,
(216) 433-8466
Headquarters program office: OAET

Micromechanical Tailoring and Fabrication Optimized Concurrently for Metal Matrix Composites

The development of residual stresses in metal matrix composites (MMC) during their fabrication has adverse effects on critical properties, such as strength and thermomechanical fatigue life. Hence, the residual stresses limit the applications of MMC as high-temperature materials and offset many of their other advantages. Although the residual stresses cannot be eliminated, their control or reduction seems possible, either by altering fabrication parameters or incorporating a fiber/matrix-interphase material. In order to obtain full benefits from this approach, a method has been devised at NASA Lewis that optimizes concurrently the fabrication of MMC and the thermomechanical properties of a fiber/matrix interphase. The objectives are to control the development of residual microstresses and avoid failures in the fibers, the matrix, and the interphase throughout the process.

The thermomechanical response of the composite during fabrication is simulated by using nonlinear micromechanics contained in the Metal Matrix Composite Analyzer (MET-CAN) in-house computer code. The theory incorporates, among other factors, three material phases (fiber, matrix, and interphase), temperature and inelastic effects on the constituents, and the residual stress buildup. The optimization is numerically accomplished by nonlinear mathematical programming using the feasible directions method. The method is encoded into another in-house code called Metal Matrix Laminate Tailoring (MMLT).

The method, as shown in Figure 8, was evaluated by using it to minimize the matrix residual stresses of an ultra-high-modulus graphite (P100)/copper composite. The following two cases were investigated: (1) the individual optimization

Lewis contact: Dimitris A. Saravanos,
 (216) 433-8466; and Christos Ci Chamis,
 (216) 433-8466.
 Headquarters program office:

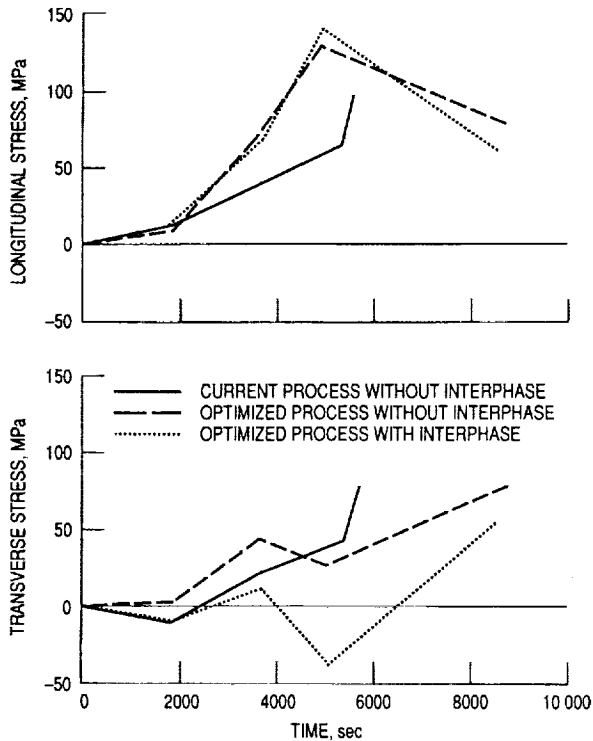


FIGURE 8. - PREDICTED RESIDUAL STRESS DEVELOPMENT FOR P100/COPPER.

of the fabrication process; and (2) the concurrent optimization of the fabrication process and the interphase properties. The resultant optimal fabrication processes with and without interphase tailoring indicated similar trends. The most significant trend was the gradual, but significant increase in consolidation pressure as the temperature decreased, which contributed to the reduction of the residual matrix microstresses. All residual thermal strains were forced to develop when the matrix and the interphase were highly nonlinear, such that high thermal strains induced low thermal stresses.

The importance of a compatible tailored interphase was also demonstrated. The concurrent fabrication-interphase tailoring reduced the longitudinal and transverse matrix stresses by 41 and 24 percent, respectively; fabrication optimization alone reduced these stresses by 21 and 0 percent only.

It is expected that both the obtained results and the computer code, still under development, will have a definite impact on the development of high-temperature composites.

Bibliography

Morel, M.R.; Saravanos, D.A.; and Chamis, C.C.: Micromechanical and Fabrication Processes Optimization for Advanced Metal-Matrix Composites. Proceedings, Structural Engineering and Optimization, J. Zarka and O. Ohtmer, eds., 1990, pp. 245-254. (Also NASA TM-103670).

Finite Element Computational Simulation of a Three-Dimensional Fiber Push-Out Test

Bonding phenomena between fiber and the matrix (interfacial) are generally regarded as playing an important role in the mechanical behavior of composite materials in general, and ceramic matrix composites in particular. Bond degradation is often a critical factor in determining the ultimate strength of a composite material, as well as its fatigue resistance, impact resistance, and other important properties. The strength of the bonding between fiber and the matrix plays a major role in the ability of the composite to bridge cracks or deflect cracks along the interface, contributing to the composite fracture toughness.

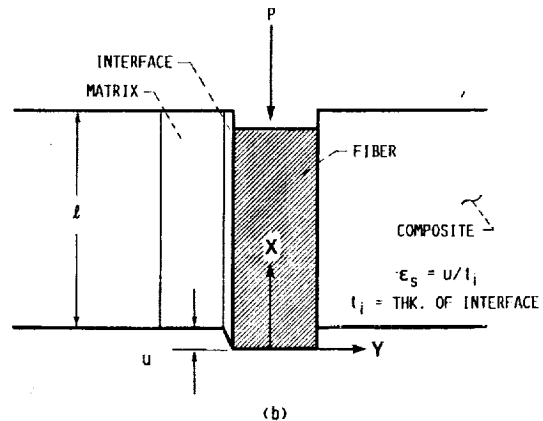
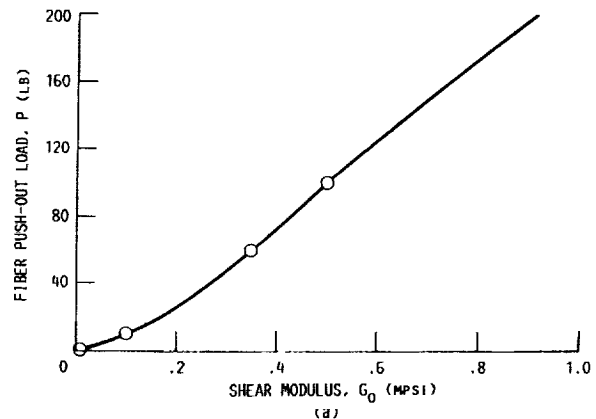


FIGURE 9. - VARIATION OF FIBER PUSH-OUT LOAD VERSUS SHEAR MODULUS OF INTERFACE IS SHOWN IN (a); (b) IS A SCHEMATIC REPRESENTATION OF FIBER PUSH-THROUGH TECHNIQUE.

The three-dimensional finite element model used in this procedure, as shown in Figure 9 parts (a) and (b), consists of a group of nine fibers, all unidirectional, in three- by-three unit cells ("nine-cell model"). The composite system consists of a 0.35 fiber-volume ratio SiC/Ti15 metal matrix composite. The concepts adopted in the computational simulation arise from the physics of the fiber push-through process. As the load is applied on the fiber, interfacial debonding initiates and progresses until the full fiber length is debonded and the fiber slides out.

This procedure, which was developed in-house, can be used to predict fiber push-through load at any temperature. Average interfacial shear strength and its component two parts—one due to frictional stresses and the other due to chemical adhesion, mechanical interlocking, etc.—can be obtained. Step-by-step procedures are described to perform the computational simulation, establish bounds on fiber push-out load, and to interpret the interfacial bond quality.

Bibliography

Fiber Push-Out Test: A Three-Dimensional Finite Element Computational Simulation. NASA TM-102565, 1990.

Lewis contact: C.C. Chamis,
(216) 433-3252
Headquarters program office: OAET

Metal Matrix Composites Microfracture: Computational Simulation

Microfracture (fiber/matrix fracture or local interface debonding) in metal matrix composites is critical to assess fatigue resistance, durability, impact resistance, and other important properties. In a recent in-house study, 3-D finite element simulation was used to evaluate effects of partial debonding on ply composite properties. It was shown that, in general, single fiber fracture and/or debonding have little effect on most of the ply-level properties. The present research, as shown in Figure 10, is an extension of that work with emphasis on microfracture, microfracture propagation, and the extent of stress redistribution in the surrounding fiber/matrix due to brittle fracture of fiber/matrix or interface debonding. A computational simulation procedure has been developed, based on global strain-energy release rates, to predict fracture toughness, fracture propagation direction, hierarchy of failure modes, and stress redistribution due to longitudinal, transverse, shear, and bending loads.

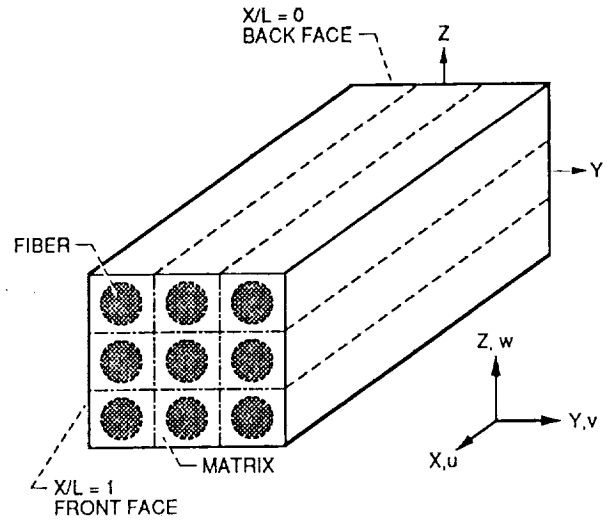


FIGURE 10. - SCHEMATIC DIAGRAM OF NINE-CELL MODEL.

The finite element model used in this procedure consists of nine-cell models. The procedure is illustrated by using a 0.35 fiber-volume ratio SiC/Ti15 metal matrix composite. Load and boundary conditions are applied to the model through enforced displacements. Fracture is simulated by placing duplicate node points on either side of the microfracture site. These duplicate nodal or grid points have the same geometrical location, but no connectivity exists between them, which in effect produces a local crack of zero width. For a given microfracture configuration, fixed boundary conditions are applied to the model in a given direction. Resulting nodal forces corresponding to those applied displacements are found by the finite element analysis. Comparison of resulting nodal forces is made for reduction in global stiffness. Corresponding strain-energy release rates are computed for perturbed microfracture configurations. Step-by-step procedures are outlined to evaluate composite microfracture and to establish hierarchy of fracture modes for a given composite system.

Typical results indicate that if the composite is subjected to longitudinal (along the fiber) loading, interface debonding does not initiate by itself. It instantaneously follows fiber or matrix fracture. Similarly, if the composite is subjected to transverse loading, debonding along the interface is the only likely event for the fracture propagation.

Bibliography

Mital, S.K.; Caruso, J.J.; and Chamis, C.C.: Metal Matrix Composites Microfracture: Computational Simulation. NASA TM-103153, 1990.

Lewis contact: C.C. Chamis,
(216) 433-3252
Headquarters program office: OAET

Compliant Layer Effects on Metal Matrix Composite Behavior

Metal matrix composites (MMCs) are prime candidates for high-temperature applications. They present a unique challenge to today's researchers. The large operating temperature (range, greater than 2000 °F) and the mismatch between the thermal expansion coefficients (CTE) of the fiber and the matrix pose great difficulties in fabrication and low-thermal cycling resistance. Both of these increase the matrix stress to critical proportions and often lead to failure. Solutions to this problem have been proposed (such as, matching CTE for fiber and matrix) with little success. One suggestion is to use a compliant layer (CL) as a buffer between the fiber and the matrix. The goal of this CL is to reduce the matrix stress without degrading the fiber, the matrix, or the composite. Finding a suitable material, however, may prove a challenge.

In an attempt to find such CL materials, two computational simulation approaches, as Figure 11 shows, were used in-house in order to evaluate CL in MMC systems for high temperature applications under thermal loads. The first is a three-dimensional linear finite element method with temperature dependent material behavior. The other is nonlinear micro-mechanics. Compliant layers are evaluated with two common but very different metal matrices reinforced with SiC (SCS 6) fibers. Computation simulation results show that an effective compliant layer for the SCS 6 (SiC)/Ti-24Al-11Nb (Ti₃Al+Nb) and SCS 6 (SiC)/Ti-15V-3Cr-3Sn-3Al (Ti-15-3) composite systems should have a

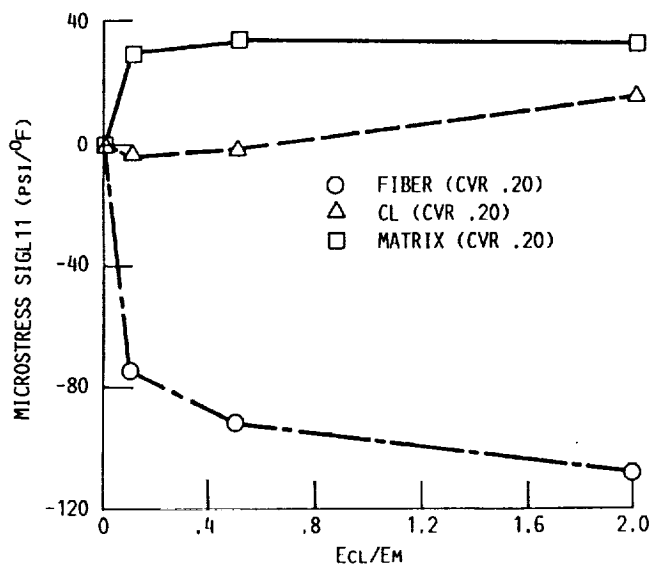


FIGURE 11. - ROOM-TEMPERATURE LONGITUDINAL CONSTITUENT MICROSTRESS (SIGL11) FOR A 20-PERCENT FVR SCS6/TI3Al AT L/D = 2.21. CL CTE = 4.67 PPM; FIBER CTE = 2.7 PPM; MATRIX CTE = 6.5 PPM.

modulus 15 percent that of the matrix, and a compliant layer coefficient of thermal expansion roughly equal to that of the composite system without the CL. Matrix stress in the longitudinal and the transverse tangent (hoop) directions is tensile for the Ti₃Al+Nb and Ti-15-3 composite systems upon cool down from fabrication. Fiber longitudinal stress is compressive from fabrication cool down. Addition of a recommended compliant layer will reduce the composite modulus.

Bibliography

Caruso, J.J.; Chamis, C.C.; and Brown, H.C.: Parametric Studies to Determine the Effect of Compliant Layers on Metal Matrix Composite Systems. NASA TM-102465, 1990.

Lewis contact: C.C. Chamis
(216) 433-3252
Headquarters program office: OAET

Probabilistic Micro- and Macromechanics of Polymer Matrix Composites

An ongoing in-house research activity involves development of probabilistic structural analysis methods (PSAM). Current effort utilizes the Numerical Evaluation of Stochastic Structures Under Stress (NESSUS) computer code which was developed under contract pursuant to the PSAM activity. The NESSUS methodology formally describes and quantifies observed scatter in the behavior of advanced polymer matrix composites.

The properties of polymer matrix composites display considerable scatter because of variation inherent in the properties of constituent materials. To quantify uncertainties in properties of composites, one has to take into account variations in the properties starting from the constituent (fiber and matrix) level and integrating progressively to arrive at the global or composite-level properties. Typically, these uncertainties may occur at the constituent level (fiber and matrix properties), at the ply level (fiber-volume ratio, void-volume ratio, etc.) and the composite level (ply angle and layup). To illustrate the approach, a probabilistic evaluation of an eight-ply graphite epoxy, quasi-isotropic laminate was completed.

Two computational simulation approaches, as shown in Figure 12, were used to capture the stochastic behavior of the composite laminate. The first approach was to use a Monte Carlo simulation technique. The second approach was to use

Structural Mechanics

Developments Made in the Physics of Viscoplasticity

The theory of viscoplasticity is used to describe the deformation behavior of crystalline solids (e.g., metals) brought about by thermal and mechanical loadings. This theory had its origin in the early 1900. Over the last two decades, the theory has undergone rapid development—in part because of the availability of computers to solve the complex system of differential equations that define viscoplasticity. For the most part, this development has been phenomenological. At NASA Lewis, a concentrated effort has been under way for nearly 10 years to replace some of this phenomenology with physics in the hope of simplifying the model and improving its predictive capability. Much has been accomplished toward this goal.

An important aspect of viscoplastic physics is the development of a thermodynamically admissible viscoplastic theory. NASA Lewis and the Office National D'Etudes et de Recherches Aérospatiales (ONERA) in Châtillon, France, formed a

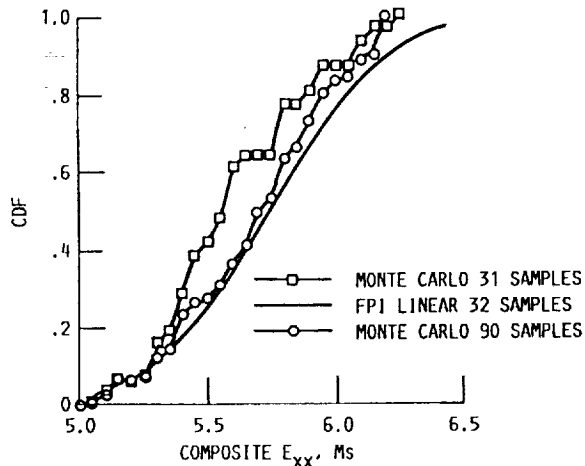


FIGURE 12. - CUMULATIVE DISTRIBUTION FUNCTIONS (CDF'S) FOR COMPOSITE MODULUS E_{xx} SIMULATED WITH MONTE CARLO AND FPI TECHNIQUES. GRAPHITE/EPOXY QUASI-ISOTROPIC LAMINATE [0/45/90/-45]_s.

the fast probability integration (FPI) technique. For the micromechanics and macromechanics of the composite, the Integrated Composite Analyzer (ICAN) was used. The input variables for which uncertainties were accounted for included fiber and matrix properties, fiber misalignment using ply substructuring, fiber-volume ratio, void-volume ratio, ply thickness and ply layup angle. The output was obtained in terms of the cumulative distribution functions (CDF's) for select laminate properties using Monte Carlo simulation as well as FPI techniques. It was demonstrated that the use of an FPI can greatly reduce the computations needed to generate composite CDF's. Furthermore, FPI provides valuable information regarding the sensitivities of composite properties to fiber and matrix properties, fiber-volume ratio, and void-volume ratio. This investigation demonstrated that an integrated program combining ICAN and FPI is feasible. Such an integrated approach offers great potential for a computationally efficient, probabilistic composite mechanics methodology.

Bibliography

Mase, G.T.; Murthy, P.L.N.; and Chamis, C.C.: Probabilistic Micromechanics and Macromechanics of Polymer Matrix Composites. NASA TM-103699, 1990.

Lewis contact: P.L.N. Murthy,
(216) 433-3332
Headquarters program office: OAET

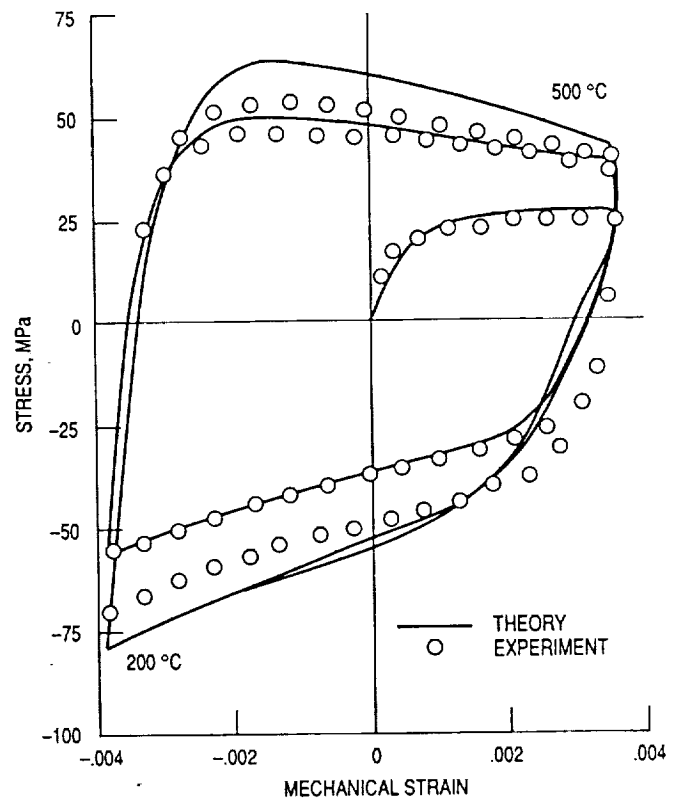


FIGURE 13. - VISCOPLASTIC CAPABILITY, THEORY VERSUS EXPERIMENT.

cooperative agreement involving exchanges of personnel for the purpose of addressing this and other issues. Four cooperative research projects have been completed as a consequence, with the result being an enhanced understanding of viscoplastic thermodynamics.

Another important area of viscoplastic research is defining how the internal state variables of the theory evolve. Our concentration here has been in simplifying these equations from the point of view of material characterization. An approach has been put forth, as shown in Figure 13, that enables the viscoplastic theory to analytically reduce to classical creep theory in the steady-state limit. This has simplified the theory and furthered its physical foundation.

A final area of research that has been undertaken at NASA Lewis for the advancement of viscoplasticity is the development of new and improved algorithms for the numerical integration of the viscoplastic constitutive equations. This is of particular importance in nonlinear finite element analyses, where the bulk of the supercomputer's computation time is taken up by numerical integration of the constitutive equations. Preliminary studies indicate computational improvements by as much as a factor of 30 over conventional methods, and this is accomplished with an improvement in accuracy. These results have important ramifications for the magnitude and complexity of structural analyses that can be undertaken in support of NASA missions.

Lewis contact: Dr. Alan D. Freed,
(216) 433-3262
Headquarters program office: OAET

Multi-Objective Shape and Material Optimization of Composite Structures Including Damping

The importance of damping to the dynamic performance of advanced structural applications demanding light weight and superior dynamic performance is well documented. Composites can provide significant damping in addition to low density, high stiffness and strength. It has been shown that composite damping is highly directional as most other properties, but follows the opposite trend than stiffness and strength. Because of the complexity, multitude of design parameters, and competing requirements, in-house research was performed on the optimal tailoring of composite structures for optimal dynamic response.

In-house research, as shown in Figure 14, involved development of a novel multi-objective optimal design methodology for light-weight, low-cost composite structures with improved dynamic performance. Design objectives include minimization of resonance amplitudes (or maximization of modal damping), weight, and material cost. The design vector includes parameters from multiple structural levels, such as, micromechanical, laminate, and structural shape variables. Performance constraints are imposed on static displacements, dynamic amplitudes, natural frequencies, and static/dynamic stresses. The effects of damping on the dynamics of composite structures are incorporated.

Evaluation of the method on cantilever Gr/Epoxy composite beams and plates illustrated that the proposed multi-objective optimization, as opposed to single-objective functions. The significance of composite damping in the design of advanced composite structures was also demonstrated. Evidence suggested that previous design methods, based on undamped dynamics, may fail to improve dynamic performance near resonances.

Application of the method on these basic composite structures appeared very encouraging. An in-house research code is available and is expected to contribute to programs involving

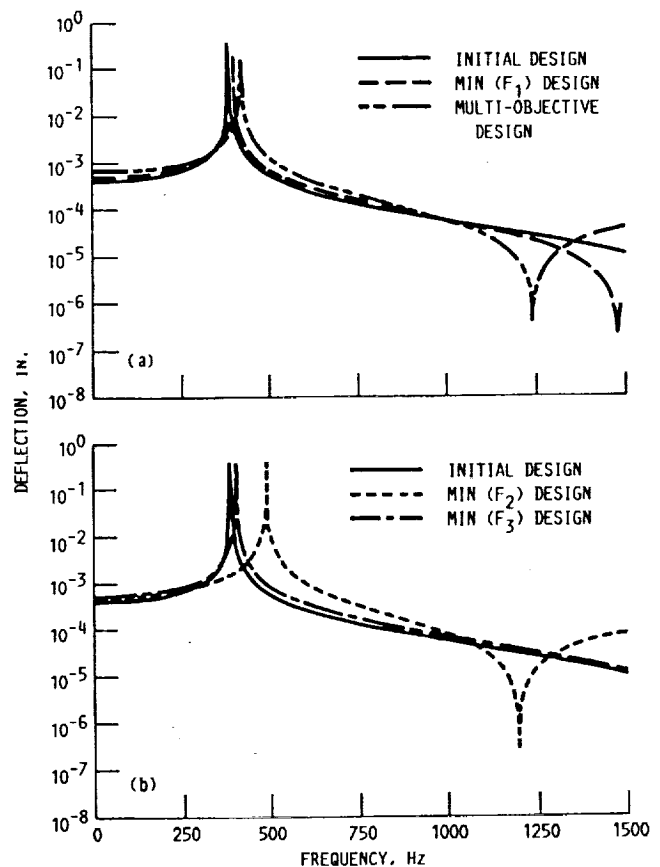


FIGURE 14. - FREQUENCY RESPONSE FUNCTIONS OF THE INITIAL AND OPTIMAL DESIGNS OF A COMPOSITE BEAM.

design of composite structures requiring improved dynamic or aeroelastic stability and fatigue endurance (composite engine blades) or improved vibration control and positioning accuracy (space station type structures, space antennas, and space mechanisms).

Bibliography

Saravanos, D.A.; and Chamis, C.C.: Multi-Objective Shape and Material Optimum Design of Composite Structures Including Damping. 31st AIAA/ASME/ASCE/AHS/ASC Structures, Structural Dynamics, and Materials Conference, Apr. 2-4, 1990, Long Beach, CA. (Also, NASA TM-102579).

Lewis contacts: Dimitris A. Saravanos,
(216) 433-8466; and Christos C. Chamis,
(216) 433-8466.
Headquarters program office: OAET

Computational Simulation of Metal Matrix Composites

High-temperature, metal matrix composites (HTMMC) offer great potential for use in advanced aerospace structural applications. Realization of this goal, however, requires concurrent developments in fabrication techniques, experimental measurement techniques, and computational methods. In development of HTMMC, initial simulation of their behavior through computational method proves beneficial. Besides providing an initial assessment of the HTMMC, this method helps minimize costly and time-consuming experimental efforts that would otherwise be required.

In-house research into computational methods for simulation of the nonlinear behavior of HTMMC has resulted in development of the Metal Matrix Composite Analyzer METCAN computer code. METCAN incorporates various levels of composite mechanics models with a nonlinear constituent material model to perform a comprehensive analysis of composite behavior. Development and verification (comparisons to experimental data) of METCAN are ongoing. Recently, material properties were generated by METCAN for seven candidate metal-matrix composites to assess their potential use in high-temperature structural applications.

Results of the latest METCAN verification activity indicate that the code can be used with confidence to predict high-temperature nonlinear behavior of metal-matrix composites. Two composites (SiC/Ti-15-3 and SiC/Ti-6-4) in the High-

Temperature Engine Materials Program (HITEMP) were studied at room and high temperatures. SiC/Ti-15-3 verification includes room-temperature comparisons for modulus, Poisson's ratio, strength, and stress-strain behavior, and high-temperature comparisons for strength and stress-strain behavior. Verification of SiC/Ti-6-4 includes a room-temperature transverse stress-strain curve and transverse strength at temperatures. For all cases examined, METCAN predictions are considered to be in good to excellent agreement with experimental data.

Bibliography

Lee, H.J.: METCAN Simulation of Candidate Metal Matrix Composites for High Temperature Applications. NASA TM-103636, 1990.

Lee, H.J.; Murthy, P.L.N.; and Chamis, C.C.: METCAN Updates for High Temperature Composite Behavior: Simulation/Verification. NASA TM-103682, 1991.

Lewis contact: Ho-Jun Lee,
(216) 433-3316
Headquarters program office: OAET

NASTRAN Improved for Low-Velocity Impact Analysis

A fundamental drawback in using many advanced composite materials in critical load-bearing aerospace structures is their brittle fracture behavior, particularly when subjected to impact loading. Computational tools are required to simulate the initiation and development of impact damage in brittle composite structures. A numerical analysis package has been developed at NASA Lewis that has significantly enhanced the capabilities of NASA Structural Analysis (NASTRAN) in this area.

Damage prediction in an impacted structure requires accurate calculation of local stresses in the region of contact with the impactor. During low-velocity impact, a region of nonlinear elastic deformation forms near the impact point, and regions of the structure remote from the impact deform in a linear elastic manner. An accurate, yet computationally efficient impact analysis must couple the linear elastic deformation of the global structure with the nonlinear elastic local deformation near the impactor. A new computational algorithm has recently been incorporated into the NASTRAN finite element analysis program to accomplish this, as Figure 15 shows. The

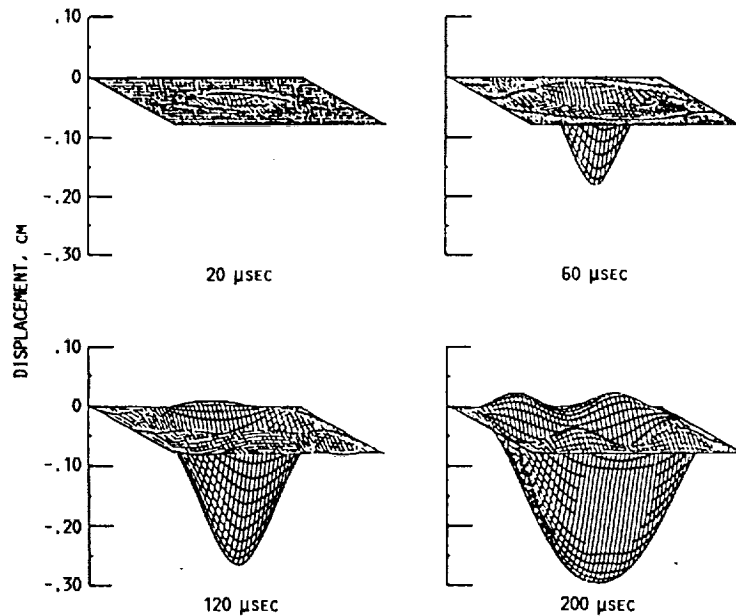


FIGURE 15. - CALCULATED DISPLACEMENT RESPONSE FOR COMPOSITE PANEL.

result is a greatly simplified impact-analysis package, which is available for public distribution through Computer Software Management Information Center (COSMIC) at the University of Georgia.

This modified finite element analysis package is used at the Naval Weapons Center and Johns Hopkins University Applied Physics Laboratory to computationally simulate the dynamic response of composite rocket motor cases to sudden impact loading. It is used at Lewis, for example, to calculate transient-impact force, local-contact deformation, and remote-strain response in composite structures. Calculated values show excellent agreement with experimental results.

Bibliography

Trowbridge, D.A.; Grady, J.E.; and Aiello, R.A.: Low Velocity Impact Analysis With NASTRAN. 18th NASTRAN User's Colloquium, NASA CP-3069, 1990, pp. 115-134.

Lewis contact: Dr. Joseph E. Grady,
(216) 433-6728
Headquarters program office: OAET

Neural Nets Capture Design Expertise

The human brain has a few hundred billion neurons, each connected to a few thousand of its neighbors. During learning, such as the accumulation of experience, a pattern of

connection strengths develops in this immense network. Neural nets attempt to model various brain functions, such as learning, by simplified representations of neurons and their connectivities. The models consist of artificial neurons that accumulate weighted input signals received from other neurons. The sum is presented to an activation function that triggers the neuron to send its output to other neurons. There are many neural net paradigms. The most interesting to this research is the supervised learning, forward feed net with a learning algorithm that adjusts the connection strengths of the net to minimize an error measure of its predictions versus the desired output of the training set. The trained neural net can be viewed as a device to quickly map input signals into desired output signals that closely approximate the output the real process would produce in response to the input.

An in-house feasibility study, as shown in Figure 16, tested the capability of neural nets to capture design expertise within a domain of design requirements. A truss structure was subjected to geometry changes as design requirements were varied. Optimum structures were obtained for each geometry by a conventional optimization method once a random set of geometric variables was selected. Using the design requirements and the resulting optimum design variables as a set of training pairs, the net was trained by the learning algorithm. When new design requirements were selected and exposed to the trained net, the structure responded with optimum designs in negligible computer times. The accuracy of its estimates was checked against optimum designs obtained by conventional optimization.

Efforts are presently underway to explore the capabilities of various neural net paradigms to capture material behavior

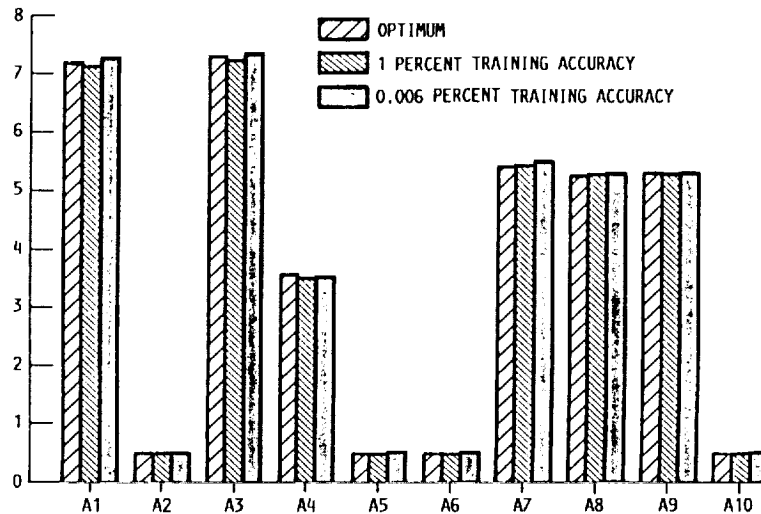


FIGURE 16. - NEURAL NET ESTIMATES OF DESIGN VARIABLES COMPARED WITH OPTIMUM DESIGN.

directly from test results. Such trained neural nets could then serve as material implant in nonlinear structural analysis codes, providing increased accuracy in simulating structural response of propulsion systems both in deterministic and probabilistic fashion.

Bibliography

Berke, L.; and Hajela, P.: Applications fo Artificial Neural Nets in Structural Mechanics. NASA TM-102420, 1990.

Rummelhart, D.E.; and McClelland, J.L.: Parallel Distributed Processing, Volume 1: Foundations. The MIT Press, Cambridge, MA, 1988.

Yoh-Han Pao: Adaptive Pattern Recognition and Neural Networks. Addison-Wesley Publishing Co., 1989.

Lewis contact: Laszlo Berke,
(216) 433-3212
Headquarters program office: OAET

Transverse Crack Detection in Composites Improved

The use of ultrasound to obtain images of flaws or damage in polymer composite laminates is well established and quite effective. In a common procedure, called C-scan, an ultrasound transducer scans an area of the laminate. The amount

of energy transmitted through the laminate (through-transmission method) or reflected back from the laminate (pulse-echo method) is displayed to produce an image that shows flaws or defects. This technique is particularly effective in detecting debonding between plies of the laminate. However, cracks that occur through the thickness are not easy to detect, since the waves propagate parallel to the crack, often leaving them undetected. Transverse cracks are important because they are often the first type of damage to occur as a result of either thermal or mechanical loading. A modified C-scan technique that uses oblique shear waves was developed at NASA Lewis to improve detection of these transverse cracks. See Figure 17. Normal longitudinal waves are used with the standard method.

When a longitudinal wave traveling in a fluid is incident at an angle on an anisotropic solid, such as a composite laminate, three types of waves are typically generated in the solid. These waves are termed quasi-longitudinal (QL), vertically polarized quasi-shear (QSV), and horizontally polarized quasi-shear (QSH) waves. In the technique developed at Lewis, the incident angle is calculated such that the QL waves are completely reflected from the solid and QSH waves are not generated. The remaining QSV waves, which are transmitted through the laminate at an oblique angle, are used to detect the presence of transverse cracks. An advantage of this technique is that it can be used with very little modification to standard C-scan equipment.

Initial results have shown that this technique is more effective in detecting transverse cracks than the standard procedure. It is being used in an ongoing research project to measure damage progression in polymer composites.

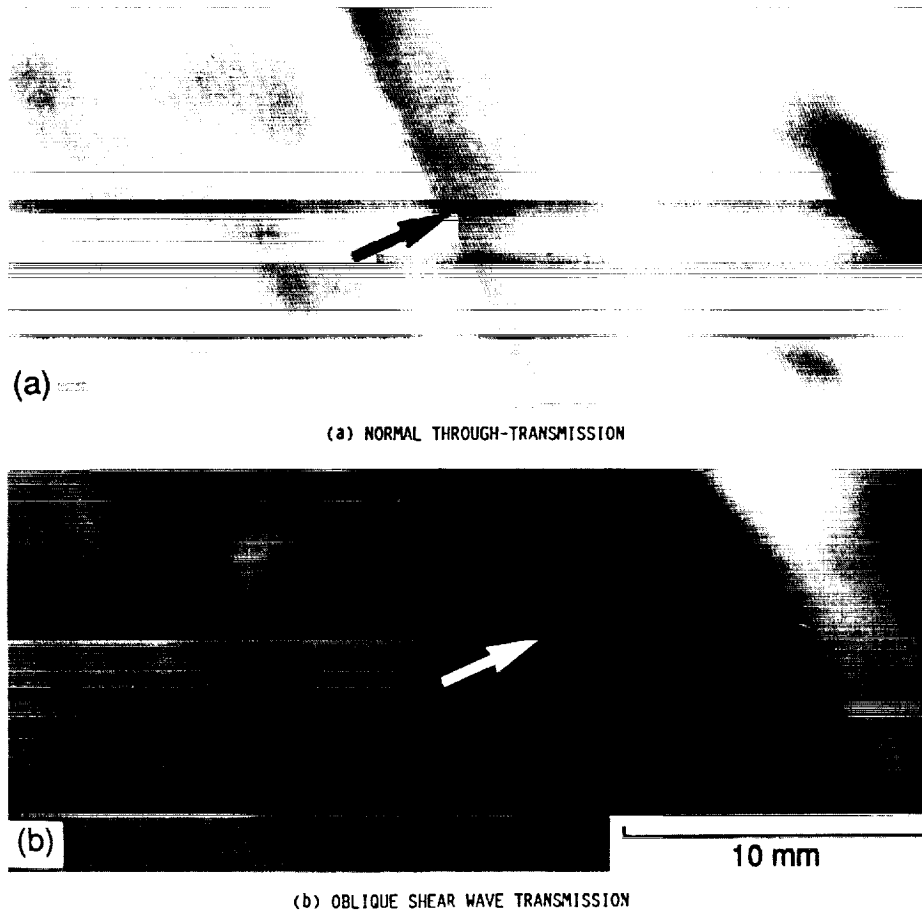


FIGURE 17. - IMAGES OF A TRANSVERSE CRACK IN A 60° OFF-AXIS UNIDIRECTIONAL SAMPLE USING THE TWO TYPES OF C-SCANS. THE SHEAR WAVE METHOD PRODUCES AN ENHANCED IMAGE. ARROWS INDICATE LOCATION OF CRACK.

Bibliography

Pereira, J.M.; and Generazio, E.R.: Improved Transverse Crack Detection in Composites. NASA TM-103261, 1990.

Lewis contacts: Michael Pereira, 433-6738; and
 Edgard Generazio, 433-6018
 Headquarters program office: OAET

Computational Simulation of Structural Fracture in Composites

It is generally accepted that flawed structures fail when the flaws grow or coalesce to a critical dimension such that (1) the structure cannot safely perform as designed and qualified, or (2) catastrophic fracture is imminent. This is true for structures either made from traditional homogeneous materials or fiber composites. One difference between fiber composites and traditional materials is that composites have multiple

fracture modes that initiate local flaws, compared to only a few for traditional materials. Any predictive approach to simulate structural fracture in fiber composites needs to formally quantify: (1) these multiple fracture modes, (2) the types of flaws they initiate, and (3) the coalescence and propagation of these flaws to critical dimensions for imminent structure fracture.

An ongoing in-house research activity, as shown in Figure 18, is directed toward development of a methodology for computational simulation of structure fracture in fiber composites. Part of this methodology consists of step-by-step procedures to simulate individual and mixed mode fracture in a variety of generic composite components. Another part has been incorporated into an integrated computer code identified as COD-STRAN (Composite Durability Structural Analysis).

The generic types of composite structural fracture include: (1) single and combined mode fracture in beams; (2) laminate free-edge delamination fracture; and (3) laminate center flaw progressive fracture. Structural fracture is assessed in one or all of the following: (1) the displacements increase very rapidly; (2) the frequencies decrease very rapidly; (3) the

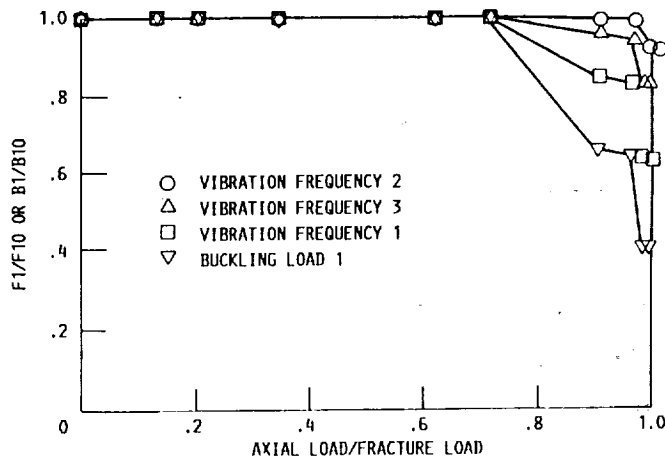


FIGURE 18. - THE EFFECT OF STRUCTURAL DEGRADATION ON NATURAL FREQUENCIES AND BUCKLING LOAD.

buckling loads decrease very rapidly; or (4) the strain energy release rate increases very rapidly. These rapid changes are assumed to denote imminent structural fracture. Based on these rapid changes, parameters/guidelines are identified which can be used as criteria for (1) structural fracture, (2) inspection intervals, and (3) retirement for cause.

Bibliography

Murthy, P.L.N.; and Chamis, C.C.: Computational Composite Mechanics for Simulation of Structural Fracture in Composites. NASA TM-102505, 1990.

Murthy, P.L.N.; and Chamis, C.C.: Interlaminar Fracture Toughness: Three-Dimensional Finite-Element Modeling for End-Notch and Mixed Mode Fracture. NASA TM-87138, 1985.

Murthy, P.L.N.; and Chamis, C.C.: Composite Interlaminar Fracture Toughness: Three-Dimensional Finite Element Modeling for Mixed Mode I, II, and III Fracture. NASA TM-88872, 1986.

Murthy, P.L.N.; and Chamis, C.C.: A Study of Interply Layer Effects on the Free Edge Stress field of Angleplied Laminates. NASA TM-86924, 1984.

Wilt, T.E.; Murthy, P.L.N.; and Chamis, C.C.: Fracture Toughness Computational Simulation of General Delaminations in Fiber Composites. NASA TM-101415, 1988.

Chamis, C.C.; and Smith, G.T.: CODSTRAN: Composite Durability Structural Analysis. NASA TM-79070, 1978.

Chamis, C.C.: Computational Simulation of Progressive Fracture in Fiber Composites. NASA TM-87341, 1986.

Minnetyan, L.; Murthy, P.L.N.; and Chamis, C.C.: Structural Behavior of Composites with Progressive Fracture. NASA TM-102370, 1989.

Lewis contact: P.L.N. Murthy,
(216) 433-3332
Headquarters program office: OAET

Probabilistic Composite Analysis

Probabilistic composite mechanics and probabilistic composite structural analysis are formal methods used to quantify the scatter observed in composite material properties and structural response. Observed scatter in composite material properties is the range of measured values in modulus, strength, and thermal expansion coefficient, for examples, while the scatter in structural response is the range of measured values for displacement, frequency, buckling load, etc. Formal methods relate scatter in the observed values to the corresponding scatter in the physical parameters which make up the composite and/or the composite structure. For example, these parameters include constituent material properties, fabrication process variables, structural component geometry, and any other variables which contribute to the composite behavior and/or structural response.

Development of these types of formal methods has been the subject of considerable in-house research. This research has led to computational simulation methods for relating scatter (uncertainties) in the composite properties or composite structural response to corresponding uncertainties in the respective parameters (primitive variables) which are used to describe the composite in all its inherent scales—micro, macro, laminate, and structural. This paper summarizes salient features of these computational simulation methods and presents typical results to illustrate their applications.

Specifically, the work contains: (1) a brief description of the fundamental concepts; (2) a probabilistic micromechanics composite; (3) a probabilistic laminate theory; (4) a probabilistic laminate tailoring; and (5) an elementary probabilistic structural analysis. Typical sample cases are included to illustrate the formal procedure for the computational simulation. Collective results of the sample cases demonstrate that uncertainties in composite behavior and structural response can be probabilistically quantified.

Bibliography

NASA TM Under Preparation: Probabilistic Composite Analysis.

Lewis contacts: Pappu L.N. Murthy,
(216) 433-3332; and C.C. Chamis,
(216) 433-3252
Headquarters program office: OAET

Lewis contact: Pappu L.N. Murthy,
(216) 433-3332
Headquarters program office: OAET

Application of Artificial Neural-Network Concepts To Structural Mechanics Problems

Artificial neural networks can provide improved computational efficiency relative to existing methods when an algorithmic description of functional relationships is either totally unavailable or is complex in nature. The amount of computational effort (CPU time) saved is naturally a function of complexity of the relationships between the various input and output variables of interest in a given problem. Significant reductions in elapsed computation time are possible. The primary goal of this work is to study the applicability of artificial neural network concepts to structural mechanics problems. Among the various problems chosen for the study is the prediction of composite ply-mechanical properties under all possible hygrothermal environments.

The artificial neural-network program selected for this study is NETS 2.0, developed at NASA JSC. This program has been modified in-house and now resides on NASA CRAY/XMP, VAX, SUN MICRO, and IBM PC/AT systems. Significant modifications to the code include automatic scaling of input/output variables, a capability which permits creation of neural networks which work with real user-supplied data. The resulting code has been shared with the NASA JSC. The future release of the NETS code will have these modifications incorporated.

The program chosen for providing the composite mechanics data is the Integrated Composite Analyzer (ICAN). ICAN is an in-house developed computer code which performs dedicated composite mechanics analysis for polymer-based composites. Three composite systems were selected for the study: (1) S-Glass fiber with Epoxy Matrix; (2) AS Graphite fiber with a Low-Modulus, Low Strength Matrix; and (3) P-75 Fiber with a High-Modulus, High-Strength Matrix. Input variables selected are the use temperature, moisture content, fiber-volume ratio and void-volume ratio. The output consists of 37 ply-level properties (ply moduli, Poisson's ratios, strengths, etc). Sample results from this study with Root Mean Square (rms) error in percentage between the ICANpredicted and NETS computed values are extremely encouraging.

Simplified Design Procedures for Fiber-Composite Structural Components/Joints

Design of composite structural components used in advanced aerospace structures requires considerable care. Often the specific designs must be complemented with appropriate finite element analyses and strategic experiments for final design and certification. One must also take into account environmental factors such as moisture absorption, exposure to higher temperature and fatigue type loadings. Simplified procedures for the preliminary design/analysis of composite structural components under such diversified, complex loading and environmental conditions are highly desirable. The in-house research efforts toward developing such simplified design procedures are summarized.

Design of composite structural components, as Figure 19 shows, for preliminary investigation purposes involves: (1) design of panels (laminates) subjected to combined in-plane loads; (2) design of built up structures (box beams) made from composite panels; and (3) design of composite joints (adhesively bonded as well as mechanically fastened). The objective of the present effort is to describe simplified step-by-step procedures to aid in the preliminary design phase of composite structural components, specifically, the four basic types of design analyses mentioned above. Details of the step-by-step design procedures for the design of panels, box beams, and joints are presented through simple illustrative examples. Guidelines are described which can be used in the design selection process. Procedures for considering cyclic loads, hygrothermal effects, and lamination residual stresses are briefly outlined through appropriate examples. Factors affecting composite structural components design are also summarized.

Bibliography

Simplified Procedures for Designing Adhesively Bonded Composite Joints. NASA TM-102120.

Simplified Procedures of Designing Composite Bolted Joints. NASA TM-100281.

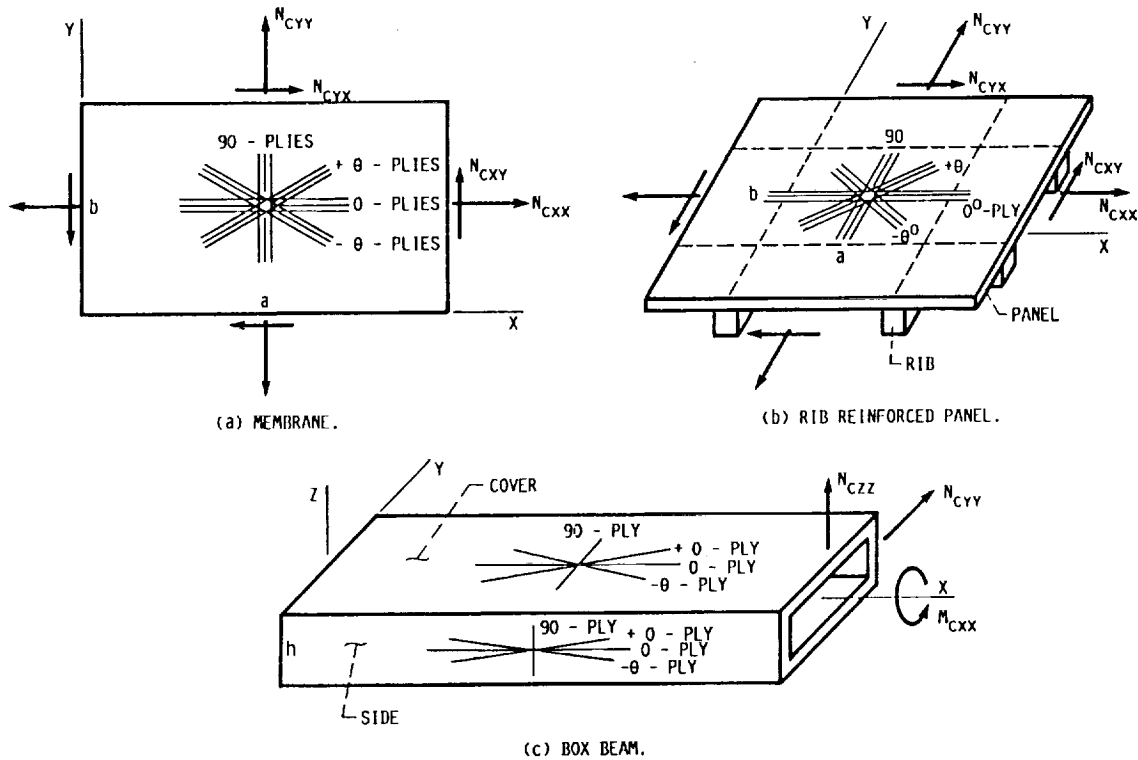


FIGURE 19. - SCHEMATICS OF SELECT COMPOSITE STRUCTURAL COMPONENTS WITH RESPECTIVE GEOMETRY AND TYPICAL LOADINGS.

Design Procedures for Fiber Composite Structural Components: Panels Subjected to Combined In-Plane Loads. NASA TM-36909.

J. Reinf. Plast. Comp. 8, 370-397 (1989), Design Procedures for Fiber Composite Box Beams.

Simplified Design Procedures for Fiber Composite Structural Components/Joints. NASA TM-103113.

Lewis contacts: Pappu L.N. Murthy,
(216) 433-3332; and C.C. Chamis,
(216) 433-3252
Headquarters program office: OAET

Fiber Substructuring Captures Greater Local Detail of Composite Response

The in-house research activity of high-temperature composite mechanics has led to the evolution of a new and unique fiber substructuring concept for the description of the micromechanical behavior of composites. The activity focuses on development of a computer code for ceramic matrix composites, and

the concept is equally applicable for any type of continuous filament reinforced composite. The computer code predicts the equivalent composite mechanical and thermal properties based on the constituent properties, and the response of the composite to combined thermal and mechanical loading.

A generic unit-cell model, as Figure 20 shows, based on a unique fiber substructuring concept is proposed for the development of micromechanics equations for ceramic-matrix composites. The unit-cell typically consists of a fiber and a matrix with or without an interphase. It is divided into several slices; the equations of micromechanics are derived for each slice. A stand-alone computer code, which contains this micromechanics model as a sub module, is developed specifically for the analysis of ceramic-matrix composites.

Typical results in the form of equivalent ply properties have been obtained for an SiC (silicon-carbide fiber)/Ti15 (Titanium matrix) composite with a 0.5 fiber-volume ratio and are compared with those obtained from customary micromechanics models. Based on results: (1) the prediction of ply mechanical and thermal properties agree with the existing models in ICAN and Metal-Matrix Composite Analyzer (MET-CAN), lending credence to the fiber substructuring approach; and (2) Fiber substructuring captures greater local detail than conventional unit-cell based micromechanical theories. This approach promises to simulate complex aspects of micromechanics in ceramic matrix composites (CMC) such as: (1) various degrees of bond around the fiber circumference

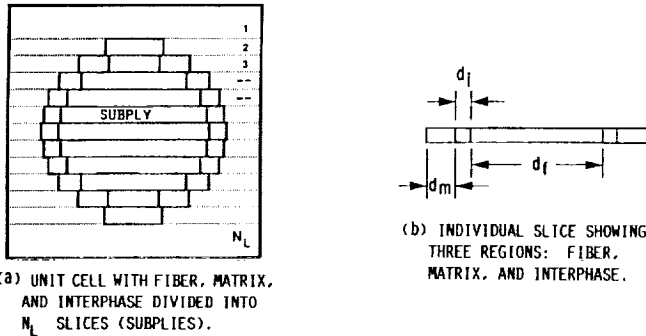


FIGURE 20. - PLY/FIBER SUBSTRUCTURING CONCEPT FOR CERAMIC MATRIX, COMPOSITE MICROMECHANICS - MECHANICS OF MATERIALS APPROACH.

and along the length, (2) fiber breaks and matrix cracking, and (3) effects of these on ply thermal and mechanical properties or responses. In addition, the approach is general and versatile. It can be applied to any type of continuous fiber-reinforced matrix composite. A nonlinear material behavior model to describe the constituent current properties as a function of the reference properties and the current response is also under development.

Lewis contact: Pappu L.N. Murthy,
(215) 433-3332
Headquarters program office: OAET

The Computational Simulation of the Global Fracture Toughness of Composite Structures

Behavior of laminated composite structures under loading is complex, especially when possible degradation with damage and fracture is considered. Internal composite damage is often initiated as delamination or separation of adjacent layers, or as transverse cracking through one or more layers. After the initiation of damage, damage growth and progression usually involves fiber-matrix debonding within individual layers and the enlargement of the damaged zone. Further degradation is in the form of fiber fracture and fracture propagation that leads to ultimate failure. Because of the infinite possibilities, it is essential to have a reliable computational capability to predict the behavior of composites under any loading condition, geometry, composite material combinations, and boundary conditions. The predictions of damage initiation, progressive damage, and progressive fracture are important in evaluating the safety and reliability of composite structures. There is also a need for an explicit fracture toughness index to evaluate the overall reliability of composite structures with localized damage and fracture.

To address the needs for design analysis, a computational method for the evaluation of global fracture toughness in laminated composites is implemented by augmentation through a university grant of the Composite Durability Structural Analysis (CODSTRAN) computer code. CODSTRAN has the in-house capability of predicting crack locations and delamination initiation as well as fracture progression and coalescence. Recent progress includes computation of the Strain Energy Release Rate (SERR) to provide a measure of global fracture toughness, considering all modes of damage and fracture during progressive degradation of composites. The cumulative total of the generated internal damage serves also as an index of structural degradation. The relationship between internal damage and structural properties such as natural frequencies and vibration mode shapes is useful for in-service evaluation of composite safety and reliability. Current analysis is being conducted on an angleplied composite plate structure subjected to in-plane tensile loading.

Bibliography

Minnetyan, L.; Murthy, P.L.N.; and Chamis, C.C.: Composite Structure Global Fracture Toughness via Computational Simulation, *Computers & Structures*, vol. 37, no. 2, pp. 175-180, 1990.

Lewis contact: Pappu L.N. Murthy,
(216) 433-3332
Headquarters program office: OAET

Reduction of Thermal-Residual Stress in Advanced Metallic Composites Via a Compensating/Compliant Layer Concept

High residual stresses within metal and intermetallic matrix composite systems can develop upon cooling from the processing consolidation temperature to room temperature, due to coefficient of thermal expansion (CTE) mismatch between the fiber and the matrix. As a result, radial, circumferential, and/or longitudinal cracks have been observed to form within the fiber-matrix interface region. Potential solutions for reducing the residual stress field and minimizing cracks have been proposed recently. Examples of some potential solutions are high CTE fibers, fiber preheating, and the compliant-layer concept. The compliant-layer concept entails the insertion or addition of an interface material between the fiber and matrix to reduce or eliminate the residual stress field, and the consequent initiation of cracks developed during cool down.

Of particular interest is the reduction in the tensile hoop stress at the fiber matrix interface, which is believed to be responsible for the predominantly observed radial cracking.

A detailed elastic and elastic-plastic parametric study was conducted using a unit cell model of three perfectly bonded concentric cylinders to determine the required "character" (i.e., thickness and mechanical properties) of the compliant layer as well as its applicability. The unknown compliant layer mechanical properties are expressed as ratios of the corresponding temperature-dependent matrix (i.e., Ti₃Al+Nb) properties. Fiber properties taken are those corresponding to SCS-6 (SiC). Results indicate that the compliant layer can be used to reduce, if not eliminate, in-plane (radial and circumferential) residual stresses within the fiber and matrix and as a result, the radial cracking. With this decrease of in-plane stresses, however, one obtains an increase in longitudinal stress, potentially initiating longitudinal cracking. Guidelines are given for selection of a specific compliant material. For example, when selecting a compliant layer material, the properties should be chosen such that (c = compliant layer, m = matrix).

- (1) CTE of the compliant layer is greater than that of the matrix.
- (2) Thickness (t/a) of the layer should be as large as other considerations allow.
- (3) $(H^c/H^m) + (\sigma_y^c/\sigma_y^m)$ should be small.
- (4) Yield point (σ_y^c) relative to matrix should be low.
- (5) Hardening slope (H^c) relative to matrix should be low.
- (6) Elastic stiffness (E^c) relative to matrix should be low.

This list is in order of importance, with respect to impact, for obtaining a minimum overall residual stress state. This requirement may not provide the maximum life under cyclic conditions.

Lewis contact: Dr. Steven M. Arnold,
(2216) 433-3334
Headquarters program office: OAET

Metal-Matrix Composite Analyzer Verification Status

Nonlinear behavior of high-temperature metal-matrix composites (HTMMC) has been investigated at NASA Lewis Research Center during the past decade. The investigation focused on the development of computational simulation procedures and attendant computer codes. A fundamental aspect of the investigation is that the computational simulation represented is parallel with the fabrication process. The

research culminated in the development of a computer code identified as Metal-Matrix Composite Analyzer (METCAN). METCAN, as shown in figure 21, has the capability to predict all aspects of HTMMC behavior, including the fabrication process, by using only room temperature properties for the fiber and matrix.

A unique feature of the computational simulation in METCAN is the introduction of the multifactor interaction model (MFIM) to represent the various nonlinearities and their mutual interactions in the constituents.

Through this MFIM, METCAN provides an effective and alternate approach to characterize HTMMC under a variety of environmental and loading conditions. The limited data available for HTMMC poses difficulties in verifying its various features. Recently, some data have been generated through the High-Temperature Engine Materials Program (HITEMP). These data are continuously being used to verify the computational simulation features of METCAN. Typical comparisons include thermal fatigue effects on room temperature tensile strength. These comparisons provide confidence that METCAN successfully simulates the complex behavior of high-temperature metal matrix composites.

The code is used by participants in the National Aerospace Plane (NASP) program to simulate high temperature composite behavior and to design experiments.

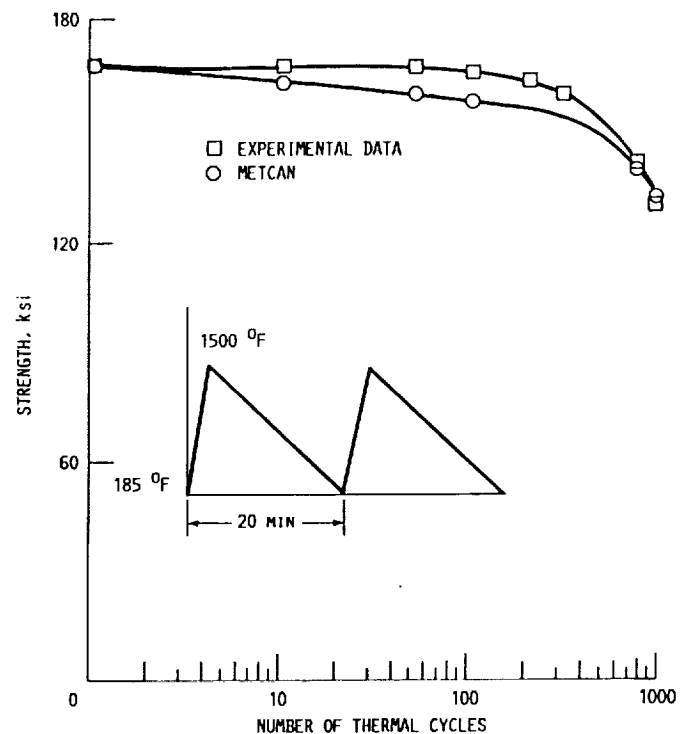


FIGURE 21. - METCAN SIMULATES THERMAL FATIGUE EFFECTS ON ROOM TEMPERATURE STRENGTH OF UNIDIRECTIONAL SiC/Ti COMPOSITE (FVR 0.35).

Bibliography

Chamis, C.C.; Caruso, J.J.; Lee, H-J; and Murthy, P.L.N.: METCAN Verification Status. NASA TM-103119, 1990.

Lewis contact: C.C. Chamis,
(2216) 433-3252
Headquarters program office: OAET

Probabilistic Simulation of Uncertainties in Composite Uniaxial Strengths

Analysis of composite structures requires reliable predictive models for material properties and strengths. However, the prediction efforts have been complicated by the inherent scatter of the experimental data. Since uncertainties in the constituent properties, fabrication variables, and internal geometry would lead to uncertainties in the measured composite properties, the question arises:

How much of the "statistical" scatter (uncertainties) of experimentally observed composite properties can be explained by reasonable statistical distribution of input parameters (primitive variables) in composite micromechanics and laminate theory predictive models?

In order to answer this question, a computational simulation procedure was developed in-house for probabilistic composite micromechanics, as shown in Figure 22. Application of this procedure for uniaxial thermal and mechanical properties was reported previously. Recently, this process was applied to fiber composite uniaxial strengths. The computational simulation is performed using ply substructuring with an existing computer code for composite mechanics in conjunction with Monte Carlo simulation. The scatter in the constituent materials strengths is selected from anticipated respective probabilistic distributions. The variables for which uncertainties are accounted include constituent strength and their respective scatter. Graphite/epoxy unidirectional composites were used to illustrate the procedure and its effectiveness to formally estimate the probable scatter in composite uniaxial strengths. Results show that ply longitudinal tensile and compressive, transverse compressive and intralaminar shear strengths are not sensitive to single fiber anomalies (breaks, interfacial disbonds, matrix microcracks); however, the ply transverse tensile strength is. A contract to extend the work to aircraft structural composites is under way.

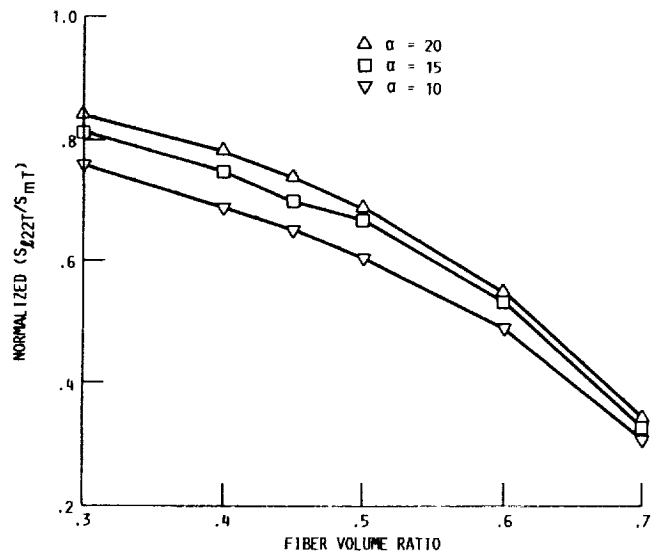


FIGURE 22. - MATRIX TENSILE STRENGTH SCATTER EFFECTS ON PLY TRANSVERSE TENSILE STRENGTH.

Bibliography

Chamis, C.C.; and Stock, T.A.: Probabilistic Simulation of Uncertainties in Composite Uniaxial Strengths. NASA TM-102843, 1990.

Lewis contact: C.C. Chamis,
(216) 433-3252
Headquarters program office: OAET

Probabilistic Laminate Tailoring With Probabilistic Constraints and Loads

There is a great potential for structural tailoring of high-performance, light-weight structures made of fiber composites. This is due to the great range of desirable properties of fiber composites and their tailoring capacity to individual design requirements. Principal among these is the ability to tailor ply properties (material selection) and fiber orientation (configuration selection) to the given mechanical, thermal, and hygral loads. A laminate is a building block that contributes to the overall thermostructural action of a component made out of composites. It's logical to concentrate on tailoring of laminate properties and configuration as a first step in the synthesis of composite structures in order to meet reliability design requirements.

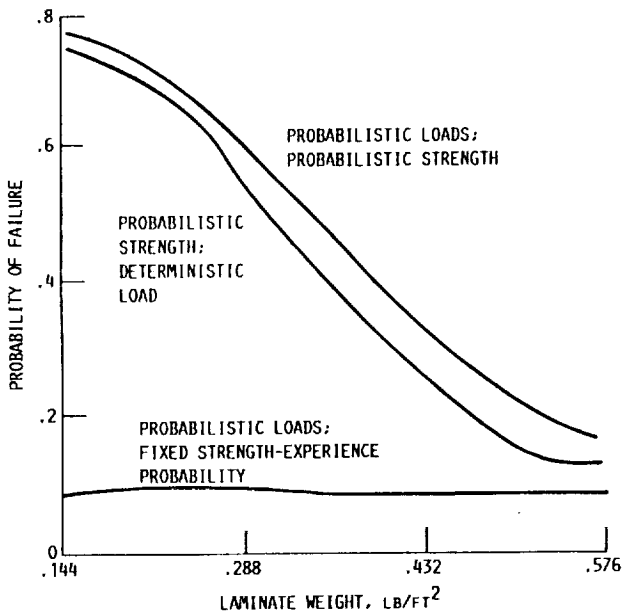


FIGURE 23. - LAMINATE TAILORING WITH PROBABILISTIC CONSTRAINTS AND LOADS.

A recent In-house research effort developed a tailoring (synthesis/optimization) procedure by combining a robust optimizer with composite mechanics and probabilistic constraints and/or loads. As Figure 23 shows, it is widely recognized that at the optimum design, one or more performance constraints are at their allowable values and any uncertainties in the given input data may, for these constraints, lead to an unsafe design. This is because the active performance constraints may become violated with variations in the input data. The procedure described herein is applied to several generic sample cases to illustrate that fiber composite laminates can be tailored to meet design requirements with assured probability of survival.

Results show that the probability of laminate failure (1) decreases as the laminate weight increases for probabilistic strength and deterministic load; (2) decreases as the laminate weight increases for combined probabilistic load and probabilistic strength; and (3) remains approximately constant as the laminate weight increases. Item (3) is relevant to designs with multiple constraints and to designs for point reliability, that is, a design to satisfy an a priori selected reliability.

Bibliography

Thanedar, P.B.; Chamis, C.C.: Composite Laminate Tailoring with Probabilistic Constraint and Loads. NASA TM-102515, 1990.

Lewis contact: C.C. Chamis,
(216) 433-3252
Headquarters program office: OAET

Fundamental Aspects of and Failure Modes in High-Temperature Composites

NASA is involved with several programs such as the National Aerospace Plane and the High-Speed Civil Transport, which will challenge the current state of technology in both materials and structures. To meet the aggressive goals set forth in these programs, high-temperature materials, including metal matrix composites (MMC) and ceramic matrix composites (CMC), are being investigated. The high-temperature nonlinear behavior of these classes of materials is very complex with limited observed characteristics (experimental data) on which to base or assess a design. As a result, a research activity was performed to identify the fundamental aspects and variables that will affect high-temperature behavior of these composite materials.

This research activity, as shown in Figure 24, led to fundamental concepts and simple equations, which are summarized to describe the fundamental aspects and failure modes in high-temperature metal matrix composites (HTMMC). These equations are explicit. They are used to identify dominant factors (variables) that influence the behavior of high-temperature materials.

$$Q = KA\Delta T/l$$

$$\epsilon = \alpha\Delta T; \sigma = E\epsilon = E\alpha\Delta T$$

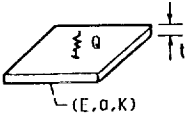
$$\Delta T = Ql/KA$$

$$\sigma = E\alpha Ql/KA = \epsilon (l/A) (\alpha Q/K)$$

— THERMAL DRIVING FORCE

— GEOMETRY CONFIGURATION FACTOR

— MATERIAL INSTANTANEOUS MODULUS



OBSERVATION: THE FOLLOWING MINIMIZES THERMAL STRESSES FOR A GIVEN HEAT FLUX:

- (1) DECREASE MODULUS (E).
- (2) DECREASE THICKNESS (l).
- (3) DECREASE THERMAL EXPANSION COEFFICIENT (alpha).
- (4) INCREASE SURFACE AREA (A).
- (5) INCREASE THERMAL HEAT CONDUCTIVITY.
- (6) INCREASE STRESS RUPTURE.

FOR A FIXED GEOMETRY DECREASE E AND alpha, AND INCREASE K

FIGURE 24. - VARIABLES THAT INFLUENCE THERMAL STRESS ARE IDENTIFIED USING ELEMENTARY HEAT TRANSFER CONCEPTS.

The simple equations, in explicit form, are for (1) strength; (2) fiber shapes; (3) load transfer, limits on matrix ductility (strain-to-fracture) to survive a given number of cyclic loadings; (4) parameters that govern thermal stresses, vibration stresses, and impact resistance; and (5) in situ matrix behavior. These equations can be used to perform parametric studies, guide experiments and constituent materials research/selection, and assess fabrication processes for specific applications. The fundamental concepts and explicit equations are presented in chart form for convenience and completeness.

Bibliography

Chamis, C.C.; and Ginty, C.A.: Fundamental Aspects of and Failure Modes in High-Temperature Composites. NASA TM-102558, 1990.

Lewis contact: C.C. Chamis,
(216) 433-3252
Headquarters program office: OAET

Progressive Damage and Fracture in Composites Under Dynamic Loading

The behavior of multi-ply composites during progressive damage and fracture has increased interest in recent years due to the extent of possibilities that use composites in practical engineering applications such as light-weight airframes, engine structures, space structures, marine and submarine structures, high-precision machinery, and structural members in robotic manipulators. Composite structures lend themselves to optimal tailoring to achieve desirable characteristics such as a high strength-to-weight ratio, dimensional stability under extreme thermal and hygral fluctuations, and the capability to allow controlled detectability such as in the Stealth technology. Because of the infinite possibilities, it is essential to have a reliable computational capability to predict the behavior of composites under any loading, geometry, material combinations, tailoring, and boundary conditions.

A new computational capability to explore the dynamic aspects of composite structural response and durability that could not be simulated previously, has been developed in-house. The present computer code, as shown in Figure 25, is able to predict the behavior of laminated composites under any loading, geometry, material combination, fiber orientation, tailoring, and boundary conditions. Structural degradation, delamination, fracture, damage growth, and propagation are included in the dynamic simulation. The properties of commercially available fiber and matrix constituent materials are compiled in a databank to allow computational simulation of any angle-plyed, multi-layer composite structure with graphite or glass fibers in an epoxy or polymer based matrix; including effects of thermal and hygral environmental conditions during manufacture and loading. The dynamic computational capabilities in the simulation of structural damage,

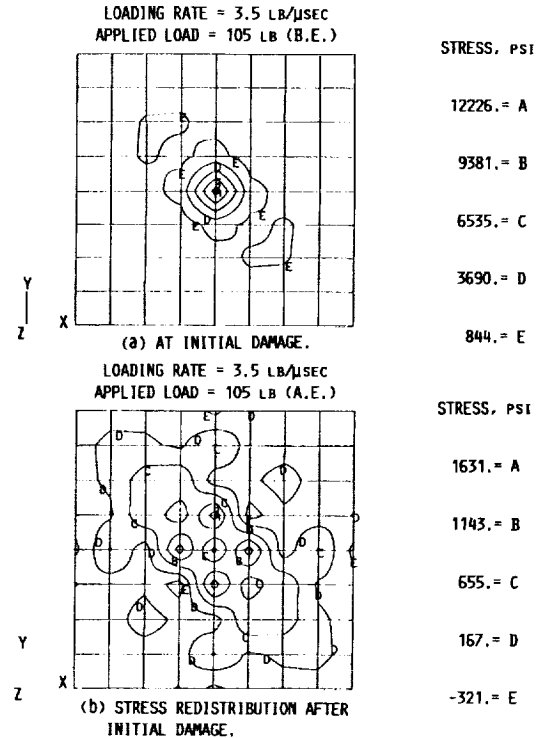


FIGURE 25. - PROGRESSIVE DAMAGE AND FRACTURE IN COMPOSITES UNDER DYNAMIC LOADING. SUPPORT MODES FREE IN X-Y PLANE, S_{22} STRESSES FOR PLY 1 (PSI).

fracture, and failure of multi-ply composites have been implemented as an augmentation of the Composite Durability Structural Analyzer (CODSTRAN) computer program.

Dynamic analysis capability of the code can be used to investigate the response of a composite structure due to loading applied at an impulsive rate to simulate impact. Under simulated impact loading, the code can be used to predict the type of failure as either localized impact penetration or more distributed flexural failure.

Bibliography

Minnetyan, L.; Murthy, P.L.N.; and Chamis, C.C.: Progression of Damage and Fracture in Composites Under Dynamic Loading. NASA TM-103118, 1990.

Lewis contact: C.C. Chamis,
(216) 433-3252
Headquarters program office: OAET

Flutter Analysis of a Supersonic Cascade in Time Domain Using a Euler Solver

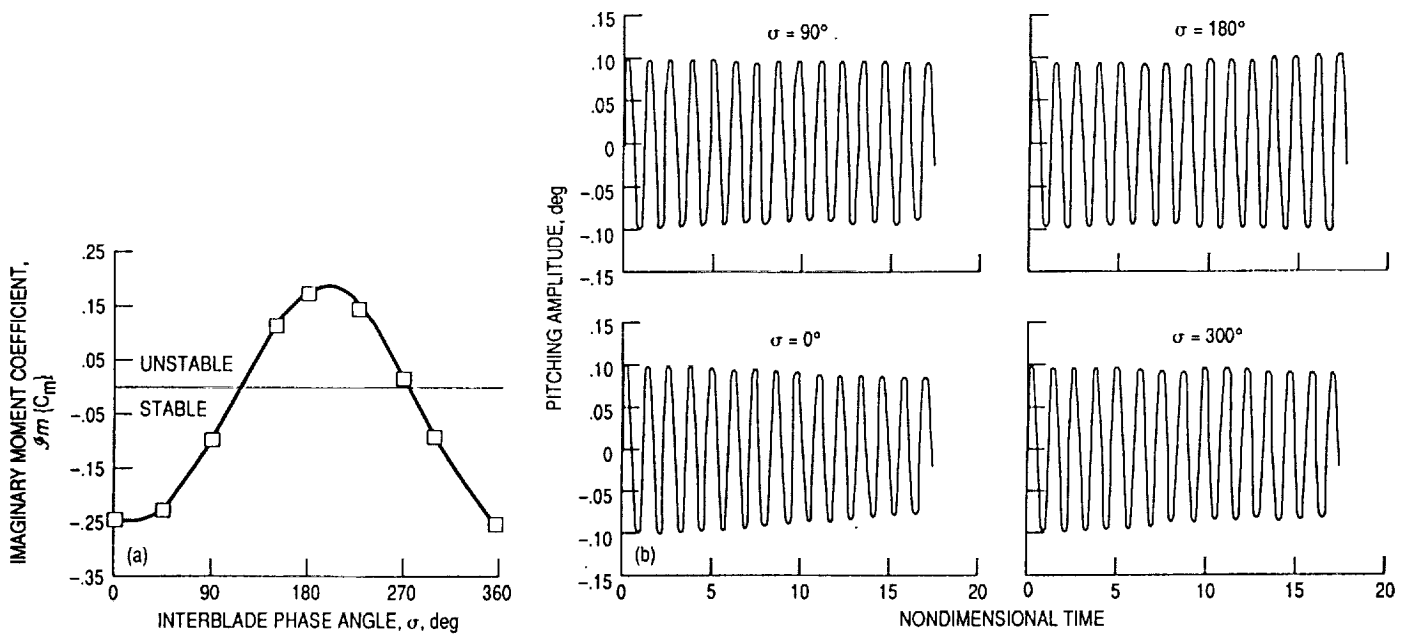
Understanding aeroelastic behavior and identifying flutter boundaries is critical in the design of the Supersonic Through-Flow Fan. Many existing aeroelastic analysis methods are based on linearized theories and are solved in frequency domain. To incorporate both aerodynamic and structural nonlinearities, however, the aeroelastic equations have to be solved in time domain. In addition, the aerodynamic model should be able to include the effects of thickness, camber of the airfoil, and the effect angle of attack in the analysis. Toward this effort, a finite difference algorithm based on Euler equations to analyze supersonic through flow fan is combined with a typical section structural model with pitching degree of freedom. A deforming grid technique is used to specify periodic boundary conditions of the cascade during oscillation. Equations are solved in time domain.

Figure 26 shows a typical result obtained for a flat plate cascade with an inlet Mach number (M_1) of 2.61, stagger angle (γ) of 28 degrees, gap-to-chord ratio (g/c) of 0.311. Block A shows the variation of the imaginary part of the moment

coefficient ($\text{Im}\{C_m\}$) with inter-blade phase angle (σ). Results are obtained from a frequency domain solution. A reduced frequency based on semi-chord (k_b) equal to 1.0 is used in the calculations. When $\text{Im}\{C_m\}$ becomes positive, the moment leads the motion of the flat plate and represents an unstable condition. It can be seen that the blade is unstable for σ between 110 and 280 deg.

For the problem analyzed, the ratio of the flutter frequency and the structural frequency is nearly one. Then the flutter speed index, V^* , used in the time-domain formulation is equal to the reciprocal of the reduced frequency, k_b . To simulate time domain characteristics, it is sufficient to show that responses at various interblade phase angles are stable or unstable for $V^* = 1.0$. Block B shows the response plots for $\sigma = 0, 90, 180$ and 300° . Corresponding solutions (in block A) are respectively stable, stable, unstable, and stable. As seen in block B, response plots predict the expected behavior. This validates development of the time domain aeroelastic code.

Lewis contact: Dennis L. Huff,
 (216) 433-3913; T.S.R. Reddy,
 (216) 433-6083
 Headquarters program office: OAET



(a) IMAGINARY PART OF MOMENT COEFFICIENT ABOUT 40-PERCENT CHORD VERSUS INTERBLADE PHASE ANGLE, σ . REDUCED FREQUENCY BASED ON SEMICHORD, k_b , 1.0.

(b) RESPONSE OF FLAT PLATE CASCADE FOR INTERBLADE PHASE ANGLES, σ , OF 0° , 90° , 180° , AND 300° .

FIGURE 26. - FLUTTER CALCULATIONS FOR A SUPERSONIC CASCADE. INLET MACH NUMBER, 2.61; STAGGER ANGLE, 28° ; GAP-TO-RATIO, RATIO, 0.311.

Multi-Input, Multi-Data (MIMD) Parallel Fortran Configuration File Generator

Implementing a parallel application on message-passing architecture involves a two-part mapping: (1) the software tasks must be mapped to the distribution processing nodes; and (2) the communications between tasks must be mapped to communications paths in the parallel architecture. After a mapping to nodes has been established, the configuration File Generator (CFG) completes the implementation by automatically generating a suitable mapping for software channels.

The purpose of this utility is to complete a configuration for a parallel FORTRAN application as mapped to a Transputer system. "Multiplexor/demultiplexor" tasks are provided everywhere multiple software channels are mapped to a single hardware channel. For communication between two tasks residing on nodes that are not connected by a physical link, a communications path is established consisting of a sequence of "intermediate" tasks on nodes between the two nodes. The duty of each intermediate node is to receive messages on the single-input channel and send them on the output channel.

Input: (1) A set of FORTRAN programs, each representing a task.

(2) A partial configuration file giving hardware declarations, task declarations, and assignment of software tasks to physical processors.

Output: (1) A complete configuration file (fconfig.cfg).

(2) Any utility tasks (multiplexor, demultiplexor, and intermediate) expressed as FORTRAN programs, as needed.

Determining a mapping of software channels to hardware channels is a complex task and prone to errors when left to the programmer. Not only does CFG ensure an error-free mapping, it facilitates frequency re-configuration during development and testing.

Lewis contact: James Kiraly, (216) 433-6023 Headquarters program office: OAET

Dynamic Substructuring by the Boundary-Flexibility Vector Method of Component-Mode Synthesis

Component-mode synthesis (CMS) is a method of dynamic analysis, for structures having a large number of degrees of freedom (D.O.F.). These structures often required lengthy computer CPU time and large computer memory resources, if solved directly by the finite-element method (FEM). In CMS, the structure is divided into independent components in which the D.O.F. are defined by a set of generalized coordinates which are defined by displacement shapes. The number of generalized coordinates is much less than the original number of physical D.O.F. in the component. Displacement shapes are used to transform the component property matrices and any applied external loads, to a reduced system of coordinates. Reduced system property matrices are assembled, and any type of dynamic analysis is carried out in the reduced coordinate system. Final results are back transformed to the original component-coordinate systems. In all conventional methods of CMS, the mode shapes used for components are dynamic mode shapes, supplemented by static deflected shapes. Historically, all dynamic mode shapes used in conventional CMS are the natural modes (eigenvectors) of components.

In this work, a new method of CMS, the boundary-flexibility vector method of CMS, is developed. It provides for the incorporation of a set of static Ritz vectors, referred to as boundary-flexibility vectors, as a replacement and/or supplement to conventional eigenvectors, as displacement shapes for components. Generation of these vectors does not require the solution of a costly eigenvalue problem, as in the case of natural modes in conventional CMS; thus, a substantial savings in CPU time can be achieved. The boundary flexibility vectors are generated from flexibility (or stiffness) properties of components. Formulation presented is for both free and fixed-interface components, and for both free- and forced-vibration problems. Free- and forced-vibration numerical examples are presented to verify the accuracy of the method and the savings in CPU time. Compared to conventional methods of CMS, results indicate that by using this new method, more accurate results can be obtained with a substantial savings in CPU time. A comparison of the number of operations required to obtain the boundary flexibility vectors versus normal modes of vibration, showed a substantial reduction of the number of required operations by using the boundary flexibility vectors, instead of eigenvectors. Good

agreement with finite-element and conventional methods of CMS was found after the new method was applied to a substantially large structure. An average savings of CPU time between 75 and 80 percent was attained. Results obtained by the boundary-flexibility method of CMS were also in good agreement with results obtained from direct integration of the equations of motion. In all cases considered, results obtained by the boundary-flexibility method were almost the same, and sometimes superior, to those obtained by conventional methods of CMS.

Lewis contact: Charles Lawrence,
(216) 433-6048
Headquarters program office: OAET

Active Vibration Control Test Results

Active Vibration Control (AVC) tests on the Lewis high-speed balance rig were conducted during the summer of 1989. Opposing pushers were installed at both bearings, whereas only nonopposing pushers were installed at the outboard disk in the summer of 1988 tests. Tests showed that the opposing pushers provided significantly more active damping than a single pusher and prevented misalignment due to the unidirectional preload of the nonopposing pusher configuration. The additional inboard disk in the 1989 test provided a means to vibrate both ends of the shaft. Unbalanced response testing confirmed that vibrations could be effectively suppressed along the entire shaft assembly with the sensor/actuator con-

figuration. A high-temperature (full-damping capability at 300 °F) elastomeric pad was used to provide isolation of the piezoelectric actuators from the rig's housing and bearing retainer in the 1989 test. This pad was required to isolate the piezopusher from the rig's housing in the second test. The active damper control capability increased from 6500 rpm (1988 testing) to over 13 000 rpm (1989 testing).

Static Stiffness, maximum-stroke and displacement-sensitivity tests were conducted on each of the eight pzl-100 Burleigh piezoelectric pushers, yielding the following results: static stiffness: 17 000 to 29 000 (lb/in.); max. stroke* 3.2 to 5.2 (mils, p.p); sensitivity* 1.30 to 1.40 (v/mil)

Transfer functions were also made for each piezopusher and its respective driver.

*Evaluated with $f = 200.0$ hz, $V = 1.0$ (v, p-p) sine wave input to driver.

Figure 27 shows data taken at the midspan of the rotor. The first mode at 10 100 rpm was suppressed using active stiffness. The second mode response was suppressed using a combination of active stiffness and damping.

Lewis contact: A. Kascak,
(216) 433-6024
Headquarters program office: OEST

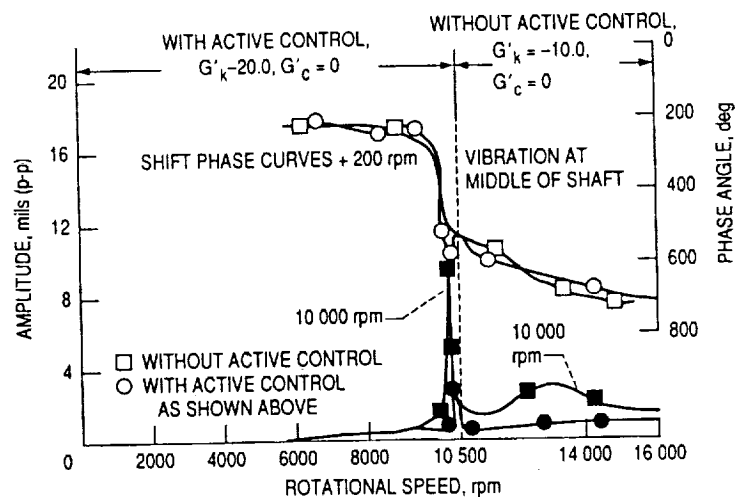


FIGURE 27. - MIDSPAN VIBRATION WITH AND WITHOUT ACTIVE DAMPING AND STIFFNESS. EFFECT OF ACTIVE STIFFNESS AND ACTIVE DAMPING ON FIRST AND SECOND MODE.

Global Approach Identifies Structural Joint Properties

Joints usually contribute significantly to the overall system stiffness, damping, and in many cases, nonlinearity. It is critical that reliable joint models be made available. For many structural systems, the constituent components often can be modeled accurately, but the joints contain considerable modeling uncertainty. Accurate system response predictions often are highly dependent on valid joint models.

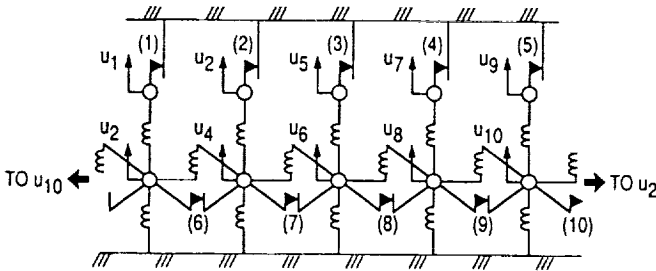


FIGURE 28. - BLADED-DISK ASSEMBLY MODEL. PARENTHESES () INDICATES PARAMETER: 1 TO 5 TIP, 6 TO 10 MIDCHORD; u INDICATES DEGREE OF FREEDOM.

NASA Lewis has developed a global approach for identifying the properties of structural joints. The procedure, which uses experimental response data, shown in Figure 28, is considered general because it is applicable to any size or type of structural system. In addition, characteristics such as damping, stiffness, and nonlinearities in joints, can be identified.

This global approach is applicable to both linear and nonlinear joints and is suitable for processing test data measured at arbitrary stations on the structural system. The approach identifies joint parameters by performing a "global" fit between the predicted and measured data. It improves on previous methods because it can better handle parameter-dependent constraints (e.g., gaps).

The approach was demonstrated with a friction-damped, bladed-disk assembly. This assembly is a relatively complex system that exhibits considerable joint damping. For typical bladed-disk assemblies, the dominant joint damping originates from blade tip rubbing or from interblade friction forces acting at the blade's shroud locations.

In order to identify connection parameters, the complete structural system was excited at various stations along the structure, and the resulting response (e.g., displacements and velocities), measured. The measurement stations may or may not be collocated with the excitation the number of measurement stations may or may not be equal to the number of input excitations. In general, it was simpler to excite the system

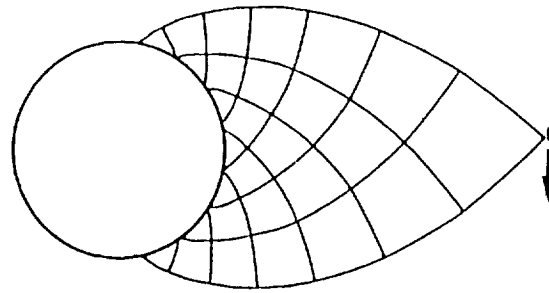
with a single input, then measure the resulting response at multiple stations. The input must be known and the output measured, regardless of the number of stations. Response measurements need not be stationed directly at the connection boundaries, but may be established at any convenient position on the system.

Lewis contact: Dr. Charles Lawrence,
(216) 433-6048
Headquarters program office: OAET

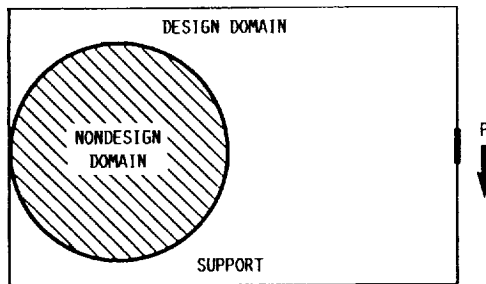
Structural Shape Optimization

As part of the computational methods effort within the Branch, automated techniques to perform structural optimization are under investigation in conjunction with the University of Michigan. A major difficulty of shape optimization of structures is caused by large domain changes during the optimization process that requires the re-discretization of the domain to conduct finite element-stress analysis. Changes of topology such as introduction of weight-saving holes in the structure are virtually impossible with existing optimization approaches, unless done manually. To resolve these difficulties and limitations of traditional shape optimization, a new method has been developed. Optimization and discretization are performed in a fixed domain using a "unit-cell" approach to automatically generate optimal shape and topology from a fixed domain, subject to given load and support conditions. The design domain is discretized into a grid-work pattern of unit-cells whose areas are modified sequentially until compliance of the structure is minimized subject to a user-defined weight and material strength constraints. Unit-cell areas are tailored during the optimization using a percent-void parameter that varies between 0.0 for a heavily loaded (e.g., full) unit-cell, to 1.0 for a lightly loaded (e.g., empty) cell.

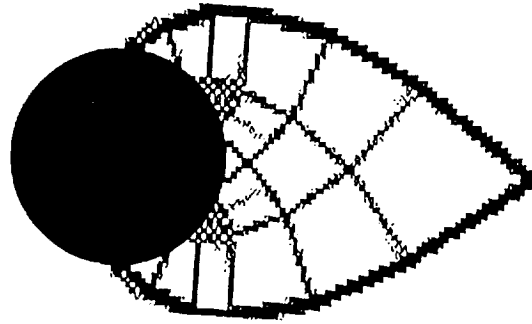
The method was successfully demonstrated, as Figure 29 shows, using the classical test case of a cantilever beam with an overhung load. The Michell Truss shown in the lower right corner of the figure is the optimal (e.g., minimum weight) truss structure for carrying bending loads to a circular attachment pin. The structural shape predicted by the unit-cell shape optimization technique is shown in the upper right corner of the figure. It bears a remarkable resemblance to the optimum. Structural designers using optimal shapes predicted from this method can easily "mentally smooth" the slightly irregular pattern and quickly complete the component's final design.



(a) ANALYTICAL SOLUTION OF MICHELL TRUSS WITH VERTICAL LOAD, P, AT FREE END.



(b) INITIAL MODEL. DOMAIN DISCRETIZED WITH UNIT CELL ELEMENTS.



(c) RESULTING OPTIMIZED STRUCTURE.

FIGURE 29. - COMPARISON OF OPTIMIZED STRUCTURE PREDICTED BY UNIT CELL APPROACH TO CLASSICAL MICHELL TRUSS.

Lewis contact: B. Stemetz,
 (216) 433-3302
 Headquarters program office: OAET

Space Station Structures Analyzed by Probabilistic Structural Methods

Probabilistic structural analysis methods (PSAM) contained in the Numerical Evaluation of Stochastic Structures Under Stresses (NESSUS) computer code are being used at NASA Lewis to analyze typical trusses that will be used in the design of the space station.

It is a common practice to evaluate the structural integrity of trusses with the aid of deterministic analysis techniques and appropriate load or safety factors. However, PSAM considers the various uncertainties in a formal quantitative manner rather than as either single values or upper- and lower-bound values. A truss is probabilistically analyzed, as Figures 30 and 31 show, by defining the primitive design variables, such as spatial truss geometry, stiffness parameters, applied loads, and moments, which are described in terms of probability density functions. The cumulative distribution functions for the response functions and the sensitivities associated with the

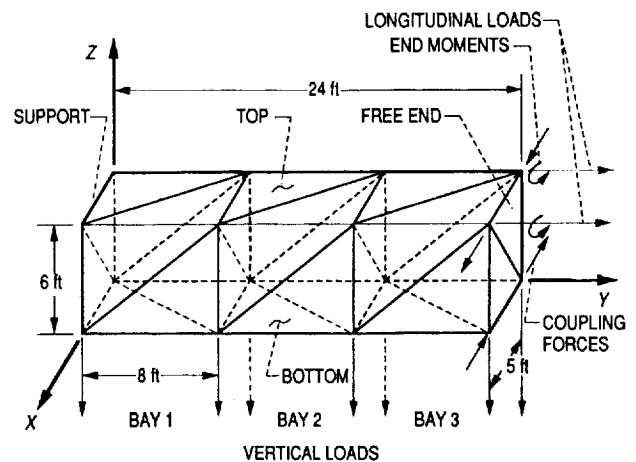


FIGURE 30. - SOLAR ARRAY PANELS MAST - TYPICAL TRUSS.

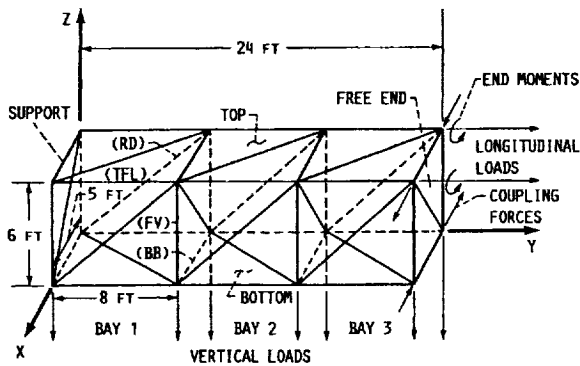


FIGURE 31. - SOLAR ARRAY PANELS MAST - TYPICAL TRUSS.

primitive variables for given responses are investigated. The probabilistic structural responses indicate substantial scatter in natural frequencies and in some member axial forces, but show less scatter in the displacements.

These methods have a prominent role in designing complex structural components because they can consider various uncertainties in the design variables and ultimately may prevent unanticipated failures.

Lewis contact: Shantaram S. Pai,
 (216) 433-3255
 Headquarters program office: OAET

Life Prediction

Multiaxial Fatigue-Life Modeling at High Temperatures

Structural components in aerospace propulsion systems of interest to NASA are frequently life limited by fatigue cracking. Invariably, fatigue cracking initiates at surface locations of high stress and strain. In addition, the local state of stress and strain is seldom uniaxial. Instead, there is a component of stress perpendicular to the maximum principal stress, i.e., the stress state is regarded as biaxial, or in more general terms, multiaxial. The degree and time phasing of multiaxiality of stress and strain is extremely important to the fatigue-cracking process, requiring quantitative models for accurate fatigue-life assessment. Multiaxial fatigue research at Lewis has been boosted in recent years with the addition of three state-of-the-art, tension-torsion biaxial testing systems. Broad,

long-range programs are underway and significant progress is being achieved.

An initial program was designed to assess the high-temperature applicability of existing, lower-temperature, multiaxial fatigue-life models. In this program, high temperature (760 °C), pure axial, pure torsional, and in-phase and out-of-phases axial-torsional fatigue tests were performed on a wrought cobalt-base alloy, Haynes 188. This alloy sees considerable use in the hot sections of various aerospace propulsion systems. These tests are part of a broader investigation into the biaxial and thermomechanical fatigue and deformation behavior of this complex dynamically strain aging alloy. Micro-mechanistic understanding of the deformation and cracking processes are being pursued in-house.

Previous multiaxial fatigue studies on other materials have shown that, under certain multiaxial stress conditions, fatigue lives can be as much as an order of magnitude lower than the fatigue lives under equivalent uniaxial strain conditions. Results to date show less sensitivity to multiaxial stress-strain states than literature results for other materials. Low-cycle fatigue lives under 90 °C out-of-phase, axial-torsional fatigue (normally considered a worst case for this type of loading) are, on average, within a factor of 3 of the fatigue lives observed in uniaxial tests. As expected, the cyclic strain hardening under out-of-phase, axial-torsional loading is much greater than for other loading conditions.

Development of critical data sets such as the one recently completed will help produce accurate and realistic multiaxial fatigue-life prediction models for use with high-temperature structural components of interest to NASA.

Lewis contact: Peter J. Bonacuse,
 (216) 433-3309; and Dr. Sreeramesh Kalluri,
 (216) 433-6727
 Headquarters program office: OSF

Nonlinear Cumulative Fatigue-Damage Model Validation

The useful lifetime of aerospace propulsion systems is frequently limited by fatigue failure. Accurate calculations of expected fatigue lifetime are important and rank with calculations of expected performance and costs. The classical linear damage rule (LDR) is used universally in engineering structural design and fatigue-life assessment. Unfortunately, it can be highly unconservative. Rather than building up linearly with usage, fatigue damage accumulates in a highly nonlinear manner. Recognition and modeling of this nonlinearity has

been a thrust at NASA Lewis for a number of years. This year, a significant advance was made in the experimental validation of our nonlinear fatigue damage accumulation models.

A complex sequence of high-, intermediate-, and low-cycle fatigue, block-loading levels was used in a validation program performed, under Grant by Case Western Reserve University, using Lewis equipment. Fatigue tests were conducted using axially loaded specimens. Experimental sequences were selected to accentuate differences between the linear and nonlinear fatigue-life prediction models. These data represent the only known results of this nature. The material, Haynes 188, a wrought cobalt-base superalloy, is used in aeronautical gas turbine engine combustors and in the liquid oxygen (LOX) positions of the main engines of the Space Shuttle. Experimental validation results have been applied to numerous NASA-developed nonlinear cumulative fatigue damage models. One nonlinear model, the Double Linear Damage Rule (DLDR), has been selected for comparison with the experimental results. It is one of the simplest models to apply to complex loading sequences. Comparison is also made with the Linear Damage Rule (LDR) model.

Only a sampling of the extensive results is displayed. Each set of bar graphs represents a different sequence among the three discrete levels of fatigue loading. Bar height indicates the number of loading blocks required for fatigue failure, whether predicted or observed. Two important observations were made. First, the classic LDR model over predicts the observed fatigue lives by factors of as much as three, producing a high degree of nonconservatism in life expectancy. Second, and equally important, experimental results agree quite well with the DLDR predictions, validating the accuracy of this nonlinear model for the prediction of fatigue lives under complex loading histories.

Lewis contact: Dr. Gary R. Halford,
(216) 433-3265
Headquarters program office: OSF

Crack Bridging in Metal Matrix Composites Modeled Analytically

The ability to predict fatigue crack growth behavior of metal matrix composites (MMC's) is of particular interest because these materials contain many crack-like defects. These cracks propagate and coalesce under cyclic loading and result in sudden catastrophic fracture. Experimental studies on a number of MMC's have shown that cracks tend to propagate in the ductile matrices, leaving behind unbroken fibers bridging

the facing crack surfaces. Crack bridging by fibers has been shown to decrease the crack growth rates by decreasing the near-crack-tip displacements. Understanding crack growth behavior in MMC's is paramount to the development of accurate life prediction models for composite structures. Future NASA missions will depend upon our ability to use MMC's in reusable structural applications where durability is essential for success.

Crack bridging has been analytically modeled, as Figure 32 shows, to determine its effects on fatigue crack propagation rates and crack opening displacements. The phenomena are complex and modeling efforts are difficult. Nevertheless, NASA Lewis has a strong continuing commitment to solve these vexing problems. The material modeled is a silicon-carbide-fiber-reinforced Ti-15-3-3-3-matrix MMC. Two different models were used to simulate crack bridging. The first model was the so-called shear lag model. This model is based on the relative sliding between the fiber and the matrix in the region where the interfacial shear stresses exceed the frictional shear stresses. The second model was the newly formulated fiber pressure model. This model assumes that the decrease in the crack driving force due to bridging is proportional to the normal and bending forces carried by the fibers.

The analytical results for both models were compared with experimental data obtained from tests performed in a specially designed loading stage mounted inside a scanning electron microscope. Use of this facility allowed for precise measurements of crack opening displacements and crack growth rates. Experimental results revealed a decrease in crack growth rates with an increase in the crack length.

Both models were successful in describing the fatigue crack growth behavior of this MMC in terms of a calculated effective crack driving force ΔK_{eff} . Also, both models accurately predicted crack opening displacements as well as the experimentally observed decrease in the crack growth rates and the

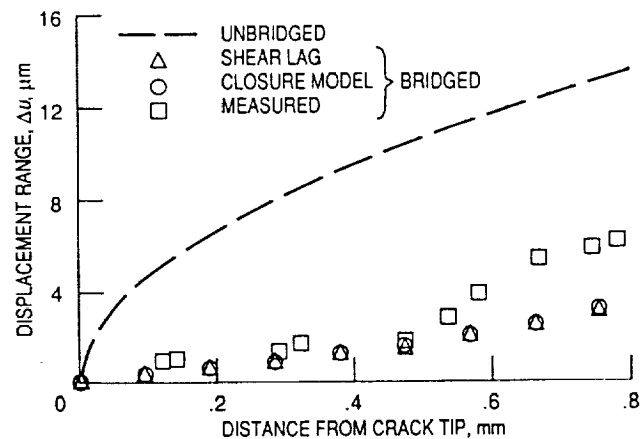


FIGURE 32. - ANALYTICAL AND EXPERIMENTAL CONFIRMATION OF BENEFIT CRACK BRIDGING.

eventual crack arrest. The advantage of the fiber pressure model is that it requires substantially less computing time than the shear lag model. Also, some of the material properties needed to run the shear lag model are difficult to obtain.

Improved crack bridging models permit more accurate life prediction modeling for structural components made of MMC's.

Lewis contact: Jack Telesman,
(216) 433-3310
Headquarters program office: OAET

High-Temperature Fatigue Modeled for a Tungsten/Copper Composite

Fatigue failure of high-temperature, metal matrix composites (MMC's) is a complex process and a subject of current intense research activity at NASA Lewis. Matrix cracking, fiber/matrix interfacial failure, and fiber fracture work together to result in fatigue failure. Depending on the failure process of the composite system of interest, a dominant failure mode can be identified, as Figure 33 shows. Modeling of dominant failure modes can serve as the basis of fatigue life prediction schemes for MMC's. Future NASA missions will require accurate predictions of MMC structure life.

A tungsten-fiber-reinforced, copper-matrix composite is a candidate material for rocket nozzle liner applications. Previous research on the fatigue behavior of a 10-volume percentage tungsten/copper composite at high temperatures had shown that the composite fails primarily due to copper-matrix degradation. Fatigue cracks initiate and propagate inside the copper

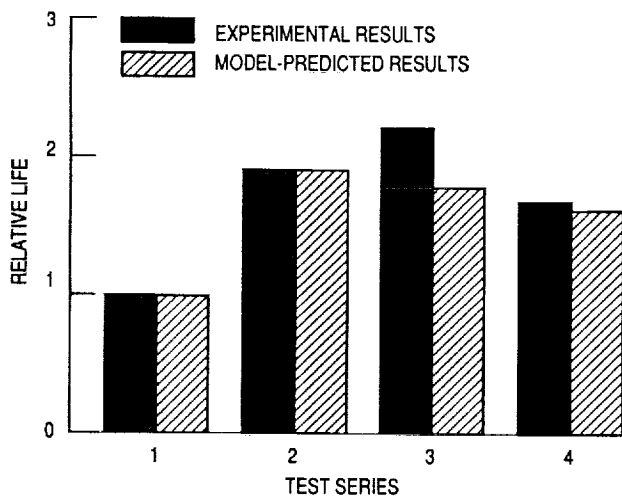


FIGURE 33. - VALIDATION OF MMC LIFE PREDICTION MODEL FOR TUNGSTEN/COPPER.

matrix through a process of initiation, growth, and coalescence of grain boundary cavities. The ductile tungsten fibers "neck down" locally and rupture after the surrounding matrix fails. Complete failure of the composite follows.

A fatigue life prediction model for the tungsten/copper composite system has been developed at NASA Lewis. The model is based on microscope-observed failure mechanisms. The composite is assumed to fail when the matrix fails. The failure mechanisms of the fiber and its contribution to the overall composite fatigue life are neglected. It is assumed that no interfacial debonding or degradation occurs. Analysis is limited currently to isothermal fatigue of a unidirectional composite.

In the model, the composite is assumed to fail when the average cavity in the matrix reaches a critical size. The cavity nucleation process in the copper matrix is neglected by assuming the pre-existence of cavities in the as-received composite. This assumption was confirmed through metallographic examinations. In addition, available literature indicates high-temperature cavity nucleation to be very fast relative to cavity growth. Cavities are assumed to begin to grow at the moment of load application, at the same rate. The average cavity growth size as a function of time is calculated by using a creep-cavity growth law. It is assumed that cavities grow with a quasi-equilibrium shape controlled by coupled diffusion and plasticity. Spatially averaged instantaneous stresses and strain rates in the matrix were used to calculate cavity size. The average matrix stress is based on an isostrain condition between the fibers and the matrix.

The model predicted fatigue lives were compared with the experimental results of a series of load controlled, tension-tension fatigue test conducted at 560 °C on 10-volume percentage tungsten/copper. Predicted lives were in agreement with experimental results. The numerically calculated cavity size was found to vary with cycle number, like the experimentally-observed cyclic change of the composite maximum tensile strain.

Lewis contact: Michael J. Verrilli,
(216) 433-3337
Headquarters program office: OAET

Characterization of Failure Mechanisms of Fiber-Reinforced Ceramic Composites Using In-Situ Non-destructive Evaluation Monitoring (NDE) Techniques

An understanding of failure mechanisms is not mature for ceramic matrix composites. We currently lack sufficient knowledge of the initiation and propagation of matrix cracks and fiber breakage. This lack of understanding also hinders composite development which primarily depends on obtaining optimal interface properties, and maintaining high fiber strength of elevated temperatures. The objectives of using in-situ Nondestructive Evaluation (NDE) monitoring techniques are: (1) to investigate and understand the mechanical behavior of SiC/RBSN composites throughout their loading history; (2) to study the effects of fiber/matrix interface debonding; and (3) to identify the occurrence and nature of damage and failure mechanisms.

By using acoustic emission and x-radiograph techniques, discrimination of failure mechanisms is possible throughout loading history. Energy, event duration and peak amplitude are key Acoustic Emission (AE) parameters. An understanding of failure sequences is achieved via three-dimensional

plots with respect to the load and strain time based parameters, as Figure 34 shows. In-situ x-ray film radiography is a helpful and practical technique for determining the interfacial shear strength based on the periodic matrix crack spacing method.

Bibliography

Chulya, A., et al.: Characterization of Damage and Fracture Mechanisms in Continuous-Fiber-Reinforced SiC/RBSN Matrix Composites by Acoustic Emissions in NASA-CP-10041, pg. 55-1 to 55-15.

Lewis contact: Dr. Abhisak Chulya/CSU,
(216) 433-8523
Headquarters program office: OAET

New Method for Determining Probability of Failure Initiation in Rotating Structures

Using probabilistic methodology, a component's design survivability can be mapped incorporating finite element analysis and probabilistic material properties. The method, as Fig-

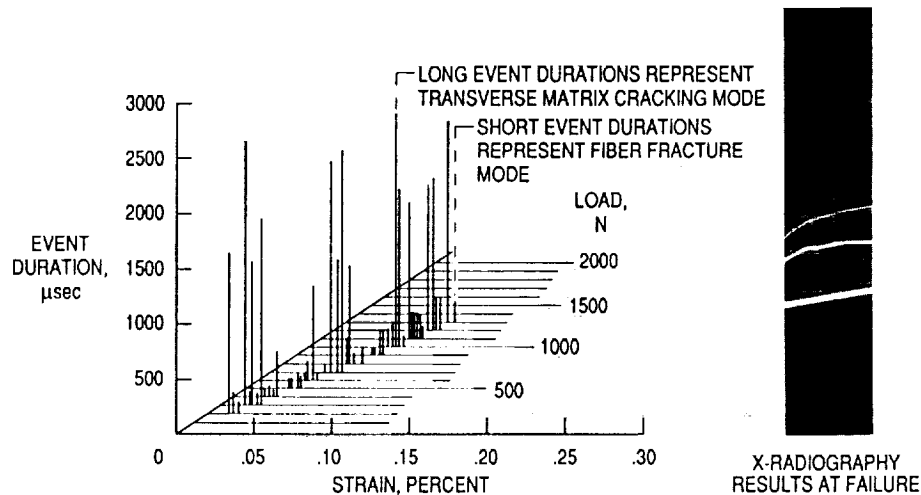


FIGURE 34. - ACOUSTIC EMISSION (AE) RESULTS FOR ENTIRE LOADING HISTORY.

ure 35 shows, evaluates design parameters through direct comparisons of component survivability expressed in terms of Weibull parameters. The method allows the use of statistical data obtained from laboratory coupon testing under environmental conditions to be integrated into life and risk analysis of full-scale engine structures.

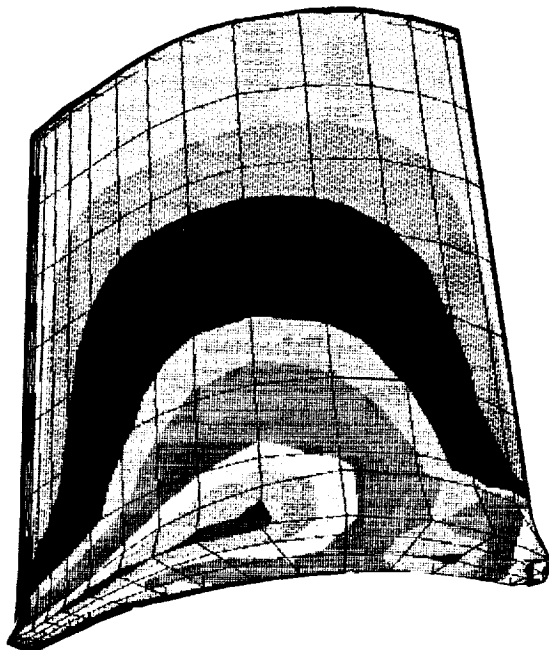
It is possible through an interactive design process to minimize the risk of failure for a given operating time or conversely to design for a finite life for a defined risk. Where the Weibull parameters and the materials stress-life exponent are unknown, it is permissible to assume these values in order to obtain a qualitative evaluation of a structural design, if not a quantitative evaluation. We are applying these methods for full-scale structures such as turbine blades and disks where full-scale component data do exist.

Lewis contact: E.V. Zaretsky,
(216) 433-3241; M.E. Melis,
(216) 433-3322; and R. August,
(216) 433-6614.
Headquarters program office: OAET

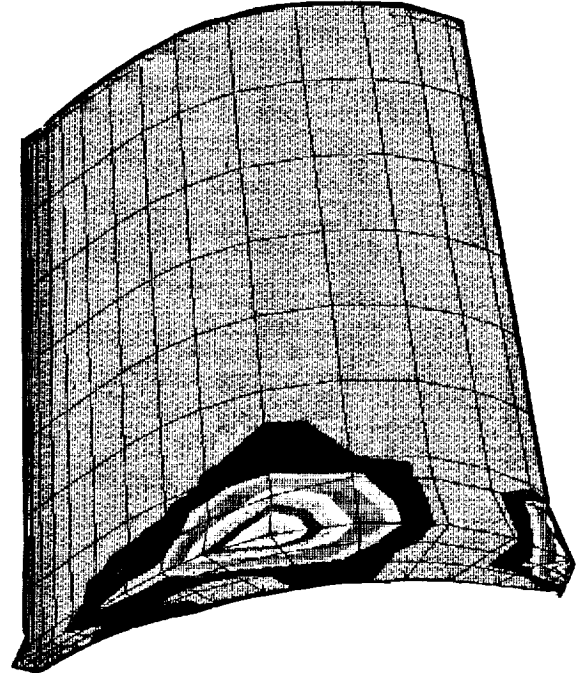
Instruments, Controls and Testing Techniques

Inductively Heated Susceptors for Thermomechanical Testing of Ceramic Matrix Composites

Ceramic matrix composites (CMC) are being considered for applications involving temperatures up to 3000 °F (1650 °C). The propulsion systems for NASA's next generation of aerospace vehicles produced from these materials will be subject to complex temperature-stress excursions as part of their normal operating conditions. These temperature-stress excursions subject the components to thermomechanical fatigue, which limits the useful lives of the CMC components. In order to provide a reliable data base for design purposes, heating methods must be employed for controlled laboratory testing that can simulate these thermal histories.



SHEAR STRESS DISTRIBUTION



PROBABILITY OF FAILURE

FIGURE 35. - NEW METHOD FOR DETERMINING PROBABILITY OF FAILURE INITIATION IN ROTATING STRUCTURES.

One method is the induction heating of a ceramic susceptor that encloses the gauge section of the test specimen. Induction heating method is preferable to other types of thermomechanical testing since it decreases the amount of time required for heating and cooling of the specimen.

In this study, a silicon-carbide susceptor, has been built that is inductively warmed. It radiantly heats a tensile specimen that is made out of a silicon nitride-matrix reinforced with silicon-carbide fibers. The temperature distribution along the gauge section was excellent resulting in a temperature gradient of only 6 °C at a temperature of 1650 °C. A temperature cycle of 1000 °C range can be performed within a 10-minute period.

This capability of performing very high-temperature tests with complex temperature and load histories enables researchers at NASA Lewis to obtain realistic data bases required to design CMC based components.

Lewis contact: Dr. Dennise Worthem,
(216) 433-3209
Headquarters program office: OAST

Flat Tensile Specimen Design for Advanced Composites

New classes of composite materials are proposed for aerospace applications involving severe thermomechanical loading. As a result, the need exists for reliable data bases of the composites' mechanical behavior for design, analysis, and processing studies. Extensive testing is required to generate the required data bases. Critical to this task is the use of specimen geometries that can provide reliable, reproducible data.

Flat, reduced gauge-section tensile specimens are used for the mechanical testing of advanced composites. Most of the new fiber-reinforced, high-temperature composites are currently available only in relatively thin plate form, which restricts specimen geometries. Concerns with the use of the reduced gauge-section specimen focus on failures occurring in the transition region between the grip region and the gauge section due to stress concentrations present there. Another concern is premature failures occurring in the grip region under or near the tab.

The goal of this study was to determine and evaluate a specimen design that would produce more consistent failures in the straight sided gauge section. Also, tab material and specimen composite combinations were evaluated to avoid premature failure in the grip region.

Finite element analyses of flat, reduced gauge-section tensile specimens with various transition contours were performed. An optimum transition contour was determined. It was also determined that transition stress values were not sensitive to the specimen material properties of interest.

Stress values in the grip region were sensitive to specimen composite and/or tab material properties. It was found that an evaluation of stresses with different specimen composite/tab-material combinations must account for material nonlinearity of both the tab material and specimen composite. Material nonlinearity can either relieve the stresses in the composite under the tab, or elevate them to cause failure under the tab.

Lewis contact: Dr. Dennis Worthem,
(216) 433-3209
Headquarters program office: OAST

Stable Poisson Loaded Specimen for Mode I Fracture Testing of Ceramic Materials

Monolithic and toughened composites are candidate materials for aerospace application where very high-temperature capabilities are required. These ceramic-based materials contain small crack-like defects developed during processing. These defects grow in a stable manner under applied loading until the crack reaches critical length, which leads to a catastrophic failure. The ability to investigate and model fatigue crack growth and fracture in monolithic and toughened ceramic materials has been hindered by the inability to produce stable crack growth. Stable crack growth in ceramic materials is complicated by the low damage tolerance and relatively high stiffness exhibited by ceramic materials. Experimental studies conducted at NASA Lewis have shown that, with common fracture tests, the unavoidable transfer of elastic energy from the test fixture to the specimen critically affects propagation stability.

Both the Chevron and beam indentation specimens provide methods of producing stable crack growth in brittle materials, however, questions regarding R-curve behavior and crack driving forces are as yet unresolved. Extensive subcritical, through thickness, crack growth has been obtained with the Stable Poisson Loaded (SPL) specimen developed at NASA Lewis. The SPL specimen utilizes the diametral expansion of a compressively loaded cylinder to apply displacements to a ceramic test sample. The loading configuration and specimen design ensures subcritical crack growth by providing an extremely high degree of applied displacement control.

Subcritical growth was achieved by minimizing the transfer of stored elastic energy to the specimen during fracture. The geometrical symmetry of the radially expanded load pin, and self-alignment of the load pin with the test specimen are added benefits of the test method. The test fixture shown allows optical monitoring of crack growth at high magnification with a traveling microscope.

Through-thickness, subcritical crack growth has been sustained in soda lime glass, alumina, silicon-carbide, and silicon-nitride specimens for distances in excess of 20 mm. The test program is proceeding with an investigation of the R-curve behavior in unreinforced alumina.

Lewis contact: Anthony M. Calomino,
(216) 433-3311; and David N. Brewer,
(216) 433-3304
Headquarters program office: OAST

In-Situ X-Ray Monitoring of Damage Accumulation in SiC/RBSN Tensile Specimens

Ceramic matrix composite (CMC) systems are being developed for heat engine applications. The ultimate goal of

current research is an understanding of composite behavior to better optimize the composite properties for different hot section applications. CMC's are being developed because they provide enhanced material toughness while maintaining the useful properties of monolithic ceramics. In order to use CMC's more effectively, their failure processes and damage tolerances must be understood; and, in turn, their failure analysis and mechanics models improved. In-situ x-ray radiography can help in imaging failure sequences and damage accumulation in composite specimens under loading. Information gathered from such in-situ monitoring can help in the development and validation of analytical models, and in the coordination between experiment and theory. Damage and failure mechanisms, such as, transverse matrix cracking, fiber-matrix debonding, fiber breaking, fiber pullout, and delamination can be better understood if imaged and identified as they occur. Such in-situ examination will help identify and clarify the sequence in which these mechanisms take place. Plus, it aids in the identification of deformation controlling properties, i.e., whether they are matrix-dominated properties, fiber-dominated properties, or a combination of both.

An in-situ x-ray and materials testing system (IX-MTS), as shown in Figure 36, was developed to conduct in-situ x-ray monitoring of materials under loading. The IX-MTS was capable of: (1) monitoring damage accumulation in silicon carbide-fiber-reinforced, reaction-bonded, silicon-nitride (SiC/

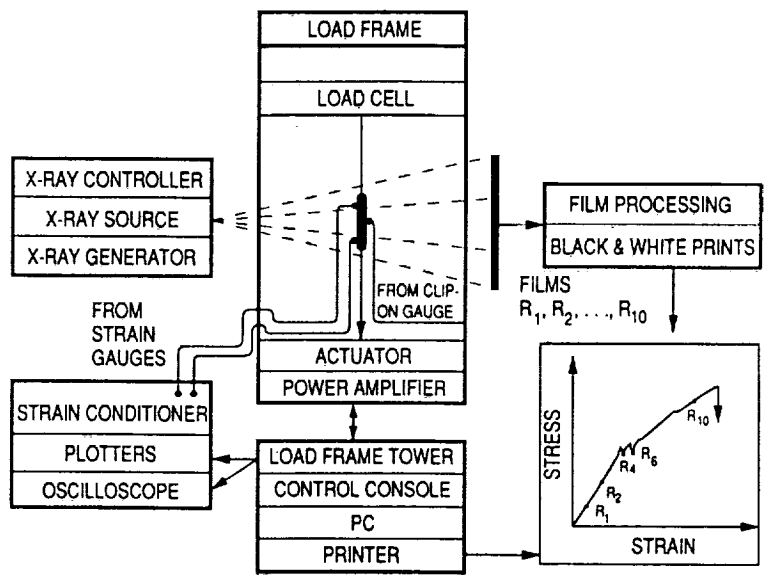


FIGURE 36. - SCHEMATIC DIAGRAM OF IN-SITU X-RAY AND MATERIALS TESTING SYSTEM (IX-MTS).

RBSN) composite specimens; and (2) of determining interfacial shear strength between the SiC fiber and the RBSN matrix by the matrix crack spacing method. The IX-MTS was used to study the effect of local density variations on the fracture behavior of composites. Further, the IX-MTS approach can be used to study thermal and oxidation effects on the interfacial shear strength of composites. The conclusion is that this approach can provide a basis for interpretation of mechanical tests, for validation of analytical models, and for verification of experimental procedures.

Lewis contact: Geroge Y. Baaklini,
(216) 433-6016; and Ramkrishna T. Bhatt,
(216) 433-5513
Headquarters program office: OAET

Ultrasonic Theory and Experimental Technique Developed to Nondestructively Evaluate Ceramic Composites

Composite materials with low densities and good high-temperature properties are being developed for use in the next generation of aerospace systems. Both the National Aerospace Plane (NASP), a transportation system that will take off like a conventional aircraft, fly at Mach 25 directly into orbit, and land like a conventional aircraft, and the High-Speed Civil Transport (HSCT), an aircraft that will transport 250 passengers at Mach 3.2 for 5000 n mi, will require advanced composite materials for propulsion and structural components.

The strength and toughness of ceramic composites are limited by the degree of bonding between the fiber and the matrix material. Unfortunately, the only way to determine the quality of this bond has been by destructive testing. However,

the nondestructive technique called angular power spectrum scanning (APSS) has been developed at NASA Lewis, see Figure 37, that makes use of the sensitive interaction of ultrasound with the pores, fibers, and grains which make up these ceramic composites.

To nondestructively evaluate composite materials, we need to understand the interaction of ultrasound with each of the scattering components in the composite. Ultrasonic scattering mechanisms for ceramic composites have been identified by examining the interaction of ultrasound with individual fibers, pores, and grains. The following are dominant ultrasonic scattering mechanisms for ceramic composites:

- (1) Symmetric diffractive scattering at individual pores;
- (2) Symmetric diffractive scattering at the fiber/matrix interface; and
- (3) Asymmetric refractive scattering at density gradients in the matrix material.

Grain boundary scattering in the matrix material has been found to be negligible for both (silicon carbide and silicon nitride) SiC and Si₃N₄.

The new nonintrusive, ultrasonic evaluation technique, angular power spectrum scanning takes advantage of the symmetry of the scattering mechanisms. APSS uses a collimated ultrasonic beam directed at one side of a composite sample. The ultrasonic energy is measured as a function of the half-solid angle on the other side of the sample. The energy as a function of angle and constant-energy contours can be obtained at each point on the sample.

Composites having a uniform microstructure yield symmetric angular power spectrums. Any asymmetry in the observed angular power spectrums indicates the presence of porosity gradients. Diffractive patterns created by the interaction of ultrasound with the fiber and the fiber/matrix interface can be used to identify variations in bond quality throughout the bulk of the material. This information is not available by any other nondestructive technique.



(a) BEFORE THERMAL CYCLING. (BANDS ARE CAUSED BY GOOD FIBER/MATRIX BOND.)

(b) AFTER THERMAL CYCLING. (MISSING BANDS INDICATE DEGRADATION IN BOND QUALITY.)

FIGURE 37. - APSS ULTRASONIC IMAGES.

Bibliography

Generazio, E.R.: Theory and Experimental Technique for Nondestructive Evaluation of Ceramic Composites. NASA TM-102561, 1990.

Lewis contact: Dr. Edward R. Generazio,
(216) 433-6018
Headquarters program office: OAET

Improved Transverse Crack Detection in Composites

The use of ultrasound to obtain images of flaws or damage in polymer composite laminates is well established and quite effective. In a common procedure, called the C-scan, an

ultrasound transducer scans an area of the laminate. The amount of energy transmitted through the laminate (transmission method), or reflected back from the laminate (pulse-echo method), is displayed to produce an image showing flaws or defects. This technique, as shown in Figure 38, is particularly effective in detecting debonding between plies of the laminate. However, cracks that occur through the thickness are not easy to detect since the waves propagate parallel to the crack, often leaving them undetected. Transverse cracks are important because it is often the first type of damage to occur as a result of either thermal or mechanical loading. A modified C-scan technique was developed in-house to improve the detection of these transverse cracks by using oblique shear waves as opposed to normal longitudinal waves used with the standard method.

When a longitudinal wave traveling in a fluid is incident at an angle on an anisotropic solid, such as a composite laminate, three types of waves are typically generated in the solid. These waves are termed quasi-longitudinal (QL), vertically

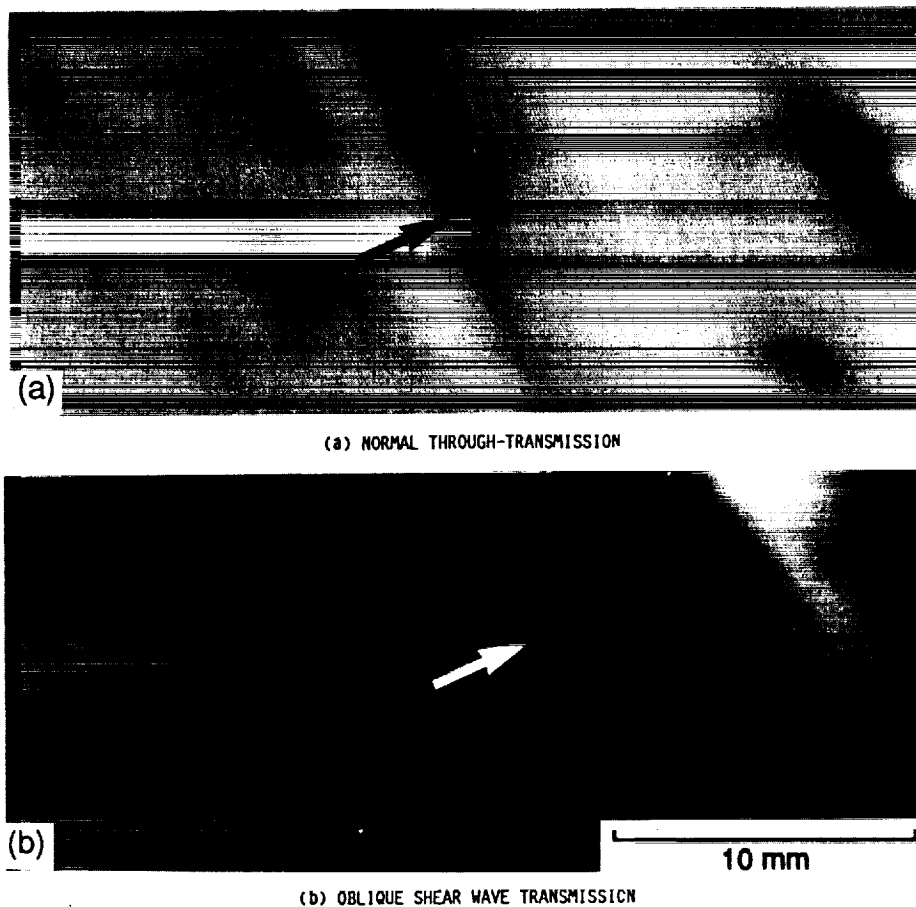


FIGURE 38. - IMAGES OF A TRANSVERSE CRACK IN A 60° OFF-AXIS UNIDIRECTIONAL SAMPLE USING THE TWO TYPES OF C-SCANS. THE SHEAR WAVE METHOD PRODUCES AN ENHANCED IMAGE. ARROWS INDICATE LOCATION OF CRACK.

polarized quasi-shear (QSV) and horizontally polarized quasi-shear (QSH) waves. In the technique developed here, the incident angle is calculated such that the QL waves are completely reflected from the solid, and QSH waves are not generated. The remaining QSV waves, which are transmitted through the laminate at an oblique angle, are used to detect the presence of transverse cracks. An advantage of this method is that it can be used with very little modification to standard C-scan equipment.

Initial results have shown that this technique is more effective in detecting transverse cracks than the standard method. It is being used in an ongoing research project in the Structures Division to measure damage progression in polymer composites.

Bibliography

Pereira, J.M.; and Generazio, E.R.: Improved Transverse Crack Detection in Composites. NASA TM-103261, 1990.

Lewis contacts: Michael Pereira,
(216) 433-6738; and Edward Generazio,
(216) 433-6018
Headquarters program office: OAET

Mechanisms

Contact Area Temperature Profile of an Engaging Sprag Clutch

The sprag overrunning clutch is an integral part of a helicopter's drive train. It transmits torque from the engine to the combining gearbox and overruns when the gearbox output rotates faster than the engine. These clutches operate on the wedging action of small sprags located between the inner and outer race. The kinematics of an engaging sprag are understood; however, what is occurring at the sprag-inner race contact area has not yet been studied. During lock-up, the sprag rotates and produces high pressures and temperatures due to the squeezing of the oil film. A four-square test rig has been constructed to determine the magnitudes of these temperatures since they may approach the tempering range of the inner race material. Data from this test will then help validate a finite element computer code which models the engagement process of the clutch.

Figure 39 shows the layout of the four-square test rig. Power is supplied by a 200 hp variable speed dc electric motor and is transferred to the system through a pulley and belt arrangement. The closed-loop is configured with two end gearboxes, with ratios of 1.5 and 1.286, which allow for a difference in

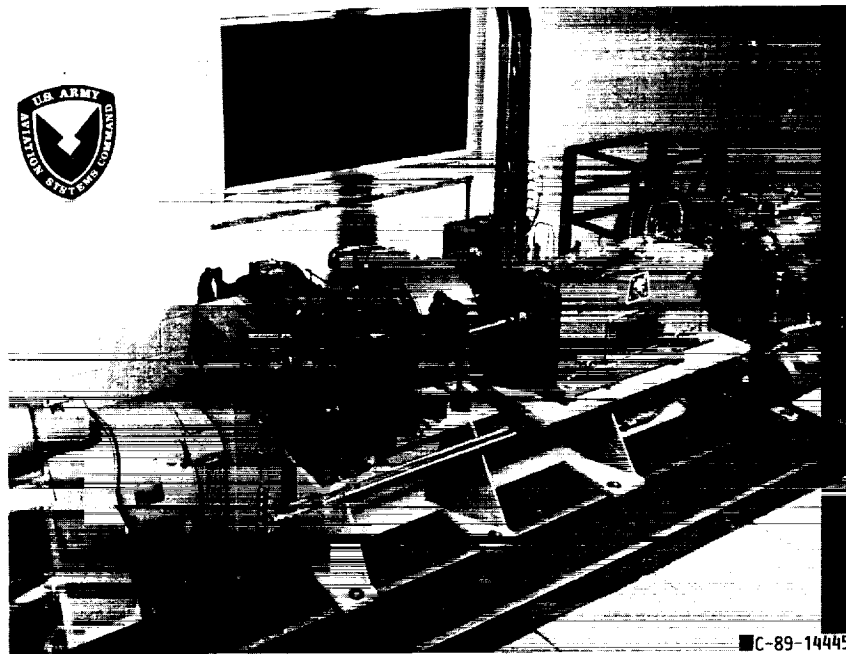


FIGURE 39. - SPRAG CLUTCH ENGAGEMENT TEST RIG.

rotating speeds to occur between the input and output shafts of the magnetic clutch. The sprag clutch test assembly is located on the highspeed shaft with the outside race of the clutch driving the inside race. The inner race has been instrumented with eight thermocouples positioned to give the greatest probability of being near an engaging sprag.

The test will be run with the clutch test assembly rotating at 5000 rpm. During the operation of the rig, the sprag clutch is initially engaged due to the inertia of the shafts and gears. Full sprag lock-up occurs when a voltage is manually applied across the magnetic clutch causing an increase in torque and a decrease in speed of the sprag clutch's output shaft. At that time, temperature measurements will be taken. This will be repeated for a number of engagement cycles since it is difficult to determine when a sprag is directly over a thermocouple. The highest readings from all the cycles performed will be taken as true sprag engagement temperatures.

Lewis contacts: K. Radil,
(216) 433-5047; and A. Kascak,
(216) 433-6024
Headquarters program office: OAET

Active Vibration Control (AVC) Test Results

A limiting factor in achieving higher levels of active damping is electromechanical instability. This phenomena results from the nonideal behavior of any sensor or actuator, and is characterized by increasing phase lag with frequency. The achievable level of active damping (while maintaining stable operation) can be raised by structural or electrical means. Phase lead and filtering circuits may aid by decreasing phase lag or eliminating certain bands of the feedback spectrum. These devices also have detrimental effects including low-frequency amplitude attenuation and phase lag. Consideration of these factors has convinced the PI that the optimum implementation of the piezoelectric actuator Active Vibration Control (AVC) will involve simultaneous design of the electrical control system and the structural rotor-bearing system. This design tool is under development at Texas A&M and consists of software to predict the instability onset gain level. The capability of the software will be tested by comparing its output with results obtained on the Lewis transient dynamics rig during the summer of 1989. The unstable mode of the Lewis rig occurred at approximately 2100 Hz. The corresponding mode shape was identified from transient recorder plots.

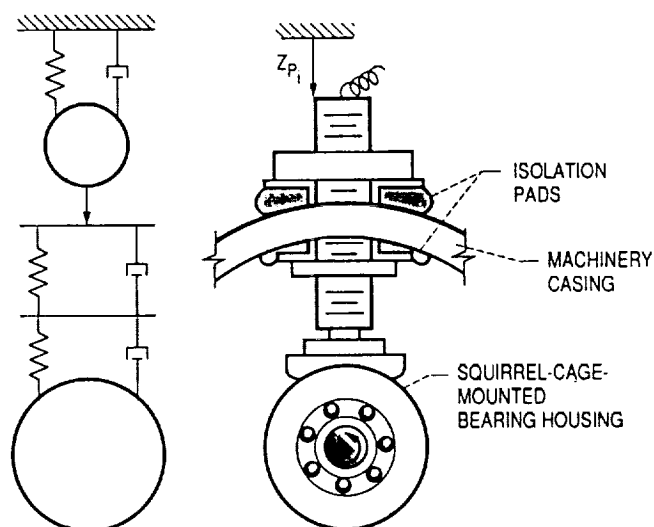


FIGURE 40. - IDEALIZED REPRESENTATION OF THE PUSHER AND ITS CONNECTIONS.

Figure 40 shows a sketch for an isolated bearing in an active damping type vibration control. The opposing piezoelectric actuators are soft mounted on flexible springs (elastomer). Figure also shows the equivalent electro-mechanical model of this setup. Both the piezoelectric pusher and its driver are represented as second order electrical, low-pass filters. This representation was formulated based on measured transfer functions of the pusher and its driver.

Areas for future work include:

- (1) Development of a digital filter to remove high-frequency phase lag of actuators and sensors without introducing any additional phase lag of its own.
- (2) Development of a digital control system which will utilize the excitation capability of the actuator for detection of significant changes in the rotor natural frequencies. This is a good indicator of structural flaws, as part of a maintenance program.
- (3) Development of a digital control system which will measure modal characteristics with the piezoelectric actuators and use this to develop a control strategy.

Lewis contact: A. Kascak,
(216) 433-6024
Headquarters program office: OEST

Hybrid Magnetic Bearing Developed for Cryogenic Applications

A new magnetic bearing has been designed and fabricated by Avcon Incorporated under contract to NASA Lewis. This

bearing is called a hybrid magnetic bearing with permanent magnet bias because it contains both permanent magnets and electromagnets. This new concept has the advantages of reduced size, weight, and electrical power consumption over magnetic bearings currently used in industry. These features make this bearing very attractive for aerospace applications. The bearing was designed for possible use in future space shuttle main-engine turbopumps.

Conventional magnetic bearings employ only electromagnets to achieve suspension and control of rotors. They require large amounts of electric power at all times to suspend the rotor and to produce a bias magnetic flux. The bias magnetic flux linearizes the force-to-current relationship of the bearing and thus simplifies the bearing control system. In the hybrid magnetic bearing the permanent magnets provide the bias magnetic flux so that electric power is not required to perform this function. The electromagnets use only a small amount of electric power to keep the rotor centered in the presence of random disturbances and to counter any high dynamic forces on the rotor. Hybrid bearings use much less electric power than conventional magnetic bearings.

In previous permanent magnet bias bearings, the electromagnet flux had to pass through the permanent magnets, an inefficient use of the electromagnet flux. In this new concept, as shown in Figure 41, the permanent magnets are not in the electromagnet flux path so that the efficiency of the electromagnets is not compromised. The permanent magnets are arranged to produce flux lines along the rotor axis, whereas the electromagnet flux lines are circumferential.

The hybrid magnetic bearing designed under this contract has a radial load capacity of 500 lb. The bearing has a 3.0-in. air-gap diameter, a 5.25-in. stator outside diameter, and a 4.12-in. length. The bearing was installed into an existing rig capable of operating up to 15 000 rpm. The speed is limited by the rig, not the magnetic bearing.

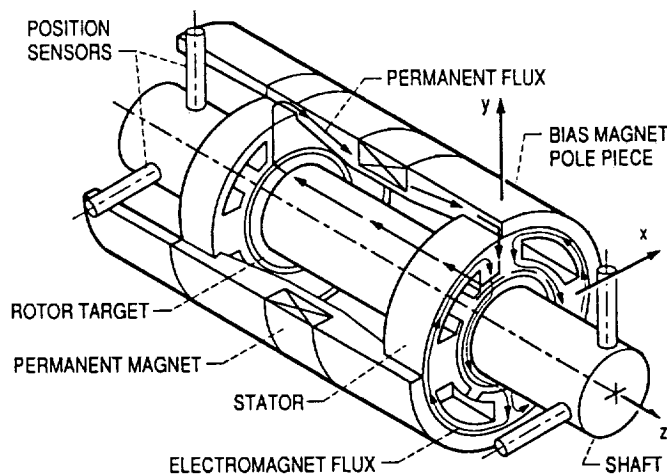


FIGURE 41. - HYBRID MAGNETIC BEARING WITH PERMANENT MAGNET BIAS.

Preliminary tests of the bearing have been performed at room temperature for radial loads up to 400 lb, stiffness up to 100 000 lb/in., and speeds up to 9800 rpm.

Lewis contacts: Eliseo DiRusso,
(216) 433-6027; Dr. Gerald V. Brown,
(216) 433-6047; Albert F. Kaschak,
(216) 433-6024; and Dr. David P. Fleming,
(216) 433-6013
Headquarters program office: OAET

Bearing Elastohydrodynamic Lubrication Formula Made Simple

The lubricant film separating the moving components in a ball or roller bearing is referred to as the elastohydrodynamic (EHD) lubricant film. The theoretical EHD film thickness is reduced by the lubricant's inability to flow into the bearing contact zone fast enough to supply the volume required to establish this theoretical film thickness. An adequate film thickness is necessary for the successful operation of rolling-element bearings. The proper bearing must be chosen for a particular application so that the appropriate film thickness can be obtained. Calculating this film thickness for the selection process is a complex operation.

NASA Lewis has developed a method that reduces the previous complicated EHD formula to a simplified form that requires only the rolling-element bearing's inside and outside diameters, the speed (in revolutions per minute), the lubricant type, and the lubricant viscosity at temperature (in centipoise). In 1990, a graph, as Figure 42 shows, was provided for the first time that was based upon experimental data. It gave the EHD film reduction factor as a function of contact lubricant flow number. This reduction factor accounts for lubricant starvation with the ball or roller-race contact. By using this corrected EHD film thickness, rolling-element bearing life can be determined with reasonable engineering certainty.

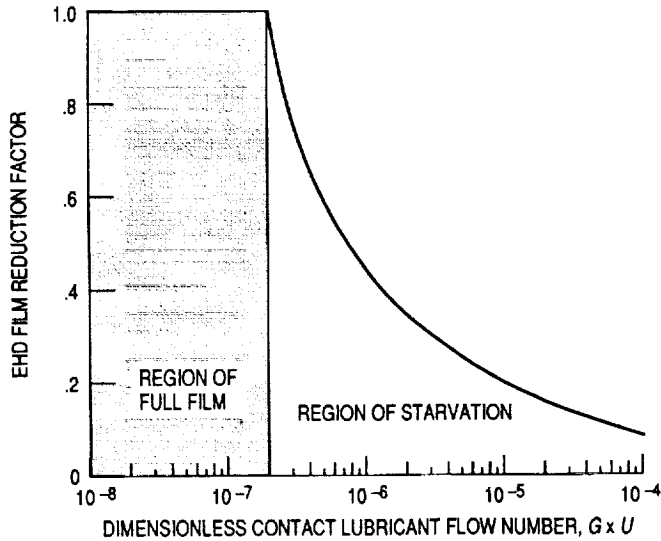


FIGURE 42. - EHD FILM REDUCTION FACTOR AS A FUNCTION OF CONTACT LUBRICANT FLOW NUMBER.

Bibliography

Zaretsky, E.V.: Bearing Elastohydrodynamic Lubrication: A Complex Calculation Made Simple. NASA TM-102575, 1990.

Lewis contact: Erwin V. Zaretsky,
(216) 433-3241
Headquarters program office: OAET

Closed-Form Solution for Hoop Stress in a Ball-Race Contact

In order to prevent motion of the inner race around a shaft, designers have been specifying extremely tight interference fits between the inner race and the shaft when it is not practical to provide a keyway or locknut arrangement. The interference fit is usually based on the anticipated growth of the shaft and the bearing under the most severe operating conditions. These conditions sometimes exist only for short periods in the machine's operating cycle. Nevertheless, it is an extremely important design consideration for both safety of operation and maintainability. In recent years, as shown in Figure 43, some engineers have noticed that bearings with higher than usual press (or interference) fits may have shorter field lives than anticipated or calculated. The failure mechanism is usually classical rolling-element (subsurface) fatigue. There has been no public documentation of the phenomenon.

A finite element method (FEM) analysis of a generic dimensionally normalized inner race of an angular-contact ball bearing was performed under varying conditions of speed and press (or interference) fit of the inner-race bore on a journal. Results of the FEM analysis at the ball-race contact were used to derive an equation from which was obtained the radius of an equivalent cylindrical bearing race with the same or similar hoop stress. The radius of the equivalent cylinder was used to obtain a generalized closed-form approximation of the hoop stresses at the ball-inner-race contact in an angular-contact ball bearing. Results obtained for an angular-contact ball bearing from a space shuttle main engine (SSME) liquid-oxygen turbopump by both the FEM analysis and the closed-form approximation are compared. Although it varied with the speed and the stress caused by the press fit, the difference between the FEM analysis and the closed-form solution was not more than 4.1 percent. For the conditions calculated, the hoop stresses can reduce inner-race life by as much as 85 percent.

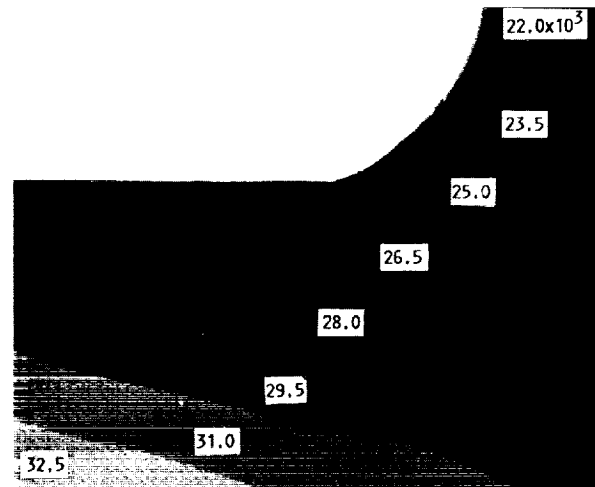


FIGURE 43.- FEM ANALYSIS OF HOOP STRESSES IN SSME LIQUID-OXYGEN TURBOPUMP 45-MM BORE ANGULAR-CONTACT BALL BEARING INNER RACE. SPEED, 25 000 RPM; PRESS FIT, 2000 PSI.

Bibliography

Zaretsky, E.V.; and August, R.: Closed-Form Solution for Hoop Stress in a Ball-Race Contact. Advanced Earth-to-Orbit Propulsion Technology 1990, R.J. Richmond; and S.T. Wu, Eds., Vol. 2, NASA CP-3092, 1990, pp. 387-399.

Lewis contact: Erwin V. Zaretsky,
(216) 433-3241
Headquarters program office: OAET

Space Mechanisms Technology Needs

In order to assess whether the current technology in space mechanisms (mechanical components/tribology) was adequate to meet the requirements of present and future proposed NASA missions, a questionnaire was sent to government and industry individuals known to be working in the field. The questions dealt with the adequacy of current technology, whether an infrastructure is needed to coordinate mechanisms research and what such an infrastructure's functions might be, what types of testing/qualification methods might be needed, and what are the areas where new technology research should be established.

Approximately 400 questionnaires were sent out. The majority were sent to attendees of the Aerospace Mechanisms

Symposium, the remainder to individuals working in tribology. The general consensus of the 130 respondents was that the current technology base is not adequate to meet requirements of future long duration NASA missions, and that new technology research programs need to be implemented.

A NASA Technical Manual is being processed, listing the replies returned. The names and affiliations of the individuals have not been given with the responses, but an alphabetized list of those responding is given at the end of the report. Responses have been separated into three categories: NASA response, other government responses, and industry responses.

Lewis contact: Robert L. Fusaro,
(216) 433-6080
Headquarters program office: OAET

Aeropropulsion

Materials

Computed Tomography Guides Machining and Structural Modeling

Metal matrix composites (MMC's) are being developed to provide gas turbine engine components that can be used at temperatures of 425 to 1315 °C. Before full-scale MMC structures can be made, subscale engine components must be prototyped, and related life prediction analyses must be performed and experimentally verified. Further, nondestructive evaluation (NDE) technologies must be explored in concert with the different fabrication methods and the complex geometric nature of the finished product. Consequently, Pratt & Whitney Aircraft and NASA Lewis, under a nonbinding cooperative program, are studying a silicon-carbide-fiber-reinforced, titanium-metal-matrix composite system (SCS-6/Ti-15V-3Cr-3Al-3Sn) for the manufacture of three subscale rings. The activities include life prediction systems, NDE, and processing aspects. The work highlighted herein is part of the NASA NDE activity.

Computed tomography (CT) with 250- to 350-mm resolution, as Figure 44 shows, provides three-dimensional density information for metal matrix composite, subscale-engine components. In tests of the subscale rings, CT cross-sectional density information differentiated between the monolithic case and the composite core. Density variations imaged in the composite core were due to poor consolidation, fiber bunching, and poor bonding. Distortion of the composite core and its closeness to the top edge of the ring were due to fabrication and tooling problems. CT can help locate the composite core before final machining to prevent machining through the

fibers. Identification of the precise three-dimensional geometry and density of both the monolithic case and the composite core can aid in developing more realistic finite element models for stress analysis and life prediction of MMC engine components.

Lewis contact: George Y. Baaklini,
(216) 433-6016
Headquarters program office: OAET

Structural Mechanics

Probabilistic Analysis of Blade Disks and the Effect of Mistuning

The dynamic analysis of bladed disks (rotor) in a probabilistic sense has gathered many researchers' attention recently. The inherent uncertainties associated with the blade geometry, material properties, damping, mass, and forces result in uncertainties of the blade's dynamic response. Consequently, the safety margin for a rotor designed using deterministic methods is never certain. Thus, it is difficult to quantify the risk involved in the conventional designs. Due to variations in the blade geometry, material properties, and mass, each blade on a rotor does not have the same fundamental frequencies. These differences alter blade responses. It is essential from design viewpoint to account for such response variations manifested by uncertainties in the primitive variables. Therefore, the probabilistic analysis of structures is necessary to assess the reliability of a design governed by design variables that are uncertain. NESSUS (Numerical Evaluation of Stochastic Structures Under Stress), a computer code developed in-house has various reliability methods to determine re-

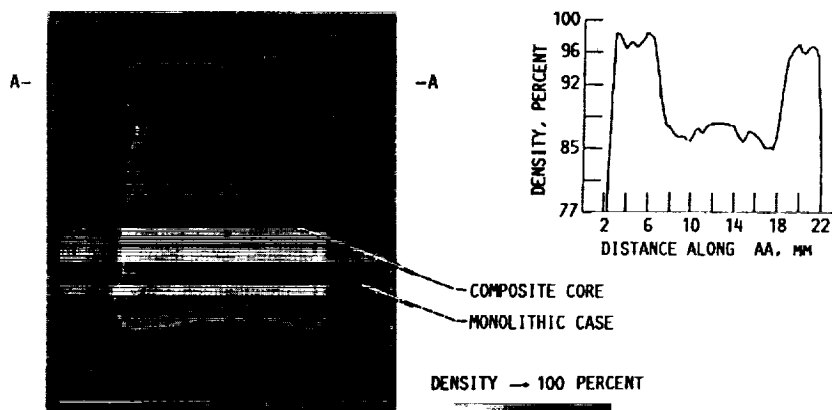


FIGURE 44. - CROSS-SECTIONAL SLICE OF NASA/PBW MMC RING.

sponse uncertainties caused by random (primitive) variables. NESSUS has been used to quantify the reliability of mistuned rotors. Rotors with 10 and 20 blades are analyzed to study the effect of the number of blades. Also, the effects of the order of excitation (multiple of blade frequency) are studied. The sensitivity of each primitive variable is quantified.

Results of the analysis, as seen in Figure 45, show that the uncertainties in the frequency of excitation significantly affect blade responses. Amplification of the response depends on the difference between mean blade frequency, mean excitation frequency, and their coefficient of variation. Inclusion of uncertainties in blade frequency and excitation is very important in analysis. The blade can be designed for a given probability level. The cumulative distribution function obtained can be used to quantify reliability risk. The primitive variable sensitivity information can be used to upgrade the design, quality control, inspection procedure and, consequently, the risk. Typical results include blade amplitudes and primitive variable sensitivity effects.

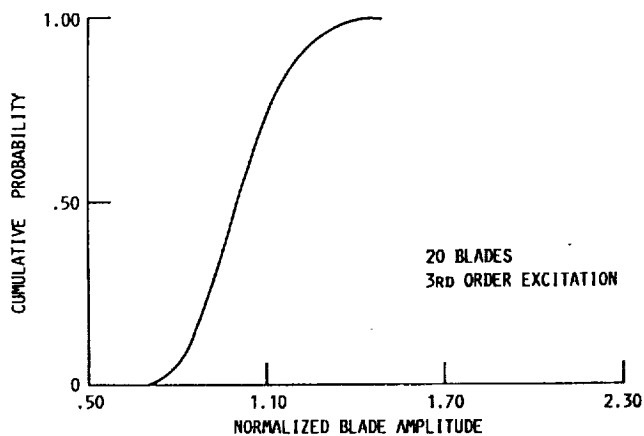
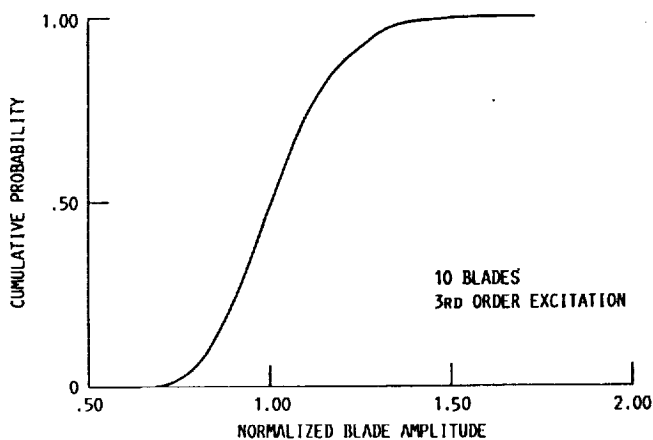


FIGURE 45. - CUMULATIVE DISTRIBUTION FUNCTION OF NORMALIZED AMPLITUDES.

Bibliography

Shah, A.R.; Nagpal, V.K.; and Chamis, C.C.: Probabilistic Analysis of Bladed Turbine Disks and the Effect of Mistuning. NASA TM-102564, 1991.

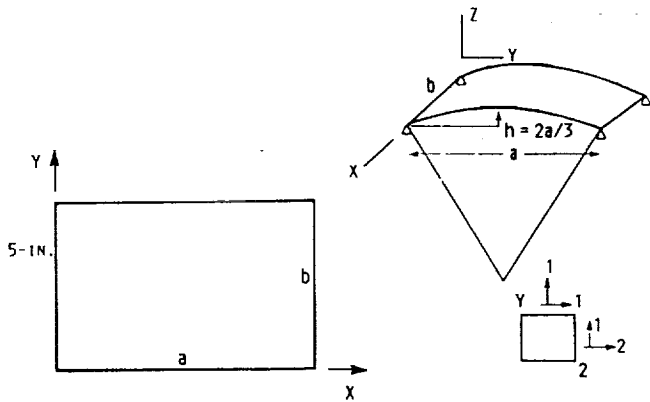
Lewis contact: C.C. Chamis,
(216) 433-3252
Headquarters program office: OAET

Structural Tailoring of Select Composite Structures

Design of composite structures for aerospace propulsion systems is a multidisciplinary activity where participating variables from each discipline are traded off in order to meet specified designer requirements for: (1) safety; (2) durability; (3) performance; (4) maintenance; and (5) cost. Therefore, multidisciplinary design is a complex activity of competing objectives which result in compromised designs. The multidisciplines that are generally associated with aerospace composite structures include the following: (1) aerodynamics; (2) structural mechanics; (3) aeroelasticity; (4) acoustics; (5) composite mechanics; (6) mechanics for fatigue and fracture; (7) life-prediction methods; (8) economics; and perhaps several others. Each of these independent disciplines requires that seasoned expertise be utilized in order to effectively provide for several variables that affect the design. Obviously, these comprise a larger number of variables that need to be traded off to obtain a compromised design.

Presently each discipline iterates to come up with the best configuration which satisfies specified designer requirements within that discipline. After that has been done, a compromise is achieved by one or more sequential iterations among participating disciplines. This process is time consuming and results in inefficient use of engineering effort. An alternative to the present procedure is to formalize this multidisciplinary design process. When the formalization is driven by structural consideration, it is appropriately called structural tailoring. The objective of the current effort is to describe structural tailoring methods that have been developed at Lewis, as Figure 46 shows, for select propulsion composite components, illustrate their applications via sample cases, present results obtained therefrom, and discuss their significance.

The sample cases include aircraft engine blades, propfans (turboprops), and flat and cylindrical panels. Typical results illustrate that the use of these codes enables the designer to obtain designs which meet all design requirements with maximum benefits in efficiency, noise, weight, or thermal



LOADING CONDITIONS	PANEL/COMPOSITE		OBJECTIVE FUNCTION
	FLAT	CYLINDRICAL PANEL	
BIAXIAL LOAD 2/1/1	(1) AS/E (1) HM/E	(1) AS/E (2) HM/E	MINIMUM DISTORTION
ΔT THROUGH THICKNESS	(1) AS/E (1) HM/E	(1) AS/E (2) HM/E	MINIMUM DISTORTION

AS/E - AS-GRAPHITE-FIBER/EPOXY-MATRIX; HM - GRAPHITE FIBER/EPOXY-MATRIX

NOTES: a = 11 in.; b = 5 in.; $\Delta T = 100^\circ F$

FIGURE 46. STRUCTURAL TAILORING OF SELECT COMPOSITE PANELS. GEOMETRY AND LOADING CONDITIONS.

distortions. Recently, the code has been extended in-house to flat and cylindrical panels. For both panels, the structural tailoring procedure substantially reduced the distortion (as high as 40 times), compared to the initial design.

The computer code is used by the Pratt & Whitney and General Electric Companies to design engine fan and compressor blades at reduced engineering effort.

Bibliography

Chamis, C.C.; and Rubenstein, R.I.: Structural Tailoring of Select Fiber Composite Structures, NASA TM-102484, 1990.

Lewis contact: C.C. Chamis,
(216) 433-3252
Headquarters program office: OAET

Demonstration of Capabilities of the High-Temperature Composites Analyzer Code

High-temperature metal matrix composite (HTMMC) materials are potentially promising candidates for developing 21st

century propulsion systems. Unlike conventional materials, the thermo-mechanical properties of components made from HTMMC materials exhibit a nonlinear dependence on parameters such as temperature, stress, and stress rate. This phenomenon may alter the structure response significantly. Commercially available codes are not capable of handling such complexities for HTMMC materials. And, experimental investigations are high in cost. Hence, computational models including nonlinear material behavior simulating the real-life response of components made from HTMMC materials are required.

Although enhancement of the code continues, in its current form, it is applicable to a wide variety of composite structural analysis problems, as shown in Figure 47. High-temperature composites analyzer (HITCAN) offers a self-contained (independent of commercial codes) modular code. It will help in material selection for specific applications, in analyzing sensitivity of structural response to various system parameters, and in providing structural response at all levels of material constituents.

Various features of the code have been published and are demonstrated through illustrative examples for typical structures including beams, plates, rings, curved panels, and built-up structures. These features make HITCAN a powerful, cost-effective tool for analyzing metal matrix composite structures and components.

EFFECTS OF	DISP. (CENTER POINT), in.	STRESSES, PLY 4 (CENTER POINT), ksi		
		LONG.	TRANS.	SHEAR
BASE CASE*	0.0135	23.0	0.8	1.3
FIBER DEGRADATION	0.0151	21.8	1.4	1.1
FABRICATION	0.0140	18.4	5.8	0.4
PLY ORIENTATIONS (0/45) ₃ (0/90) ₃	0.0144 0.0140	11.3 13.5	7.1 4.7	1.6 0.0
NONLINEAR MULTIFACTOR INTERACTION CONSTITUTIVE MODELS				
P = CONSTANT	0.0119	22.7	2.0	1.1
P = f(T)	0.0133	25.5	0.9	1.3
P = f(σ)	0.0121	21.5	1.0	1.1
P = f($\dot{\sigma}$)	0.0118	22.7	2.0	1.1

*BASE CASE IS FOR NO FIBER DEGRADATION, NO FABRICATION, (0/ ± 45 /90) PLY ORIENTATIONS, AND P = f(T, σ , $\dot{\sigma}$) CONSTITUTIVE MODEL.

NOTATION:
P = MATERIAL PROPERTY
 σ = STRESS
T = TEMPERATURE
 $\dot{\sigma}$ = STRESS-RATE

FIGURE 47. SENSITIVITY ANALYSIS.

Bibliography

Singhal, S.N.; Lackney, J.J.; Chamis, C.C.; and Murthy, P.L.N.: Demonstration of Capabilities of High Temperature Composite Analyzer Code HITCAN. NASA TM-102560, 1990.

Lewis contact: C.C. Chamis,
(216) 433-3252
Headquarters program office: OAET

Three-Dimensional Full Potential Method for the Aeroelastic Modeling of Propfans

Propfans are designed to operate at high subsonic cruise Mach numbers of about 0.8 with advance ratios around 3. At these conditions, the local Mach numbers vary from high subsonic at the hub to supersonic at the blade tip. Thus, the flow-over part of the blade is transonic. Linearized compressible theories are incapable of modeling shock waves that occur in transonic flow; therefore, a nonlinear aerodynamic model such as the full potential model is required. The three-dimensional full potential solver has been validated for steady calculation by comparison with experimental data for SR3 and SR7 blades. Additional comparisons have also been made between steady and unsteady results from the full-potential code, a Euler code, and a linearized potential (panel) code. In the frequency domain flutter analysis, the eigenvalues determine stability. Generalized force derivatives that are required in the eigenvalue problem are determined from the full-potential solver.

Figure 48 shows the variation of frequency and damping with Mach numbers calculated using full-potential and panel codes. Frequency predictions agree very well and the full-potential code results show systematically lower damping values, with a near neutral stability point at a Mach number of 0.7, which is not present in the panel code results. The reason for this difference is currently being investigated. The predicted loss of stability near Mach 0.7 may or may not be a real nonlinear effect.

The main benefits of the three-dimensional full-potential code are its ability to model nonlinear phenomena such as shock waves encountered in transonic flow. The full-potential code requires less computational time and storage as compared to similar Euler codes even though it models all flowfield characteristics considered important for the propfan.

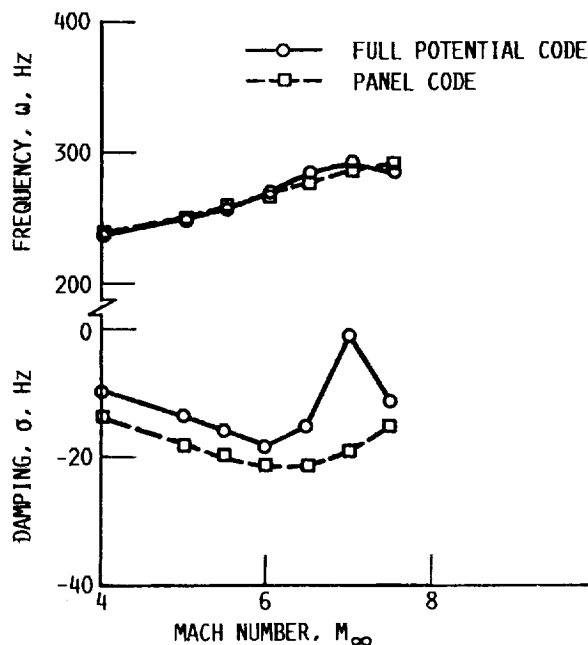


FIGURE 48. - COMPARISON OF FREQUENCY AND DAMPING COEFFICIENTS FOR SR3 BLADE, ADVANCE RATIO $J = 3.46$, BLADE SETTING ANGLE $\beta = 56.6^\circ$, INTERBLADE PHASE ANGLE = 0° .

Lewis contact: George L. Stefko,
(216) 433-3920
Headquarters program office: OEST

Application of an Efficient Hybrid Scheme for Aeroelastic Analysis of Advanced Propellers

The aerodynamic and acoustic requirements of advanced propellers (propfans) have resulted in design with thin, swept, and twisted blades of low-aspect ratio and high solidity compared to conventional propellers. The aeroelastic problem is inherently nonlinear due to large deflections caused by centrifugal and aerodynamic loads. Analytical aeroelastic models can't account for nonlinear aerodynamics, real-blade airfoil geometry (including thickness and camber), and flow incidence. Developments in numerical methods and high-speed computers, however, have made it possible to develop numerical models that can account for these effects.

A three-dimensional hybrid finite-difference Euler solver has been developed for solving flow field around propeller type

geometries. The hybrid solution scheme treats the radial direction fluxes semi-implicitly, and the other two direction fluxes implicitly, reducing computational time and memory requirements. Performance, spanwise, and chordwise load calculations with this scheme correlated well with measured data.

This aero-code has been interfaced with a finite element structural model (NASTRAN) to study the effect of structural flexibility on the advanced propeller performance. Blade structural deflections are obtained with the combined effects of centrifugal and aerodynamic loading. These deflections then provide the new blade shape. The process is repeated until the blade setting angle at a 75 percent span from two consecutive iterations is within a given tolerance.

In figure 49, the relative change in blade-setting angle over the span is plotted with an iteration for SR7L propeller for a Mach number, $M = 0.775$, and advance ratio, $J = 3.088$. Variation in the blade-setting angle is nonlinear and the large deflection occurs near the tip, with practically no deflection at the root section. This shows that a rigid body rotation of the blade to account for changes in blade geometry under operating conditions may not be sufficient for accurate performance and blade-load calculations.

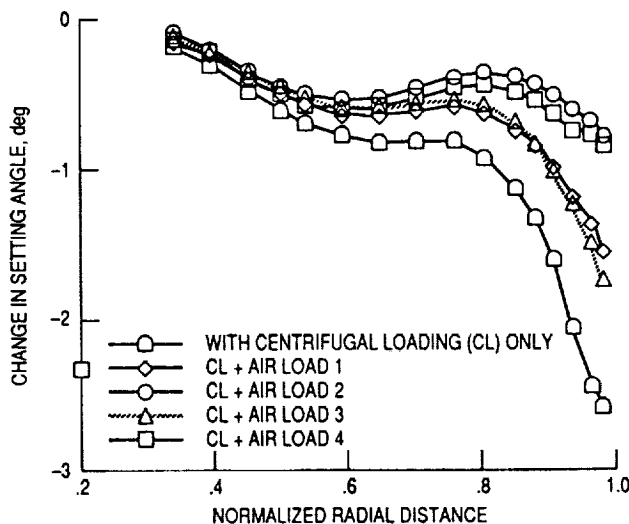


FIGURE 49. - CHANGE IN BLADE SETTING ANGLE VERSUS BLADE SPAN FOR SR-7L TWO-PROPFAN. ADVANCE RATIO, 3.088; MACH NUMBER, 0.775.

Lewis contact: D.L. Huff,
(216) 433-3913
Headquarters program office: OAET

Full Potential Solver Used for Time-Domain Flutter Analysis of Cascades

The traditional approach to calculating the flutter of bladed disks (stators and rotors) has been the frequency-domain analysis. The aerodynamic forces that are typically used with this approach are based on a linear potential theory which neglects the effects of blade loading due to thickness, camber, and angle of attack, and is not suitable for transonic flows. At NASA Lewis, the unsteady full potential equation has been used as the basis for a two-dimensional cascade flow model, as Figure 50 shows, that can represent flows over a wide range of Mach numbers from low subsonic to supersonic, including transonic flows with weak shocks.

In the time-domain method of flutter analysis the equations of motion for the blades are integrated simultaneously with the full-potential equation governing the inviscid, irrotational fluid flow. Starting with the steady flow field, one blade in the cascade is given a small disturbance in the form of a pitching velocity. The variation of blade pitching and plunging displacements with time is used to determine the stability of the cascade. The blade motions either decay or grow with time, depending on the reduced flow velocity, indicating stability or instability, respectively. The main benefits of the time-

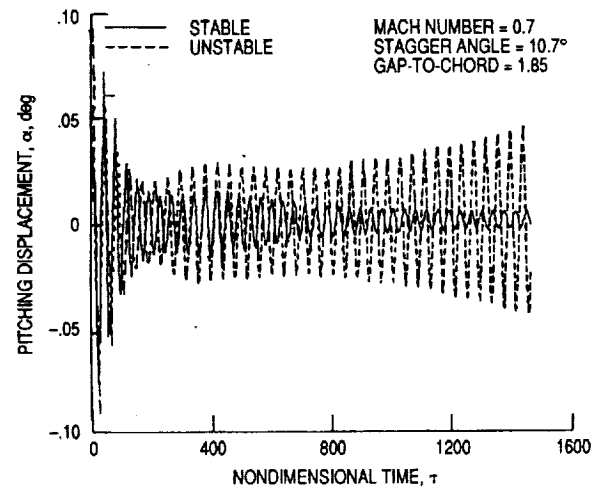


FIGURE 50. - BLADE MOTIONS AT STABLE AND UNSTABLE CONDITIONS: CASCADE GEOMETRY REPRESENTATIVE OF SR5 PROPFAN.

domain approach are the ability to handle nonlinear structural models and aerodynamic forces that are nonlinearly dependent on blade displacements. The time-domain approach allows a realistic simulation of the motion of the fluid and of the cascade blades for a better physical understanding.

Lewis contact: George Stefko,
(216) 433-3920
Headquarters program office: OAET

Reduced Order Models for Nonlinear Aerodynamics

A semi-empirical model has been developed for predicting unsteady aerodynamic forces on arbitrary airfoils under stalled and unstalled conditions. Aerodynamic forces are modeled using second-order ordinary differential equations for lift and moment, with airfoil motion as the input. The fluid lift forces has the characteristics of a damped harmonic oscillator because of the fluid's inertia, dissipation, and compliance. Airfoil motion is assumed to drive the fluid-lift oscillator. Pitching moment is represented similarly. Parameters in these equations are determined from comparison with airfoil load data for small-amplitude oscillatory motion from a Navier-Stokes solver.

This model is then used to provide the aerodynamic loads input to a two degrees-of-freedom structural dynamics model. To study the flutter behavior of a NACA 0012 airfoil at a Mach number of 0.3, the time response for a two degrees-of-freedom structural-fluid system using these equations is compared with those from the Navier-Stokes solver and the classical incompressible potential flow model. The savings in computer time and memory requirement, due to this model, are significant in comparison to methods based directly on the Navier-Stokes equations.

Flutter boundary, as a function of initial angle of attack, is plotted in Figure 51. It can be observed that for angles less than 10 degrees, a particular value of V_F^* gives stable oscillations. For V^* greater than this value, growing oscillations occur and for V^* less than this value, decaying oscillations occur. The flow over airfoil is fully attached for these initial angles of attack. For angles greater than 10 degrees, stable oscillations occur over a range of values of V^* instead of one particular value. Below this range, decaying oscillations are seen; above this range, growing oscillations occur. It should be noted, however, that the range of V^* , over which the limit cycle is observed, is somewhat different for the two fluid-dynamic models.

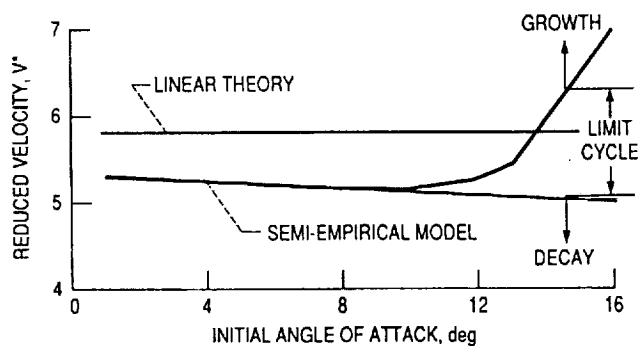


FIGURE 51. - FLUTTER BOUNDARY AS A FUNCTION OF INITIAL ANGLE OF ATTACK.

Lewis contact: George Stefko,
(216) 433-3920
Headquarters program office: OEST

Updated Flutter Analysis of Supersonic Fan Stator

A flutter analysis for supersonic fans with supersonic axial flow has been modified to include Lighthill's nonlinear piston theory. This allows representation of airfoil thickness and camber, upstream of the shock impingement point, on the airfoil downstream of the shock impingement point. The code uses Lane's linear potential theory which represents the airfoil by a flat plate of zero thickness. Lane's potential theory was used over the full airfoil before this improvement.

The code was used to perform a flutter analysis of the NASA Lewis Supersonic Fan Stator 5. The stator design had been changed to a pin-pin support from the original design's cantilevered support. Results of the flutter analysis are shown in Figure 52. Two calculated flutter boundaries are shown, as well as the operating line for the critical stator mode, which is first torsion. The figure shows that the stator operating line is in the stable region for 0.2 percent structural damping, but in the unstable region of 0.0 percent structural damping. Measurements made from a stator blade show that the structural damping is greater than 1.4 percent for the first torsion mode. Therefore, the supersonic fan stator is predicted to be flutter free.

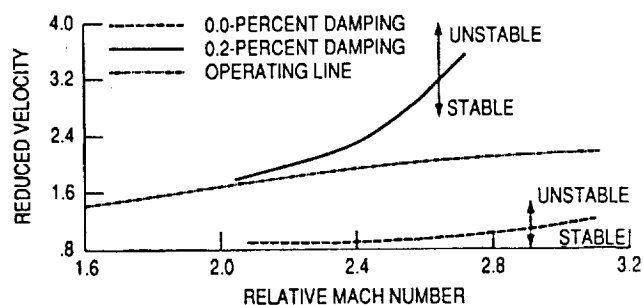


FIGURE 52. - FLUTTER BOUNDARY PREDICTION FOR THE NASA LEWIS SUPERSONIC FAN STATOR 5 USING LIGHTHILL'S NONLINEAR PISTON THEORY AND LANE'S POTENTIAL THEORY.

Lewis contact: Joan M. Lucro,
(216) 433-2684
Headquarters program office: OAET

Aeroelastic Analysis of Propfans Adapted for Concurrent Processing

Propfans offer significant fuel savings (30 to 50 percent) over current turbofan engines for the next generation of transport aircraft. A propfan is a radically new aircraft propeller that can operate at the high flight speeds of turbofan engines. Unlike conventional propellers, propfans have thin, flexible blades that undergo large deflections and have large variable sweep. Analysis programs have been developed to predict, and thus avoid, aeroelastic instabilities, which can lead to catastrophic failure of propfan blades.

An advanced aeroelastic analysis program was adapted to run efficiently on a shared-memory, multiple-processor computer, an Alliant FX/80. The program, Aeroelastic Stability and Response of Propulsion Systems (ASTROP3), uses a three-dimensional, compressible, unsteady aerodynamic model and blade normal modes to calculate the aeroelastic stability and response of propfan blades.

Within ASTROP3, the major amount of execution time is used in the computation of aerodynamic influence coefficients. In a representative case with a model of the SR3C-X2 propfan blade, the coefficient computation used 97 percent of the total execution time. Fortunately, this computation is highly independent and can be done concurrently on separate processors.

For efficient execution in a parallel processing environment, the overhead time involved in setting up for vector and concurrent processing must be minimized as Figure 53 shows. Overhead can be controlled by selective use of compiler options and directives to enable vectorization or concurrentization only where a reduction in execution time will result. In the ASTROP3 code, changes were made to enable the concurrentization of the entire influence coefficient computation. Further modification rescheduled the parallel subtasks such that idle time of available processors was reduced.

Speedups attained on the Alliant FX/80 using different numbers of processors were recorded for the flutter analysis of a SR3C-X2 propfan rotor and compared with ideal and theoretical speedups. For seven processors, the actual speedup was 5.28, or 75.4 percent of ideal.

Bibliography

Murthy, D.V.; and Janetzke, D.C.: Concurrent Processing Adaption of Aeroelastic Analysis of Propfans. AIAA Paper 90-1036, April 1990. (Also NASA TM-102455.)

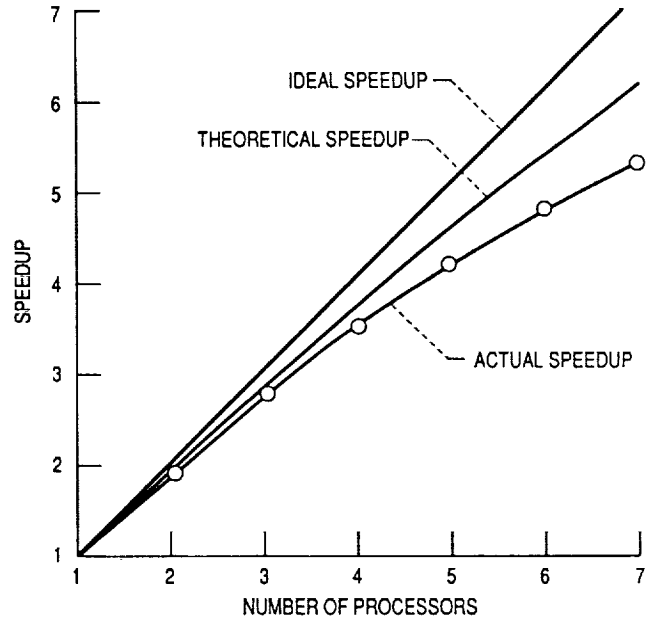


FIGURE 53. - EXECUTION TIME PERFORMANCE OF PARALLEL PROCESSING FOR PROPFAN AEROELASTIC ANALYSIS.

Lewis contacts: David C. Janetzke,
(216) 433-6041; and Durbha V. Murthy,
(216) 433-6714
Headquarters program office: OAET

Linearized Unsteady Aerodynamic Analysis for Application to Turbomachinery Flutter and Forced Response

The objective of this research program is to develop theoretical unsteady aerodynamic models and a Linearized Unsteady Flow computer code (LINFLO) for predicting compressible unsteady inviscid flows through blade rows of axial-flow turbomachines. These analyses are required for understanding the impact of unsteady aerodynamic phenomena on the structural dynamic stability, reliability, and aerodynamic performance of such blading. The research effort is devoted mainly toward application to low-speed turbomachinery, such as the SSME turbopump turbines which have encountered reliability problems. This research applies more generally to the prediction of flutter and forced response in turbomachinery fan, compressor, and turbine blading, operating in the subsonic and transonic regimes.

The unsteady aerodynamic behavior of turbomachinery blading is strongly dependent upon the steady aerodynamic flowfield surrounding the cascade. Blade rows of axial-flow turbomachines often consist of airfoils varying from very thin to thick cross-sections, all with varying degrees of camber. Such blades operate in a nonuniform steady flow due to effects of airfoil thickness and flow incidence entering the cascade.

Linearized unsteady potential formulation models the small unsteady disturbances occurring in the cascade as first-order perturbations of the flow variables occurring in the mass, momentum and energy conservation equations. The unsteady perturbations, due to blade motion or incident aerodynamic disturbances, are linearized about a nonlinear, isentropic, irrotational steady potential flow.

Special consideration must be given to flows in which the unsteady disturbance is due to aerodynamic excitations. These excitations may be due to low-frequency gusts, high-frequency wakes, or pressure waves. For subsonic or transonic flows containing weak shocks, the mean steady flow is irrotational and isentropic. Under these conditions, the inviscid conservation equations become greatly simplified. Analytical expressions exist for the linearized inviscid equations which use a splitting technique to study the behavior of vorticity and entropy gusts for flows which have a steady potential form. The unsteady velocity field is split into irrotational and rotational parts leading to three linear variable-coefficient equations which, sequentially coupled, permit their solution in order.

A distinct advantage of this formulation is that the unsteady behavior in a flow field can be resolved very accurately using the linearized potential approach, at a greatly reduced computational effort.

Lewis contact: George Stefko,
(216) 433-3920
Headquarters program office: OAET

Blade Aeroelastic Stability Analysis for Cruise Missile Counter Rotation Propfan Models

The ASTROP2 (Aeroelastic Stability and Response of Propulsion Systems) code was used to analyze three counter rotation (CR) propfan models in a 6x6-way configuration for cruise missile application. This is in support of a Navy sponsored wind tunnel test in the NASA Ames 14-foot wind

tunnel. The purpose of the test is to investigate propfan/airframe interactions for cruise missiles.

Two of the propfan model blades were designed at NASA Lewis and the third was provided by Garrett Corporation. One Lewis blade model, CM1, is representative of a low tip-speed geared design (tip diameter 16.5 in.). The other Lewis design, CM2, is representative of a high tip-speed gearless design (tip diameter 14.25 in.). In addition, the Lewis design had to satisfy aerodynamic performance and integral order structural criteria. Four organizations at Lewis worked together to accomplish the designs. Multiple iterations were required before acceptable designs were found. The final Lewis designs are called CM1d and CM2d. The Garrett design had to be checked for aeroelastic stability only.

The ASTROP2 code is a single rotor modal analysis that uses a fully coupled-motion, normal-mode structural model and a two-dimensional strip unsteady cascade aerodynamic model. A frequency domain solution, the code predicts frequency, damping and phase angle of the aeroelastic modes. The forward and aft rotor of each CR model were analyzed separately. However, the analytical representation of the steady flow into each rotor includes the interaction between the rotors.

The analyses, as shown in Figure 54, were performed at the blade design angle of each blade over the full range of tunnel operating conditions planned: Mach 0.4 to 0.9; rotor tip speeds from 450 ft/sec to 850 ft/sec for the CM1 and Garrett

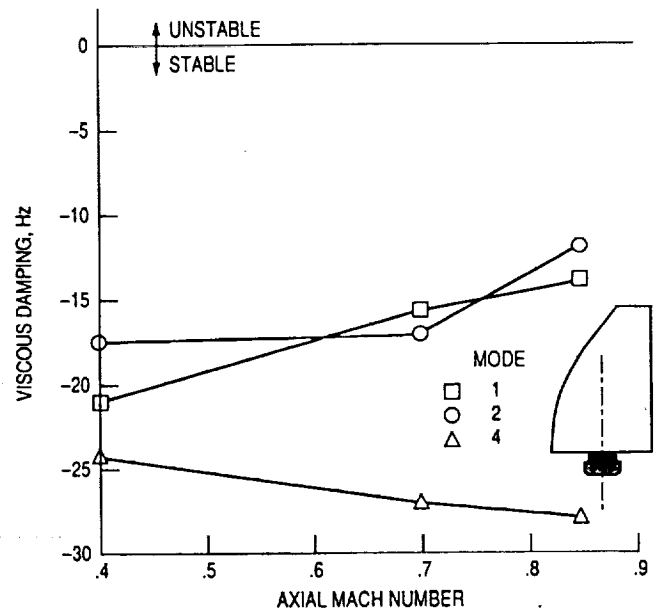


FIGURE 54. - LRCSW 0.55-SCALE-MODEL AEROELASTIC STABILITY PREDICTION FOR CM1d FORWARD SIX-BLADED ROTOR. NO STEADY AIRLOADS; TIP SPEED, 750 FT/SEC; BLADE SETTING ANGLE AT 75-PERCENT SPAN, 58.5°.

blades; and 600 ft/sec to 950 ft/sec for the CM2 blades. Typical results for the CM1d design are shown in the Figure. It shows the damping of only the three lowest damped blade modes, although six blade modes were used in the analyses. The figure shows the blades remain in the stable region over the full Mach number range. These results are typical for all the conditions analyzed for CM1d, CM2d, and the Garrett forward and aft blades.

Lewis contact: John Lucero,
(216) 433-2684
Headquarters program office: OAET

Counter Rotation Propfan Unstalled Flutter Experimentally Investigated

Propfans may have unstalled flutter in their operating range. The thin airfoil sections, high blade sweep, high solidity, low aspect ratio, and transonic to supersonic tip speeds of propfans give them this potential. Unstalled flutter has been investigated experimentally for single-rotation propfans and has guided the development of flutter analyses. A shift in interest

to counterrotation required a similar investigation for this configuration. Therefore an experiment was planned and conducted using a counterrotation propfan model with a front rotor that had flutter. The objectives were to study the characteristics of the flutter and the effect that the aerodynamic interactions between the rotors had on it.

The model, called F21/A21, was installed in the Lewis 8-by-6-foot Supersonic/Transonic Wind Tunnel. As Figure 55 shows, there were 13 blades on the front rotor and 10 blades on the rear rotor. The rotor diameters were nominally 2 ft. First, the front rotor was tested alone to map its stability. Then, both rotors were tested, with the rear rotor at different powers, and the front rotor stability was re-mapped to see the change. In general, the aft rotor slightly increased the stability of the front rotor—a small but favorable effect of rotor aerodynamic interactions. The stability of the rotor decreased when blade setting angle was increased, and flutter occurred in several modes over the range of the test conditions. In addition to conventional strain gauges, a laser-based optical system was used to obtain measurements at flutter. The laser data provided detailed spectral results, phases between all the rotor blades, and a density variations on the fracture behavior of composites. It will be used to study thermal and oxidation effects on the interfacial shear strength of composites. This

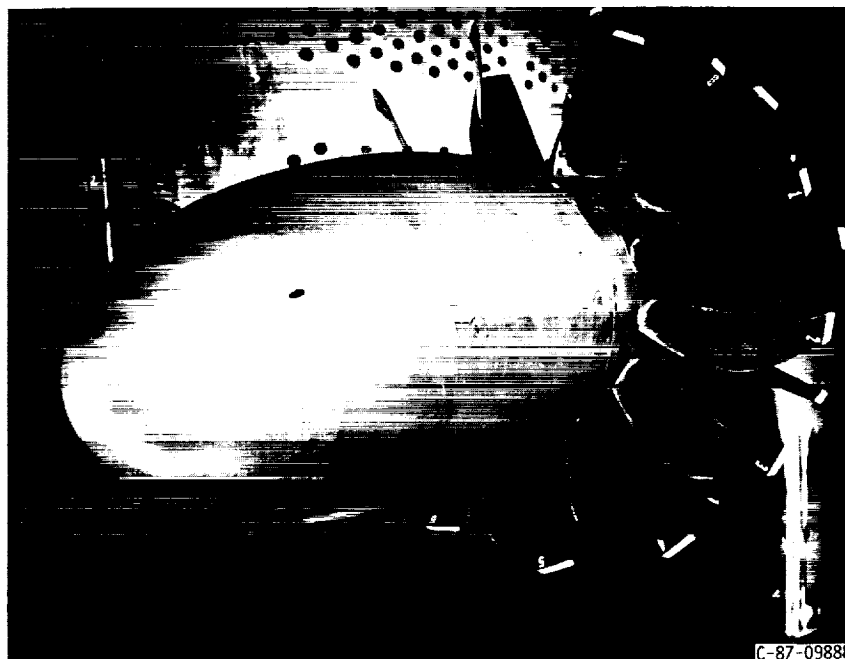


FIGURE 55. - F21/A21 COUNTERROTATION PROPELLER MODEL IN NASA LEWIS 8-FOOT BY 6-FOOT SUPERSONIC WIND TUNNEL.

approach can provide a basis for interpretation of mechanical tests, for validation of analytical models, and for verification of experimental procedures.

Lewis contacts: George Y. Baaklini,
(216) 433-6016; and Ramkrishna T. Bhatt,
(216) 433-5513
Headquarters program office: OAET

Life Prediction

Fatigue-Life Prediction of Intermetallic Matrix Composites

Intermetallic matrix composites (IMC) will aid NASA in achieving aeronautical propulsion goals of lower weight and higher operating temperatures coupled with greater efficiency, performance, and durability. Fatigue-life prediction models will be indispensable for calculating durability. Toward that end, a new IMC fatigue-life prediction model has been developed permit assessment of fatigue performance in the earliest possible stages of IMC development.

A strain-based life prediction method was developed for an intermetallic matrix composite (IMC) under tensile cyclic loadings at elevated temperatures. In general, composite life prediction theories can be separated into two types: modulus (stiffness) degradation theories; and residual strength degradation theories. The models in these classes have shown to provide good correlations between experimental and predicted fatigue lives for a variety of composite systems. All models have well defined theories that are backed by observed physical phenomena. Most of the models are statistical based, typically utilizing two- or three-parameter Weibull distributions. Like life prediction models for monolithic materials, all require extensive testing, and in most cases, specialized tests and analytical procedures to characterize the model.

It can be extremely useful to estimate fatigue lives of composites utilizing a few simple material properties such as ultimate tensile strength, modulus of elasticity and ductility. By analogy to the Method of Universal Slopes for low-temperature fatigue of monolithic alloys, the following equation was chosen:

$$N_p = A[\sigma_{ult}/E]^\alpha(\epsilon_f)^\beta(\epsilon_{max})^\gamma$$

where N_p is the predicted life, ϵ_{max} is the maximum applied strain, A is a constant, and α , β , and γ are exponents. Like

the Method of Universal Slopes method, this equation correlates composite's ultimate tensile strength (σ_{ult}), tangent loading modulus (E), and fracture strain (ϵ_f) to fatigue life.

The model parameters (A , α , β , and γ) were determined by conducting a multiple regression analysis on both tensile and fatigue data. This has been done for a 0° unidirectional SiC/Ti-24Al-11Nb IMC at temperatures of 425 and 815 °C. Fatigue data at 650 and 760 °C for this IMC from two independent sources were used to verify the model. Ninety percent of the available results fall within a factor of 2 in life from the predicted value. All data fall within a factor of 3.

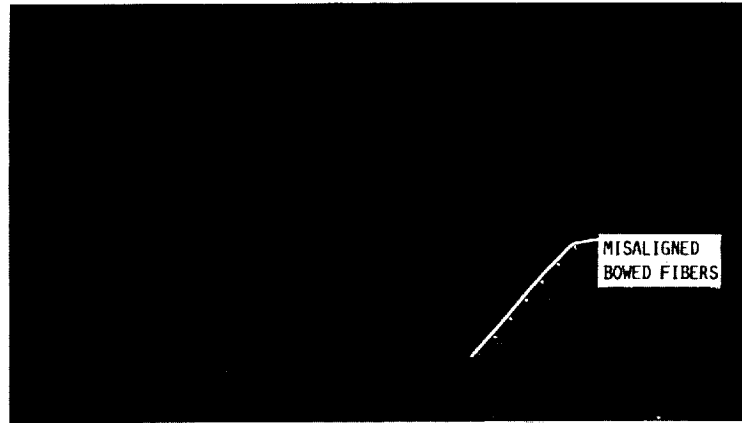
The advantage of this life approximation method is its simplicity. For a given operating temperature, a designer can evaluate the material without a costly investment of time or money. In the event the composite system appears to be a viable option, then, and only then, should a full fatigue characterization program be initiated.

Lewis contact: Paul A. Bartolotta,
(216) 433-3338
Headquarters program office: OAST

Ultrasonic and Radiographic Evaluation of Advanced Aerospace Materials: Ceramic Composites

Advanced high-temperature, low-density composite materials are being developed for use in the next generation of aerospace systems. Two examples that will require advanced composite materials for both propulsion and structural components are: (1) the High-Speed Civil Transport (HSCT), and aircraft for transporting 250 passengers at Mach 3.2 for 5000 n mi; and (2) the National Aerospace Plane (NASP), a transportation system that will take off, fly at Mach 25 directly into orbit, and land like a conventional aircraft.

Nondestructive evaluation (NDE) is being done to enhance and accelerate the development of ceramic composite materials. NDE is being done, during the processing stages, to identify subsurface features that affect the strength and life of these complex materials. Two nondestructive evaluation techniques, (a) radiographic imaging, and (b) ultrasonic C-scan can, together, provide sufficient data for an accurate nondestructive evaluation, as Figure 56 shows. Radiography is useful for identifying porosity, fiber alignment, fiber registration, fiber parallelism, and density variations. Ultrasonic C-scans identify the presence of density variations, density gradients, and the quality of the bond between laminae.



(a) X-RAY IMAGE



(b) ULTRASONIC IMAGE

FIGURE 56. - NASP LAMINATED CERAMIC COMPOSITE PANEL.

An iterative process between NDE and materials developers is used to eliminate these strength limiting subsurface features. During a feasibility study, these two NDE techniques identified crucial subsurface strength limiting material variations in laminated ceramic composite leading edge panels designed for the National Aerospace Plane (NASP).

Bibliography

Generazio, E.R.: Ultrasonic and Radiographic Evaluation of Advanced Aerospace Materials: Ceramic Composites. NASA TM-102540.

Lewis contact: Dr. Edward R. Generazio,
 (216) 433-6018
 Headquarters program office: OAET

Mechanisms

Actively Controlled Hydraulic Force Actuator

The hydraulic force actuator is a device which utilizes hydraulic pressure to apply control forces to a rotor bearing housing in order to actively control rotor vibrations. Figure 57 shows a schematic of the hydraulic force actuator system. The rig consists of a mass which is free to move horizontally but constrained vertically. Hydraulic pressure is introduced into the pressure chambers on either side of the mass. The membrane which forms the inner wall of the chamber is very flexible and deflects under the action of the hydraulic pressure, thereby transmitting a force to the mass.

The servovalve is in a closed-loop control system which controls the pressure difference in the chambers in response to electrical signal inputs. The control system can control either the amplitude of the mass or the force applied to it. Frequency response of the system is approximately 100 Hz. Focus of this work is to significantly increase the frequency response of the system so it may be used to control rotor vibrations in typical advanced aircraft engines.

Lewis contact: E. DiRusso,
 (216) 433-6027
 Headquarters programs office: OAET

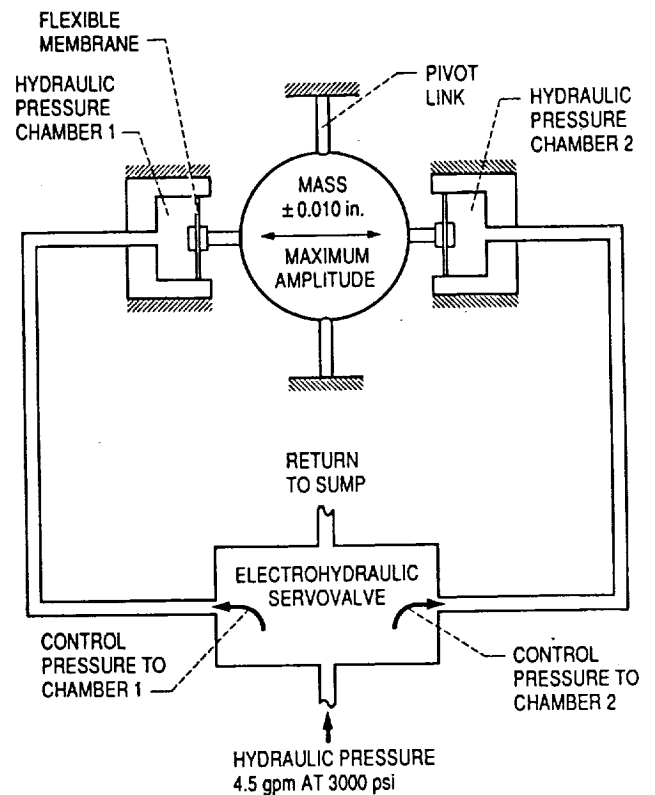


FIGURE S7. - SCHEMATIC OF ACTIVELY CONTROLLED HYDRAULIC FORCE ACTUATOR.

Space Propulsion

Materials

Fatigue Mean Stress Equations for Space Shuttle Main Engine Turbopump Blade Alloys

The NASA Space Shuttle's three main engines were designed for repeated use. However, certain critical components have been found to be fatigue-life limited to the point of having to be replaced after only a few flights. The heavily-loaded, Directionally Solidified MARM 246 + Hf turbine blades used in the first and second stages of the High-Pressure Fuel Turbo Pump (HPFTP) have been particularly prone to fatigue cracking. A promising solution is to consider an alternative material - Single-Crystal PWA 1480, an advanced nickel-based superalloy currently in commercial aeronautical gas turbine use.

In the relatively cool, cracking-susceptible shank regions of the blades, the fatigue mean stresses are exceptionally high. Consequently, the fatigue resistance of a material under high mean stresses is one of the most crucial aspects to consider when selecting an alternate material. This is the situation addressed by a recent Lewis in-house program.

Room-temperature, fatigue-life data on PWA 1480 and Mar M 246 were gathered from the existing literature for this study. A limited number of tensile mean stress fatigue tests were conducted at room temperature on Mar M 246. Data from fully reversed room-temperature fatigue tests were used to establish the zero mean stress-fatigue life relations of PWA 1480 and Mar M 246. Room temperature fatigue data with different levels of tensile mean stress were used to establish the effect of tensile mean stress on the fatigue life behavior. The applicability of commonly-used fatigue mean stress parameters to single crystal and directionally solidified nickel-base superalloys was examined. In addition, the recently proposed unified method of Heidmann and Manson, under grant at Case Western Reserve University (CWRU), was used to characterize the tensile mean stress-fatigue data of the two superalloys. The unified method allows the tensile mean-stress effect to vary at different fatigue-life levels.

The mean stress methods of Gerber and Morrow were found to be unconservative for single crystal PWA 1480 and directionally solidified Mar M 246. The methods of Goodman and Soderberg were also unconservative in several cases for these

superalloys. The unified method as proposed by Heidmann and Manson was modified to correlate the tensile mean stress-fatigue data of the superalloys studied. Analysis based on the modified unified method indicated that tensile mean stress was more detrimental in the low-cycle fatigue regime than in the high-cycle fatigue regime for PWA 1480 and vice versa for Mar M 246.

Guidelines developed in this study are useful for estimating the fatigue lives of turbopump blades made of nickel-based single crystal and directionally solidified superalloys. Such fatigue life calculations are necessary in the determination of which alloy is indeed the most fatigue resistant under a given set of circumstances. The life prediction models and tensile mean stress results will also be beneficial in assessing design and residual lifetimes of critical components.

Lewis contact: Dr. Sreeramesh Kalluri,
(216) 433-6727; and Dr. Michael A. McGaw,
(216) 433-3308
Headquarters program office: OSF

Mechanisms

Cryogenic Dampers Verification

Cryogenic turbomachinery, of the type used in liquid rocket high-pressure fuel and oxidizer turbopumps, has experienced high vibration. Subsynchronous whirl instabilities, high unbalance sensitivities, and cross talk between the turbopumps are some causes for these high vibrations. These problems arise because of a lack of damping in the pump. The damping contributed by seals may in some cases be inadequate or severely diminished as clearances increase with wear.

This research and development project, as shown by Figure 58, proposes to develop generic sources of damping by designing and testing various types of dampers in a cryogenic environment. These dampers will alleviate the problem of insufficient damping in cryogenic turbomachinery.

Major goals are to: (1) Design, fabricate and test a rotordynamics rig including an LN₂ containment vessel for immersion of the dampers; (2) Evaluate Curved Beam, Elastomeric, Active Piezoelectric Pusher, Turbulent Squeeze Film, Cartridge, Non-Newtonian Fluid and other damper prototypes, and; (3) Design and test dampers for the Cryogenic Turbomachinery Test Stand at NASA Lewis or Marshall.



C-89-14715

FIGURE 58. - CURVED BEAM DAMPER FOR CRYOGENIC ENVIRONMENT.

A general purpose, rotordynamic test rig has been developed utilizing liquid nitrogen as a working fluid. The damper containment vessel in this rig has a diameter of 24 inches and a depth of 18 inches. The installation of the rig is nearing completion and the testing of the curved beam damper will begin soon. Measured free-free modes of the rotor agree very well with predictions.

Lewis contact: Albert Kascak,
(216) 433-6024
Headquarters program office: OAET

Structural Mechanics

Viscoplastic Analysis Performed for Rocket-Thrust Chamber

Combustion gases in rocket-thrust chambers such as those in the space shuttle main engines are very hot and under high pressure. The copper material that lines the inner wall of these chambers is exposed to 6000-psi gases at temperatures of 6000 °F during firing and to cryogenic temperatures during startup and shutdown. The severe thermal and mechanical loads during each rocket firing permanently deform the linear material. Repeated firings result in undesirable distortion and

eventual thinning and cracking of the thrust chamber liner near the internal coolant channels. Ongoing research is attempting to develop a better understanding of this durability problem in order to pave the way for developing more durable materials and structural designs.

A viscoplastic stress-strain analysis of an experimental cylindrical rocket thrust chamber has been performed at NASA Lewis by Dr. Vinod Arya of the University of Toledo (Cooperative Agreement NCC3-120). A finite element solution methodology developed at NASA Lewis was employed to perform the viscoplastic analysis. A viscoplastic model has been put forth by Prof. David Robinson of The University of Akron. It incorporates a single internal state variable that represents kinematic hardening. This model was employed to investigate whether such a viscoplastic model could predict the experimentally observed behavior of the thrust chamber.

Two types of loading cycles were considered: a short cycle of 3.5-sec duration that corresponds to the experiments; and an extended cycle of 485-sec duration that is typical of the space shuttle main engine operating cycle. As shown in figure 59, the analysis qualitatively replicated the information behavior of the component as observed in experiments at NASA Lewis. It predicted the thinning of the coolant channel wall. And it indicated that the mode and location of failure in the component depends on the duration of the loading cycle—an important implication for future thrust chamber experiments. Advanced viscoplastic analyses have become an essential tool for the realistic life assessment of thrust chambers.

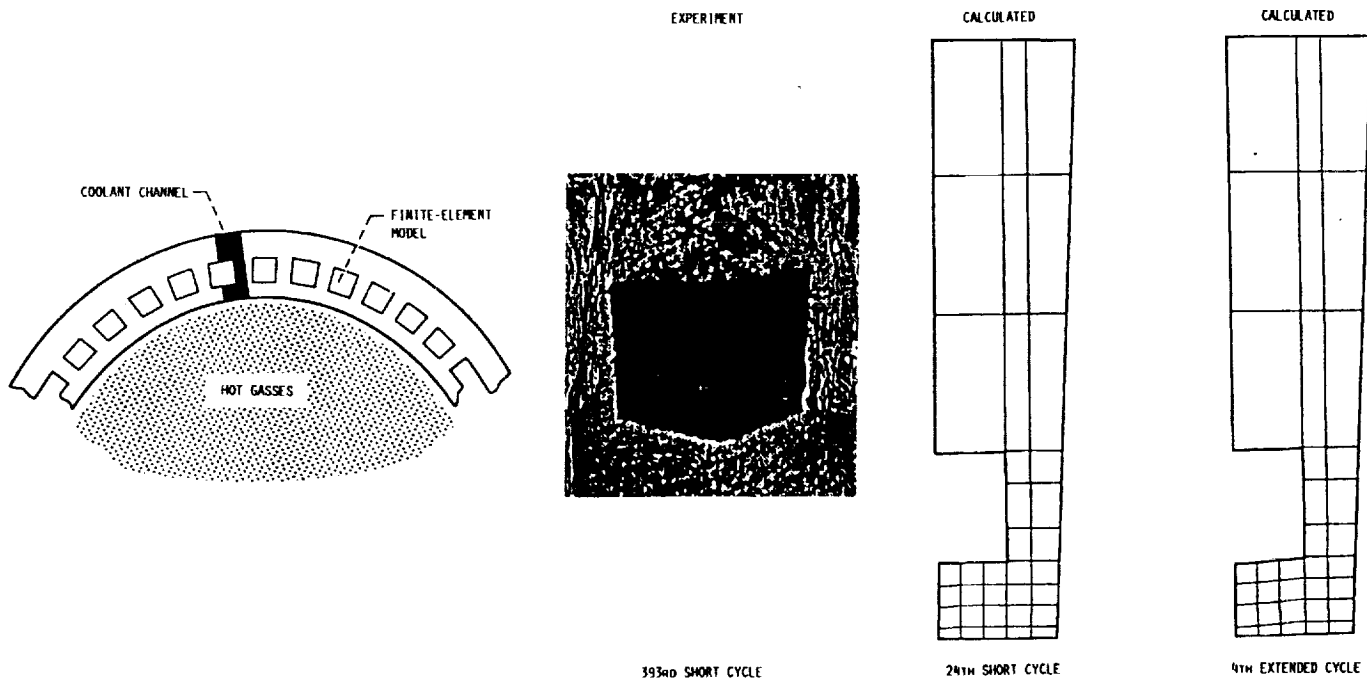


FIGURE 59. - VISCOPLASTIC PREDICTIONS OF CYCLICALLY DEFORMED THRUST CHAMBER.

Currently, research is being pursued to investigate how employing metal-matrix composites affects the deformation behavior and service life of thrust chambers.

Lewis contact: Dr. Gary R. Halford,
(216) 433-3265
Headquarters program office: OSF

Aeroelastic Stability Characteristics of the Space Shuttle Main Engine High-Pressure Oxidizer Turbopump Turbine Rotor

The dynamic analysis for the Space Shuttle Main Engine (SSME) LO₂ High-Pressure Oxidizer Turbopump (HPOT) turbine blade assesses the unsteady aerodynamic effect on the rotor stability. The method employed applies modal dynamic analysis to simulate the coupled blade/fluid system. A three-dimensional finite element model of the blade and its normal modes of vibration are used in conjunction with two-dimensional linearized unsteady aerodynamic theory. The aerodynamics are modeled by axisymmetric stream surface strips along the blade span. The blade structural and aerody-

amic dynamic behaviors are coupled within modal space. A complex eigenvalue problem is solved to determine the stability of the tuned rotor system.

The present analysis, as Figure 60 shows, was applied to the SSME HPOTP first stage turbine operating at the 109 percent rated power level. This blade was modeled using 6 axisymmetric streamsurfaces along the airfoil span and by retaining the first four normal modes of the turbine blade. The aeroelastic computations using these modes found that the aerodynamic damping levels were low (less than 0.5 percent of critical damping) for all modes of vibration. The second normal mode (edgewise mode) was found to be unstable for interblade phase angles from 18 degrees up to 221 degrees. The root locus of all calculated eigenvalues for motion in the first edgewise mode is included on the figure. This analysis did not consider the effects of mechanical and material damping on the blade stability. These damping effects will have a stabilizing influence on the blade.

Blade cracking has been a continuing problem during development of the HPOTP, although not as acute a problem since the introduction of blade-to-blade friction dampers at the blade platforms. The results from this analysis indicate that the history of blade cracking may be due to an unstable limit cycle vibration in the edgewise mode caused by flutter instability.

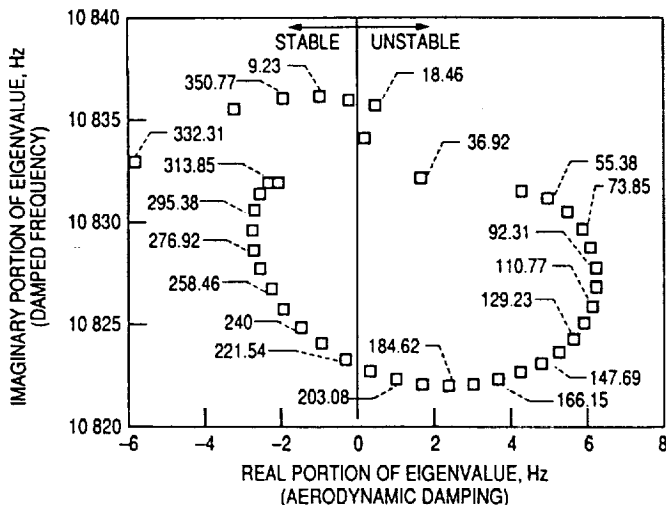


FIGURE 60. - PLOT OF ROOT LOCUS FOR TUNED HIGH-PRESSURE OXIDIZER TURBOPUMP (HPOTP) TURBINE VIBRATION. NUMBERS ON PLOT INDICATE INTERBLADE PHASE ANGLES.

Lewis contact: George Stefko,
(216) 433-3920
Headquarters program office: OEST

Life Prediction

A Method for Predicting Cumulative Creep-Fatigue Damage Interaction

Treatment of cumulative creep-fatigue damage in materials and structures subjected to a history of complex, repetitive thermal and mechanical loading has received considerable attention in recent years. It has long been recognized that the application of classical linear damage rules for both fatigue (Miner) and creep (Robinson) are too often unconservative in their prediction of material/structural durability, especially for the case of reusable space propulsion systems.

A model of cumulative creep-fatigue damage has been developed which is based on the use of nonlinear damage curve equations to describe the evolution of creep-fatigue damage for four basic creep-fatigue cycle types. A concept referred to as damage coupling is introduced to analytically account for the differences in the nature of the damage introduced by each cycle type. It provides a means of tracking the cumulative damage which accrues in complex loading histories. These concepts are synthesized into a general framework for the treatment of cumulative creep-fatigue problems.

The model properly degenerates to accepted representations of material damage, behavior for creep-fatigue and high-cycle/low-cycle fatigue interaction, as modeled by the NASA Lewis damage curve approach. The model structure is such that a relatively small number of tests are required to characterize a new material. Similarly, engineering estimates of model constants, so that approximate predictions may be made for an uncharacterized material, are straight forward in execution.

The cumulative creep-fatigue damage interaction life prediction method was developed under a doctoral degree program at Case Western Reserve University. The model has been characterized for Type 316 Stainless Steel (a material used in the Space Shuttle Main Engine heat exchanger, as well as a former liquid oxygen LOX position-injector material) at 816 °C for a large number of two-level block loading experiments involving general combinations of creep-fatigue and simple-fatigue loadings. The vast majority of results from these experiments are unconservatively predicted by the linear damage rule (in common use in contemporary structural design), but are well correlated through the use of the model proposed. The cumulative creep-fatigue damage interaction life prediction model presented is the first such model to provide a comprehensive treatment of cumulative damage for complex creep-fatigue loading histories. An order of magnitude improvement, in accuracy of prediction of life expectancy for components used in reusable space propulsion systems, can be realized from its use.

Lewis contact: Dr. Michael A. McGaw,
(216) 433-3308
Headquarters program office: OAST

Nondestructive Evaluation/Health Monitoring Opportunities for Space Propulsion Systems

Space vehicles that will transport people and supplies to and from the moon and Mars will have to be reliable for extended lifetimes. In order to develop these vehicles, nondestructive evaluation and health monitoring strategies will be required. The vehicle's propulsion system is a key element of the vehicle that will be designed to incorporate advanced health monitoring and nondestructive inspection capabilities. There are many different types of space propulsion systems being considered and developed. These systems are based on chemical, electrical, and nuclear processes. The principles of

operation vary considerably between systems. A description of each space propulsion system, its principles of operation, inspectability, reliability, and failure modes are identified and provided as a framework for nondestructive evaluation/health monitoring research.

The principles of operation of space propulsion systems can be grouped into three basic processes: thermalization (Resistojet, Arcjet, Microwave thruster, Nuclear thermal rocket); ionization (Ion and Magnetoplasmadynamic thrusters); and chemical reactions (Hydrogen/oxygen and Hydrazine thrusters), Figure 61. Each basic process has its own particular type of known failure modes. Systems that use thermalization processes have failed due to high temperature enhanced mechanisms such as grain growth, melting, and corrosion. Ionization often results in sputter erosion and oxidation that limit the life of these systems. Systems based on chemical processes have failed due to catalyst breakdown.

Reliabilities for most of these propulsion systems remain in question. How reliabilities are to be determined at a reasonable cost for these advanced space propulsion systems remains unknown. Lifetime estimates have been obtained for some of these space propulsion systems. However, nonintrusive

methods for monitoring and verifying the propulsion system's "age" and health need to be developed.

Material loss and material microstructural changes are identified as the dominant mechanisms that affect the lifetimes of these advanced propulsion systems; therefore, research should be directed to the nondestructive evaluation and health monitoring of these mechanisms. Nondestructive evaluation and health monitoring research will impact the development of space propulsion systems by taking a leading role in the development of future directions.

Bibliography

Generazio, E.R.: Overview of Space Propulsion Systems for Identifying Nondestructive Evaluation and Health Monitoring Opportunities. NASA TM-103614.(216) 433-3304
Headquarters program office: OAST

Lewis contact: Dr. Edward R. Generazio,
(216) 433-6018
Headquarters program office: OAET

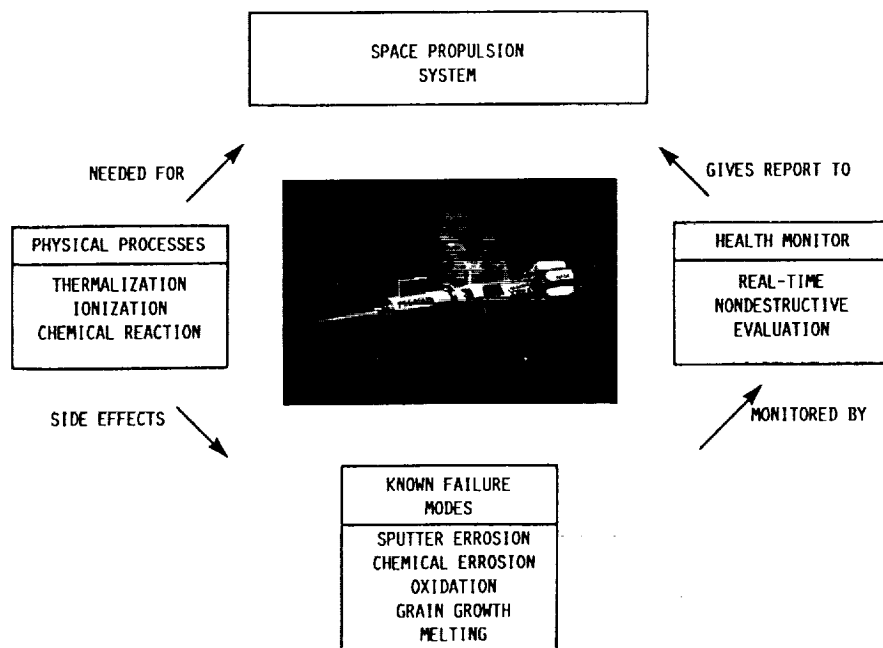


FIGURE 61. - NONDESTRUCTIVE EVALUATION TOOLS ARE USED TO MONITOR HEALTH OF SPACE PROPULSION SYSTEMS.

1990 Bibliography

- Abdul-Aziz, A., et al.: Effects of Using Serpentine Cooling Plates on Heat Transfer in Fuel-Cell Cooling Systems. Proceedings, Canadian Society of Mechanical Engineering Forum, Vol. 1, 1990.
- Afolabi, D.: Effects of Mistuning and Matrix Structure on the Topology of Frequency Response Curves. NASA TM-102290, 1989.
- Arnold, S.M.: Quantification of Numerical Stiffness for a United Viscoplastic Constitutive Model. *J. Eng. Mater. Technol.*, vol. 112, July 1990, pp. 271-276.
- Arnold, S.M.; Arya, V.K.; and Melis, M.E.: Elastic/Plastic Analyses of Advanced Composites Investigating the Use of the Compliant Layer Concept in Reducing Residual Stresses Resulting from Processing. NASA TM-103204, 1990.
- Arnold, S.M.; Tan, H.Q.; and Dong, X.: Application of Symbolic Computations to the Constitutive Modeling of Structural Materials. Symbolic Computations and their Impact on Mechanics, A.K. Noor, I. Elishakoff, and G. Hulbert, eds., ASME PVP, Vol. 205, 1990, pp. 215-229. (Also NASA TM-103225).
- Arnold, S.M.; and Tan, H.Q.: Symbolic Derivation of Potential Based Constitutive Equations. *Comput. Mech.*, vol. 6, 1990, pp. 237-246.
- Arya, V.K.: Finite Element Analysis of Structural Components Using Viscoplastic Models with Application to a Cowl Lip Problem. NASA CR-185189, 1990.
- Arya, V.K.; Melis, M.E.; and Halford, G.R.: A Finite Element Elastic-Plastic-Creep and Cyclic Life Analysis of a Cowl Lip. NASA TM-102342, 1990.
- Baaklini, G.; and Bhatt, R.T.: Preliminary X-Ray Monitoring of Damage Accumulation in SiC/RBSN. *HITemp Review 1990*, NASA CP-10051, 1990, pp. 54-1 to 54-13.
- Bakhle, M.A.; Reddy, T.S.; and Keith T.G.: Time Domain Flutter Analysis of Cascades Using a Full-Potential Solver. AIAA Paper 90-0984; Apr. 1990.
- Ballarini, R.: A Rigid Line Inclusion at a Bimaterial Interface. *Eng. Fract. Mech.*, vol. 37, no. 1, 1990, pp. 1-5.
- Ballarini, R.; and Luo, II, A.: Green's Functions for Dislocations in Bonded Strips and Related Crack Problems. NASA CR-185291, 1990.
- Bartolotta, P.A.; and Brindley, P.K.: High Temperature Fatigue Behavior of a SiC/Ti-24Al-11Nb Composite. NASA TM-103157, 1990.
- Berke, L.; and Hajela, P.: Applications of Artificial Neural Nets in Structural Mechanics. NASA TM-102420, 1990.
- Binienda, W.K.; Robinson, D.N.; Arnold, S.M.; and Bartolotta, P.A.: A Creep Model for Metallic Composites Based on Matrix Testing: Application to Kanthal Composites. NASA TM-103172, 1990.
- Bonacuse, P.J.; and Kalluri, S.: Axial-Torsional Fatigue: A Study of Tubular Specimen Thickness Effects. NASA TM-103637, AVSCOM-TM-90-C-014, 1990.
- Brown, H.C.; and Chamis, C.C.: Computational Characterization of High-Temperature Composites via METCAN. *HITemp Review 1990*, NASA CP-10051, pp. 46-1 to 46-6.
- Calomino, A.M.; and Brewer, D.N.: Controlled Crack Growth Specimen for Brittle Systems. NASA TM-103126, 1990.
- Caruso, J.J.; Chamis, C.C.; and Brown, H.C.: Parametric Studies to Determine the Effect of Compliant Layers on Metal Matrix Composite Systems. NASA TM-102465, 1990.
- Castelli, M.G.: Thermomechanical Deformation Testing and Modeling in the Presence of Metallurgical Instabilities. NASA CR-185188, 1990.
- Castelli, M.G.; Ellis, J.R.; and Bartolotta, P.A.: Thermomechanical Testing Techniques for High-Temperature Composites: TMF Behavior of SiC (SCS-6)/Ti-15-3. NASA TM-103171, 1990.
- Chamis, C.C.; and Ginty, C.A.: Fundamental Aspects of and Failure Modes in High-Temperature Composites. NASA TM-102558, 1990.
- Chamis, C.C.; and Stock, T.A.: Probabilistic Simulation of Uncertainties in Composites Uniaxial Strengths. NASA TM-102483, 1990.
- Chamis, C.C.; and Rubenstein, R.I.: Structural Tailoring of Select Fiber Composites Structures. NASA TM-102484, 1990.
- Chamis, C.C.; Caruso, J.J.; Lee, H.-J.; and Murthy, P.L.N.: METCAN Verification Status. NASA TM-103119, 1990.
- Chamis, C.C.; and Murthy, P.L.N.: Probabilistic Composite Analysis. First NASA Advanced Composite Technology Conference, Part 2, J.G. Davis Jr. and H.L. Bohon, eds., NASA CP-3104-PT-2, 1990, pp. 891-900.
- Chamis, C.C.; and Shiao, M.: Probabilistic Simulation of Uncertainties in Thermal Structures. NASA TM-103680, 1990.
- Chen, W.Y., et al.: Modeling and Characterization of Multi-Directionally Reinforced Ceramic Matrix Composite. *HITemp Review 1990*, NASA CP-10051, 1990, pp. 76-1 to 76-9.
- Choi, S.R.; Ritter, J.E.; and Jakus, K.: Failure of Glass with Subthreshold Flaws. *J. Am. Ceram. Soc.*, Vol. 73, No. 2, Feb. 1990, pp. 268-274.
- Choi, S.R.; and Salem, J.A.: Strength and Fracture Toughness of Monolithic and SiC Whisker-Reinforced Silicon Nitrides. Proceedings American Ceramic Society Symposium on Composites, Orlando, Florida, November, 1990.
- Chudnovsky, A.; and Wu, S.P.: Effect of Crack-Microcracks Interaction on Energy Release Rates. International Journal of Fracture, Vol. 44, No. 1, July 1990, pp. 43-56.
- Chulya, A.; Baaklini, G.Y.; and Bhatt, R.T.: Characterization of Damage and Fracture Mechanisms in Continuous Fiber Reinforced SiC/RBSN Ceramic Matrix Composites by Acoustic Emission. *HITemp Review 1990*, NASA CP-10051, 1990, pp. 55-1 to 55-15.

- Davy, D.; Saravanos, D.A.; Chamis, C.C.; and Hopkins, D.A.: Optimization of Tibial Knee Implants. Proceedings of 1st World Congress of Biomechanics, Aug. 30 - Sept. 4, 1990, San Diego, CA.
- DiRusso, E.; and Brown, G.V.: Experimental Evaluation of a Tuned Electromagnetic Damper for Vibration Control of Cryogenic Turbopump Rotors. NASA TP-3005, 1990.
- Dodd, W.R.; Badgley, M.B.; and Konkell, C.R.: User Needs, Benefits, and Integration of Robotic Systems in a Space Station Laboratory. NASA CR-185150.
- Doghri, I.; Jansson, S.; LeMaitre, J.; and Leckie, F.A.: Optimization of Interface Layers in the Design of Ceramic Fiber Reinforced Metal Matrix Composites. NASA CR-185307, 1990.
- Duffy, S.F.; and Arnold, S.M.: Noninteractive Macroscopic Reliability Model for Whisker-Reinforced Ceramic Composites. Journal of Composite Materials, Vol. 24, No. 3, March, 1990, pp. 293-308.
- Duffy, S.F.; Chulya, A.; and Gyekenyesi, J.P.: Structural Design Methodologies for Ceramic Based Material Systems. To appear in Flight-Vehicle Materials. Structures and Dynamics Technologies - Assessment and Future Directions, A. K. Noor and S.L. Venneri, eds. 1990, (Also, NASA TM-103097).
- Duffy, S.F.; and Gyekenyesi, J.P.: C/CARES - A Computer Algorithm for the Reliability Analysis of Laminated CMC Components. HHTemp Review 1990, NASA CP-10051, 1990, pp. 77-1 to 77-9.
- Duffy, S.F.; Wetherhold, R.C.; and Jain, L.K.: Extension of a Noninteractive Reliability Model for Ceramic Matrix Composites. NASA CR-185267, 1990.
- Freed, A.D.; Raj, S.; and Walker, K.P.: Stress Versus Temperature Dependent Activation Energies in Creep. NASA TM-103192, 1990. (In press, Journal of Engineering Materials and Technology).
- Freed, A.D.; and Walker, K.P.: A Viscoplastic Model with Application to LiF-22%CaF₂ Hypereutectic Salt. NASA TM-103181, 1990.
- Freed, A.D.; and Walker, K.P.: Model Development in Viscoplastic Ratchetting. NASA TM-102509, 1990.
- Freed, A.D.; and Walker, K.P.: Steady-State and Transient Zener Parameters in Viscoplasticity: Drag Strength Versus Yield Strength. Appl. Mech. Rev., vol. 43, no. 5, pt. 2, May 1990, pp. S328-S337. (Also NASA TM-102487).
- Fusaro, R.L.: Self-Lubricating Polymer Composites and Polymer Transfer Film Lubrication for Space Applications. Tribol. Int., vol. 23, no. 2, Apr. 1990, pp. 105-122. (Also, NASA TM-102492).
- Gayda, J.; Gabb, T.P.; and Freed, A.D.: The Isothermal Fatigue Behavior of a Unidirectional SiC/Ti Composite and the Titanium Alloy Matrix. Fundamental Relationships Between Microstructure and Mechanical Properties of Metal-Matrix Composites, The Minerals, Metals and Materials Society, 1990, pp. 497-514. (Also, NASA TM-101984).
- Generazio, E.R.: Theory and Experimental Technique for Nondestructive Evaluation of Ceramic Composites. NASA TM-102561, 1990.
- Generazio, E.R.: Ultrasonic and Radiographic Evaluation of Advanced Aerospace Materials: Ceramic Composites. NASA TM-102540, 1990.
- Ghosn, L.J.; Telesman, J.; and Kantzos, P.: Fatigue Crack Growth in Unidirectional Metal Matrix Composite. International Fatigue Series (Fatigue 90), H. Kitagawa and T. Tanaka, eds., Materials and Component Engineering Publications Ltd, England, Vol. II, 1990, pp. 893-898. (Also, NASA TM-103102).
- Gladden, H.J., et al.: Thermal Structural Analysis of Several Hydrogen Cooled Leading Edge Concepts for Hypersonic Flight Vehicles. NASA TM-102391, 1990.
- Grady, J.E.: Collision Forces for Compliant Projectiles. NASA TM-4203, 1990.
- Grady, J.E.; and Lerch, B.A.: Evaluation of Thermal and Mechanical Loading Effects on the Structural Behavior of a SiC/Titanium Composites. NASA TM-102536, 1990.
- Hajela, P.; and Berke, L.: Neurobiological Computational Models in Structural Analysis and Design. AIAA Paper 90-1133, Apr. 1990.
- Hamid, A.: Probabilistic Modeling for Simulation of Aerodynamic Uncertainties in Propulsion Systems. NASA TM-102472, 1990.
- Hickman, J.M., et. al.: Solar Electric Propulsion for Mars Transport Vehicles. NASA TM-103234, 1990.
- Hopkins, D.A.: Integrated Analysis and Applications. Aeropropulsion '87, NASA CP-3049, 1990, pp. 141-153.
- Huber, R.D.; and Green, R.E. Jr.: Acousto-Ultrasonic Nondestructive Evaluation of Materials Using Laser Beam Generation and Detection. NASA Contractor Report CR-185282, 1990.
- Janetzke, D.C.; and Murthy, D.V.: Concurrent Processing Adaptation of Aeroelastic Analysis of Propfans. AIAA Paper 90-1036, Apr. 1990 (Also, NASA TM-102455).
- Jansson, S.; and Leckie, F.A.: Reduction of Thermal Stresses in Continuous Fiber Reinforced Metal Matrix Composites with Interface Layers. NASA CR-185302, 1990.
- Jansson, S.; Leckie, F.A.; Onat, E.T.; and Ranaweera, M.P.: Materials with Periodic Internal Structure: Computation Based on Homogenization and Comparison with Experiment. NASA CR-185303, 1990.
- Jenkins, M.G.; Ghosh, A.; and Salem, J.A.: Numerical, Micro-Mechanical Prediction of Crack Growth Resistance in a Fibre-Reinforced/Brittle Matrix Composite. Proceedings of the Society for Experimental Mechanics Spring Conference, Albuquerque, New Mexico, June 4-6, 1990.
- Kalluri, S.; and Bonacuse, P.J.: A Data Acquisition and Control Program for Axial-Torsional Fatigue Testing. Applications of Automation Technology to Fatigue and Fracture Testing, ASTM-STP-1092, 1990, pp. 269-287. (Also, NASA TM-102041, AVSCOM-TR-89-C-002).
- Kalluri, S.; and McGaw, M.A.: Fatigue Behavior of PWA 1480 Single Crystal in the Presence of Tensile Mean Stress. Advanced Earth-To-Orbit Propulsion Technology, R.J. Richmond and S.T. Wu, eds., NASA CP-3092, Vol. 3, 1990, pp. 319-331.

- Kalluri, S.; and McGaw, M.A.: Effect of Tensile Mean Stress on the Fatigue Behavior of Single Crystal and Directionally Solidified Superalloys. NASA TM-103644, 1990. (Presented at the ASTM Symposium on Cyclic Deformation, Fracture, and Nondestructive Evaluation of Advanced Materials, San Antonio, TX, Nov. 1990).
- Kielb, R.E.; and Ramsey, J.K.: Flutter of a Fan Blade in Supersonic Axial Flow. *J. Turbomachinery*, vol. 111, no. 4, Oct. 1989, pp. 462-467.
- Kiernan, M.T.; and Duke, J.C. Jr.: Theoretical Basis of the Acousto-Ultrasonic Method, In: *Acoustic Emission: Current Practice and Future Direction*. ASTM STP 1077 (W. Sachse, J. Roget, and K. Yamaguchi, Eds.), American Society for Testing and Materials, Philadelphia, 1990, pp. 105-119.
- Kiernan, M.T.; and Duke, J.C., Jr.: A Physical Model for the Acousto-Ultrasonic Method, NASA CR-185294, 1990.
- Kim, K.S.; VanStone, R.H.; Laflen, J.H.; and Orange, T.W.: Simulation of Crack Growth and Crack Closure Under Large Cyclic Plasticity. *Fracture Mechanics: Twenty-First Symposium*, ASTM-STP-1074, 1990, pp. 421-447.
- Kuo, W.S.; and Chou, T.W.: Predictions of the Critical Strain for Matrix Cracking of Ceramic Matrix Composites. *Inelastic Deformation of Composite Materials*, G.J. Dvorak, ed., Springer-Verlag, 1990, pp. 639-652.
- Kuo, W.S.; and Chou, T.W.: Modeling of Flexural Behavior of Ceramic Matrix Composites. *Microcracking-Induced Damage in Composites*, G.J. Dvorak and D.C. Lagoudas, eds., ASME, 1990, pp.
- Lawrence, C.; and Huckelbridge, A.A.: A Global Approach For The Identification of Structural Connection Properties. NASA TM-102502, 1990.
- Lawrence, C.; and Kiraly, L.J.: Structural Dynamics Branch Research and Accomplishments for FY89. NASA TM-102488, 1990.
- Lee, H.-J.: METCAN Simulation of Candidate Metal Matrix Composites for High Temperature Applications. NASA TM-103636, 1990.
- Lerch, B.A.: Fatigue Behavior of SiC/Ti-15-3 Laminates. *HITemp Review 1990*, NASA CP-10051, 1990, pp. 35-1 to 35-9.
- Lerch, B.A.; and Antolovich, S.D.: Fatigue Crack Propagation Behavior of a Single Crystalline Superalloy. *Metall. Trans. A*, vol. 21A, no. 8, Aug. 1990, pp. 2169-2177.
- Lerch, B.A.; Gabb, T.P.; and MacKay, R.A.: Heat Treatment Study of the SiC/Ti-15-3 Composite System. NASA TP-2970, 1990.
- Lerch, B.A.; Hull, D.R.; and Leonhardt, T.A.: Microstructure of a SiC/Ti-15-3 Composite. *Composites*, vol. 21, no. 3, 1990, pp. 216-224.
- Logie, D.S., Kamil, H., and Umarietya, J.R., "An Application of Object-Oriented Knowledge Representation to Engineering Expert Systems," *Proceedings of 3rd AF/NASA Symposium on Recent Advances in Multidisciplinary Analysis and Optimization*, San Francisco, CA, Sept. 1990.
- McGaw, M.A.: Cumulative Creep Fatigue Damage Modeling. *Advanced Earth-to Orbit Propulsion Technology*, R.J. Richmond and S.T. Wu, eds., NASA CP-3092, Vol. 3, 1990, pp. 298-318.
- McGraw, M.A.: Modelling and Identification of Cumulative Creep-Fatigue Damage in an Austenitic Stainless Steel. Ph.D. Dissertation, Case Western Reserve University, 1990.
- Meeks, C.; DiRusso, E.; and Brown, G.V.: Development of a Compact, Lightweight Magnetic Bearing. AIAA Paper 90-2483, July 1990.
- Melis, M.E.: Comgen - A Computer Program for Generating Finite Element Models of Composite Materials at the Microlevel. NASA TM-102556, 1990.
- Melis, M.E.; and Gladden, H.J.: A Unique High Heat Flux Facility for Testing Hypersonic Engine Components. NASA TM-103238, 1990.
- Minnetyan, L.; Murthy, P.L.N.; and Chamis, C.C.: Composite Structure Global Fracture Toughness via Computational Simulation. *Comput. Struct.* vol. 37, no. 2, 1990, pp. 175-180.
- Minnetyan, L.; Murthy, P.L.N.; and Chamis, C.C.: Progression of Damage and Fracture in Composites Under Dynamic Loading. NASA TM-103118, 1990.
- Minnetyan, L.; Murthy, P.L.N.; and Chamis, C.C.: Structural Behavior of Composites with Progressive Fracture. NASA TM-102370, 1990.
- Mital, S.K.; and Chamis, C.C.: Fiber Push-out Test: A Three-Dimensional Finite Element Computational Simulation. NASA TM-102565, 1990.
- Mital, S.K.; and Chamis, C.C.: Microfracture in High-Temperature Metal Matrix Composites. *HITEMP Review 1990*, NASA CP-10051, pp. 45-1 to 45-9. (Also *Proceedings of 15th Annual Mechanics of Review*, Oct. 24-25, 1990).
- Mital, S.K.; Caruso, J.J.; and Chamis, C.C.: Metal Matrix Composites Microfracture: Computational Simulation. NASA TM-103153, 1990. (Also, *J. Computers and Structures*, Vol. 37, No. 2, 1990, pp. 141-150.)
- Morel, M. and Saravanos, D.A.: Computational Procedure to Tailor Compliant Layer Characteristics and Proceeding History for Minimum Residual Stresses," *HITEMP Review 1990*, NASA CP-10051, pp. 44-1 to 44-9.
- Morel, M.; Saravanos, D.A.; and Chamis, C.C.: Concurrent Micromechanical Tailoring and Fabrication Process Optimization for Metal-Matrix Composites. NASA TM-103670, 1990.
- Morel, M., Sarvanos, D.A., and Chamis, C.C., "Micromechanical and Fabrication Processes Optimization for Advanced Metal-Matrix Composites," NASA TM-103670, 1990.
- Murthy, P.L.N.; and Chamis, C.C.: Simplified Design Procedures for Fiber Composite Structural Components/Joints. NASA TM-103113, 1990.
- Murthy, P.L.N.; and Chamis, C.C.: Fiber Substructuring for Micromechanics of Ceramic Matrix Composites. *HITEMP Review 1990*, NASA CP-10051, pp. 75-1 to 75-8.
- Nemeth, N.N.; Manderscheid, J.M.; and Gyekenyesi, J.P.: "Ceramics Analysis and Reliability Evaluation of Structures (CARES) Users and Programmers Manual," NASA TP-2916, 1990.
- Orange, T.W.: Method and Models for R-Curve Instability Calculations. *Fracture Mechanics: Twenty-First Symposium*, J.P. Gudas, E.M. Hackett, and J.A. Joyce, eds., ASTM-STP-1074, 1990, pp. 545-559. (Also, NASA TM-100935.)
- Pai, S.S.: Probabilistic Structural Analysis of a Truss Typical for Space Station. NASA TM-103277, 1990.
- Patnaik, S.N.; Berke, L.; and Gallagher, R.H.: Compatibility Conditions of Structural Mechanics for Finite Element Analysis. NASA TM-102413, 1990.
- Patnaik, S.N.; Berke, L.; and Gallagher, R.H.: Integrated Force Method Versus Displacement Method for Finite Element Analysis. NASA TP-2937, 1990.

- Pereira, J.M.; and Generazio, E.R.: Improved Transverse Crack Detection in Composites. NASA TM-103261, 1990.
- Popp, G.J.; and Wetherhold, R.C.: Mechanical Characterization of a Woven Ceramic Fiber/Ceramic Matrix Composite. *J. Mater. Sci. Lett.*, vol. 9, no. 10, Oct, 1990, pp. 1187-1189.
- Renneisen, J.D.; and Williams, J.H., Jr.: Input-Output Characterization of Fiber Reinforced Composites by P-Waves, NASA CR-185287, 1990.
- Robinson, D.N.; and Arnold, S.M.: Effects of State Recovery on Creep Buckling Under Variable Loading. *J. Appl. Mech.*, vol. 57, June 1990, pp. 313-320.
- Roth, D.J.; Stang, D.B.; Swickard, S.M. and DeGuire, M.R.: Review and Statistical Analysis of the Ultrasonic Velocity Method for Estimating Porosity Fraction in Polycrystalline Materials. NASA TM-102501, 1990.
- Rubinstein, A.A.: Crack Path Effect on Material Toughness. *J. Appl. Mech.*, vol. 57, no. 1, Mar. 1990, pp. 97-103.
- Rubinstein, A.A.: Fracture Toughness Modeling for Materials with Complex Microstructure. *Constitutive Laws of Plastic Deformation and Fracture*, A.S. Krausz, et al., eds., Kluwer Academic, Dodrecht, 1990, pp. 215-221.
- Salem, J.A.: Strength and Toughness of Monolithic and Composite Silicon Nitrides. NASA TM-102423, January, 1990.
- Salem, J.A.; and Choi, S.R.: Toughened Ceramic Life Prediction. Ceramic Technology of Advanced Heat Engines Semiannual Contractors Report, ORNL/TM-11586, September, 1990, pp. 383-396.
- Salem, J.A.; and Choi, S.R.: Toughened Ceramic Life Prediction. Ceramic Technology of Advanced Heat Engines Semiannual Contractors Report, ORNL/TM-11719, December, 1990, pp. 341-364.
- Saravanos, D.A.; and Chamis, C.C.: Multi-Objective Shape and Material Optimization of Composite Structures Including Damping. NASA TM-102579, 1990.
- Saravanos, D.A.; and Chamis, C.C.: Unified Micromechanics of Damping for Unidirectional and Off-Axis Fiber Composites. *J. Composites Technol. Res.*, vol. 12, no. 1, Spring 1990, pp. 31-40.
- Saravanos, D.A.; and Chamis, C.C.: An Integrated Methodology for Optimizing the Passive Damping of Composite Structures. *Polymer Composites*, vol. 11, no. 6, Dec. 1990, pp. 328-336.
- Saravanos, D.A.; Murthy, P.L.N.; and Morel, M.: Optimal Fabrication Processes for Unidirectional Metal Matrix Composites: A Computational Simulation. NASA TM-102559.
- Seng, H-S; and Williams, J.H., Jr.: Ultrasonic Verification of Five Wave Fronts in Unidirectional Graphite. NASA CR-185288, 1990.
- Shah, A.R.; Nagpal, V.K.; and Chamis, C.C.: Probabilistic Analysis of Bladed Turbine Disks and the Effects of Mistuning. NASA TM-102564, 1990.
- Shiao, M.; and Chamis, C.C.: A Methodology for Evaluating the Reliability and Risk of Structures Under Complex Service Environments. NASA TM-103244, 1990.
- Shiao, M.; and Chamis, C.C.: First Passage Problem: A Probabilistic Dynamic Analysis for Degrading Structures. NASA TM-103755, 1990.
- Singhal, S.N., et al.: Demonstration of Capabilities of High Temperature Composites Analyzer Code HITCAN. NASA TM-102560, 1990.
- Smith, T.E.: Aeroelastic Stability Characteristics of High Energy Turbines. *Advanced Earth to Orbit Propulsion Technology 1990*, Vol. 2, R.J. Richmond and S.T. Wu, eds., NASA CP-3092-VOL-2, 1990, pp. 163-179.
- Srivastava, R.; et al.: Application of an Efficient Hybrid Scheme for Aeroelastic Analysis of Advanced Propellers. AIAA Paper 90-0028, Jan. 1990. (Also, NASA TM-102428).
- Steinetz, B.M.: A Test Fixture for Measuring High Temperature Hypersonic-Engine Seal Performance. NASA TM-103658, December, 1990.
- Steinetz, B.M.; et al.: High Temperature NASP Engine Seal Development. NASA TM-103716, 1990.
- Suzuki, K.; and Kikuchi, N.: Shape and Topology Optimization by a Homogenization Method. Sensitivity Analysis and Boundary Element Methods, ASME, NY, 1990, pp. 15-30.
- Szatmary, S.A.; Gyekenyesi, J.P.; and Nemeth, N.N.: Calculation of Weibull Strength Parameters, Batdorf Flaw Density Constants and Related Statistical Quantities Using PC-CARES. NASA TM-103247, 1990.
- Thanedar, P.B.; and Chamis, C.C.: Composite Laminate Tailoring with Probabilistic Constraints and Loads. NASA TM-102515, 1990.
- Thomas, D.J.: Reliability Analysis of Composite Laminates with Load Sharing. *J. Compos. Mater.*, in review.
- Thomas, D.J.; and Wetherhold, R.C.: Reliability Analysis of Continuous Fiber Composite Laminates. NASA CR-185265, 1990.
- Thomas, D.J.; and Wetherhold, R.C.: Reliability Analysis of Continuous Fiber Composite Laminates. *Composite Structures*, vol. 17, no. 4, 1991, pp. 277-293.
- Tong, M.; Steinetz, B.M.: Thermal and Structural Assessments of a Ceramic Wafer Seal in Hypersonic Engines. Prepared for Presentation at the 27th Joint Propulsion Conference cosponsored by the AIAA, ASME, SAE, and ASEE, Sacramento, CA, June 24-27, 1991, NASA TM-103651, December, 1990.
- Trowbridge, D.A.; Grady, J.E.; and Aiello, R.A.: Low-Velocity Impact Analysis with NASTRAN. NASA TM-103169, 1990.
- Umarietiya, J.R. and Kamil, H., "Implementation of Efficiency Sensitivity Analysis for Optimization of Large Structures," *Proceedings of 3rd AF/NASA Symposium on Recent Advances in Multidisciplinary Analysis and Optimization*, San Francisco, CA, Sept. 1990.
- VanStone, R.H.; and Kim, K.S.: Elevated Temperature Crack Growth. *Advanced Earth-to-Orbit Propulsion Technology 1990*, R.J. Richmond and S.T. Wu, eds., NASA CR-3092, Vol. 3, 1990, pp. 345-358.
- Vary, A.: NDE of Structural Ceramics. Proceedings 34th Sagamore Army Materials Research Conference, October 1-4, 1990, Plymouth, MA (In Press).
- Vary, A.: Acousto-Ultrasonics. Non-Destructive Testing of Fiber Reinforced Plastics, Volume 2 (J. Summerscales, Ed.), Elsevier Applied Science Publishers, Essex, England, 1990, pp. 1-54.

Verrilli, M.J.; Ellis, J.R.; and Swindeman, R.W.: Current Activities in Standardization of High-Temperature Low-Cycle-Fatigue Testing Techniques in the U.S. NASA TM-103675, 1990. (To be published in Proceedings, Harmonisation of Testing Practice for High Temperature Materials, Travedona Monate, Italy, Oct. 1990).

Verrilli, M.J.; Kim, Y.S.; and Gabb, T.P.: High Temperature Fatigue Behavior of Tungsten Copper Composites. Fundamental Relationships Between Microstructures and Mechanical Properties of Metal Matrix Composites, P.K. Liaw and M.N. Gungor, eds., The Minerals, Metals and Materials Society, 1990, pp. 479-495. (Also, NASA TM-102404.)

Walker, K.P.; Freed, A.D.; and Jordan, E.: Micro Stress Analysis of Periodic Composites. Advanced Earth-to-Orbit Propulsion Technology 1990, R.J. Richmond and S.T. Wu, eds., NASA CP-3092, Vol. 3, 1990, pp. 359-374.

Walker, K.P.; Jordan, E.H.; and Freed, A.D.: Equivalence of Green's Function and the Fourier Series Representation of Composites with Periodic Microstructure. Micromechanics and Inhomogeneity: The Toshio Mura Anniversary Volume, G.J. Weng, M. Taya, and H. Abe, eds., Springer-Verlag, New York, 1990, pp. 535-558.

Wortherm, D.W.: Flat Tensile Specimen Design for Advanced Composites. NASA CR-185261, 1990.

Wortherm, D.W.; Robertson, I.M.; Leckie, F.A.; Socie, D.F.; and Altstetier, C.J.: Inhomogeneous Deformation in Inconel 718 During Monotonic and Cyclic Loadings. Metall. Trans., vol. 21A, no. 12, Dec. 1990, pp. 3215-3220.

Yamamoto, O.; and August, R.: Structural and Aerodynamic Analysis of Large Scale Advanced Propeller Blade. AIAA Paper 90-2401, July 1990.

Yeh, H.; Solidum, E.; Schienle, J.; Karasek, K.; and Salem, J.A.: Proceeding and Mechanical Behavior of Whisker-Toughened Silicon Nitride. In: Proceedings of the 28th SAE Annual Contractors Coordination Meeting, Dearborne, Michigan, October 28, 1990.

Zaretsky, E.V.: Bearing Elastohydrodynamic Lubrication: A Complex Calculation Made Simple. NASA TM-102575, 1990.

Zaretsky, E.V.: Bearing and Gear Steels for Aerospace Applications. Advanced Materials in Aerospace Applications, ASM International, 1990, pp. AIV 1-15.

Zaretsky, E.V.: Liquid Lubrication in Space. Tribol. Int. vol. 23, no. 2, Apr. 1990, pp. 75-93.

Zaretsky, E.V.; and August, R.: Closed Form Solution for Hoop Stress in a Ball-Race Contact. To be published, Proc. 1990 Conference on Advanced Earth-to-Orbit Prop. Tech., 1990. Presented in Huntsville, Alabama, May 15-17, 1990, 1990 Conference on Advanced Earth-to-Orbit Prop. Tech.

Contractor/Grant Reports

Arya, V.K.: Application of Finite-Element-Based Solution Technologies for Viscoplastic Structural Analyses. NASA CR-185196. (Accepted for publication in Communications in Applied Numerical Methods, 1990).

Emery, A.F.; Etemad, S.; and Wolak, J.: Interfacial Temperatures and Surface Heat Fluxes During a Blade-Seal Rubbing Process. AIAA Paper 81-1165, June 1981.

Emery, A.F.; Wolak, J.; Etemad, S.; and Choi, S.R.: An Experimental Investigation of Temperatures Due to Rubbing at the Blade-Seal Interface in an Aircraft Compressor. Univ. of Washington, NAG3-7, 1983. Jan. 1990. (Grant Monitor: J. Kiraly).

Huckelbridge, A.A.; and Abdallah, A.A.: Boundary Flexibility Method of Component Mode Synthesis Using Static Ritz Vectors. Comput. Struct., vol. 35, no. 1, 1990, pp. 51-61.

Kim, K.S.; VanStone, R.H.; Malik, S.N.; and Lafien, J.H.: Elevated Temperature Crack Growth. NASA CR-182247, 1990.

Ku, C.C.; and Williams, M.H.: Three-Dimensional Full Potential Method for Aeroelastic Analysis of Propfans. AIAA Paper 90-1120, May 1990.

Malachowski, M.J.: Beam Rider for an Articulated Robot Manipulator (ARM) Accurate Positioning of Long Flexible Manipulators NASA CR-185151, 1990.

Roberson, D.N.; Binienda, W.K.; and Kavuma, M.M.: Creep and Creep Rupture of Strongly Reinforced Metallic Composites. NASA CR-185286, 1990.

Smolinski, P.J.: Transient Finite Element Computations on the Transputer System. NASA CR-185199, 1990.

Williams, M.H.: An Unsteady Lifting Surface Method for Single Rotation Propellers. NAG 3-499, July 1990. (Contract Monitor: G.L. Stefko).

Wolak, J.; Emery, A.F.; Etemad, S.; and Choi, S.R.: Preliminary Results on the Abradability of Porous, Sintered Seal Materials. Univ. of Washington, NAG3-7, 1983. Jan. 1990 (Contract Monitor: J. Kiraly).

Wolak, J.; Emery, A.F.; Etemad, S.; and Choi, S.R.: Blade Tip Geometry-A Factor in Abrading Sintered Seal Material. Univ. of Washington, NAG3-7, 1984, Jan. 1990. (Grant Monitor: J. Kiraly).

Zenas, R.; Archbold, T.; Wolak, J.; Emery, A.F.; and Etemad, S.: Metallurgical and Mechanical Phenomena Due to Rubbing of Titanium Against Sintered Powder Nichrome. Univ. of Washington, NAG3-7, 1984. Jan. 1990. (Grant Monitor: J. Kiraly).

1
2
3
4
5
6
7
8
9
10
11
12
13
14
15
16
17
18
19
20
21
22
23
24
25
26
27
28
29
30
31
32
33
34
35
36
37
38
39
40
41
42
43
44
45
46
47
48
49
50
51
52
53
54
55
56
57
58
59
60
61
62
63
64
65
66
67
68
69
70
71
72
73
74
75
76
77
78
79
80
81
82
83
84
85
86
87
88
89
90
91
92
93
94
95
96
97
98
99
100